Redox in melts and glasses

Roberto Moretti

Seconda Università degli Studi di Napoli

Dipartimento di Ingegneria Civile, Design, Edilizia & Ambiente

Via Roma 29 - 81031 Aversa (I)

INGV - Osservatorio Vesuviano
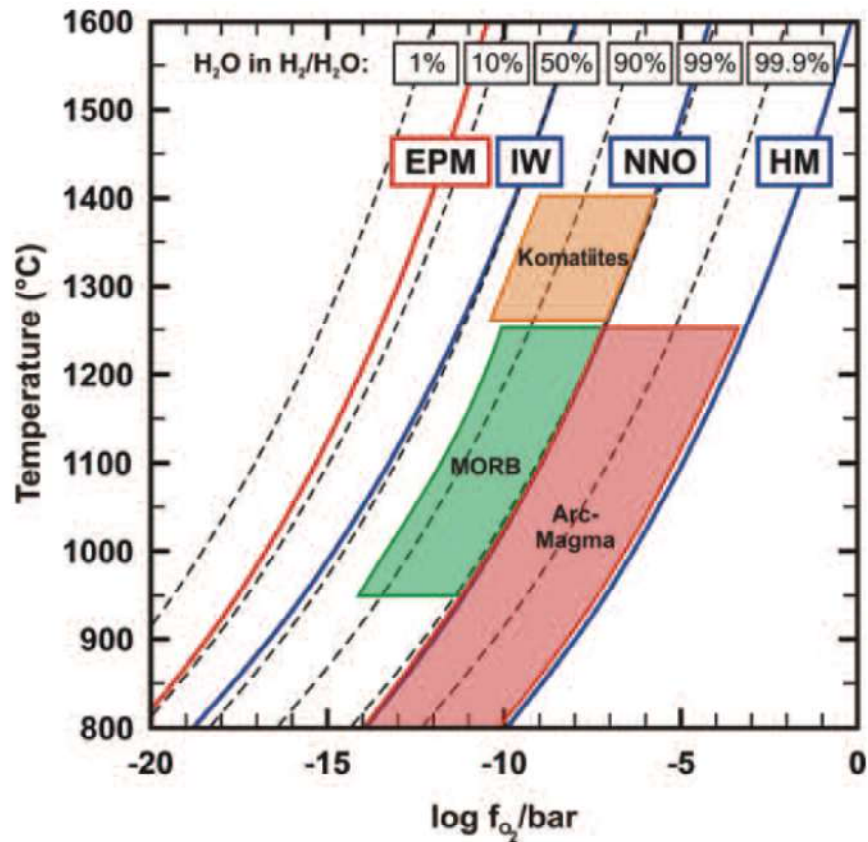
Via Diocleziano 328 - 80124 Napoli (I)

FIGURE 5 Redox conditions for terrestrial magmas in comparison with some oxygen buffers used for experimental control of the oxygen fugacity. Abbreviations: HM = hematite + magnetite, NNO = nickel + nickel oxide, IW = iron + wüstite, EPM = Earth primitive magma (magma ocean). The quartz-fayalite-magnetite (QFM) buffer, not shown on this diagram, is -0.8 log units below the NNO buffer. Dashed lines show the equilibrium H_2O fraction in H_2–H_2O gas mixtures for given T and f_{O_2}. The Earth primitive magma ocean (EPM), saturated in metal iron, is the most reduced and is in equilibrium with H_2–H_2O gas containing 8% water. Komatiites, the oldest lavas found on Earth, have redox conditions between IW +1 and NNO (Canil 2002), which correspond to a gaseous mixture containing 60 to 99% water. MORB displays moderately reducing conditions also upper bounded by the NNO buffer, whereas arc magmas, derived from subduction, are the most oxidized terrestrial lavas and also the most water rich (Carmichael, 1991). Such increase in oxidation state of magma with time, correlated with an increase in water content, is a fundamental issue that has motivated numerous experimental studies.
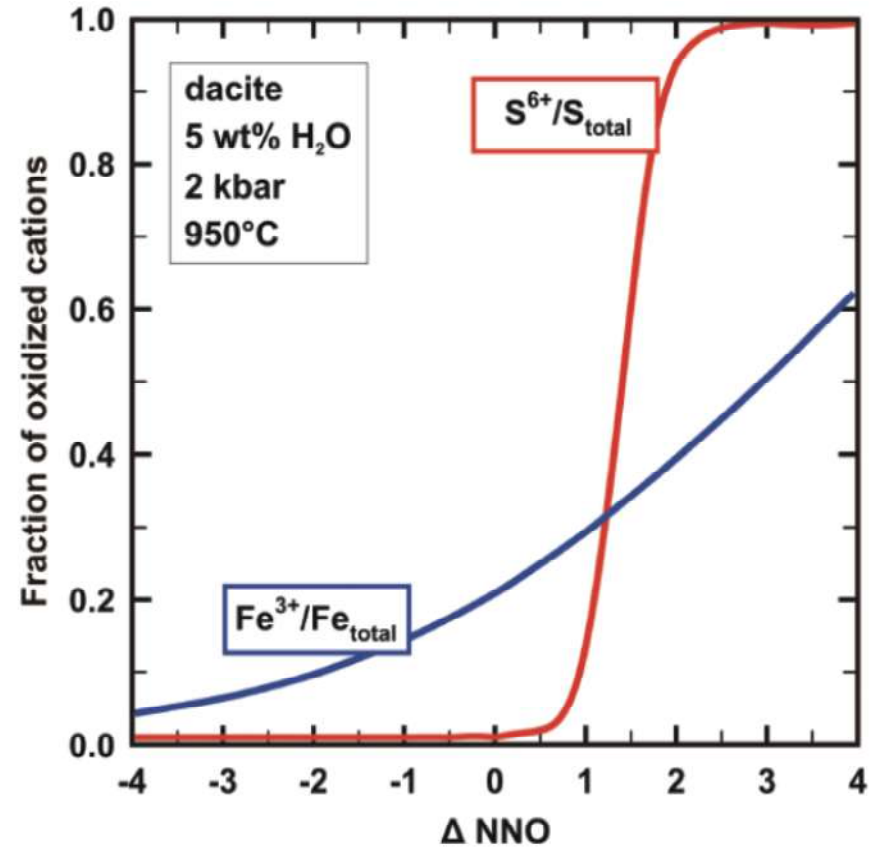
FIGURE 6 Variation of the fraction of oxidized species of sulfur (S^{6+}/total S) and iron (Fe^{3+}/total Fe) with oxygen fugacity for hydrous dacitic melts at 950°C (sulfur is calculated after Morretti and Ottonello 2005 and iron after Kress and Carmichael 1991). This diagram illustrates the sharp change in sulfur redox state centered on NNO + 1, which strongly contrasts with the smooth increase in ferric iron from NNO - 4 to NNO + 4. Because arc magmas display f_{O_2} conditions between NNO and NNO + 2, the oxidation state of sulfur can vary greatly in these magmas, which has a critical influence on their degassing dynamics (Scaillet and Pichavant 2005).

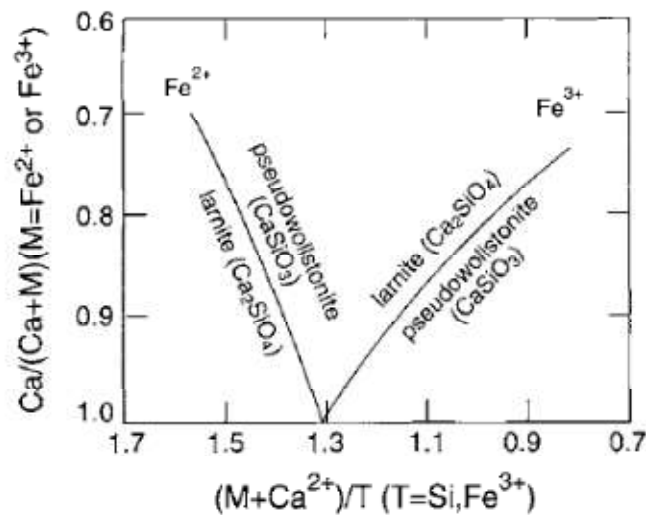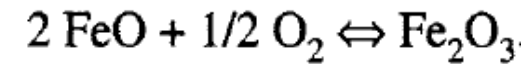$$2 \, FeO + 1/2 \, O_2 \Leftrightarrow Fe_2O_3$$

Figure 10.2 - Shift of the liquidus boundary of calcium silicates against the NBO/T of the melt whose variations result from changes in the proportions of Fe^{2+} and Fe^{3+}. Plot drawn by Mysen [1988] from the CaO-"Fe_2O_3"-SiO_2 phase diagram (see Fig. 10.7).

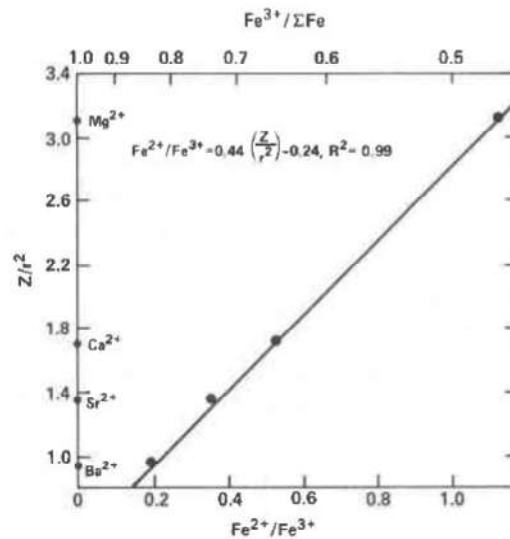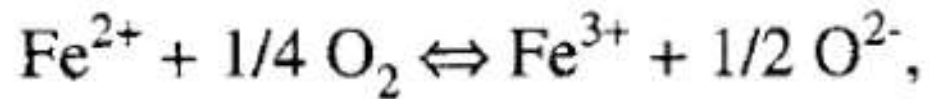$$NBO/T = 1/T \sum_{i=1}^{i} 1/n M_i^{n+}$$

$$NBO/T = (2O - 4T)/T$$

Fig. 2. Relationship between Fe^{2+}/Fe^{3+} and type of metal cation (Ba^{2+}, Sr^{2+}, Ca^{2+}, Mg^{2+}), expressed as Z/r^2 (Z = electrical charge, r = ionic radius for six-fold coordination; Whittaker and Muntus, 1970) for metasilicate melt compositions equilibrated at 1550°C in air.

$$Fe^{2+} + 1/4 \; O_2 \Leftrightarrow Fe^{3+} + 1/2 \; O^{2-},$$

$$K_{3/2} = (a_{Fe^{3+}}/a_{Fe^{2+}}) \; (a_{O^{2-}})^{1/2}/f_{O_2}^{1/4},$$

$$\log \; (Fe^{3+}/Fe^{2+}) = \log \; K_{3/2} + 1/4 \; \log \; f_{O_2} - 1/2 \; \log \; a_{O^{2-}} = A - 1/2 \; \log \; a_{O^{2-}}$$

Figure 10.12. Iron redox ratio of alkali silicate melts at 1400°C in air against SiO_2 concentration [Paul and Douglas, 1965]. Total iron content of 0.41 wt %.
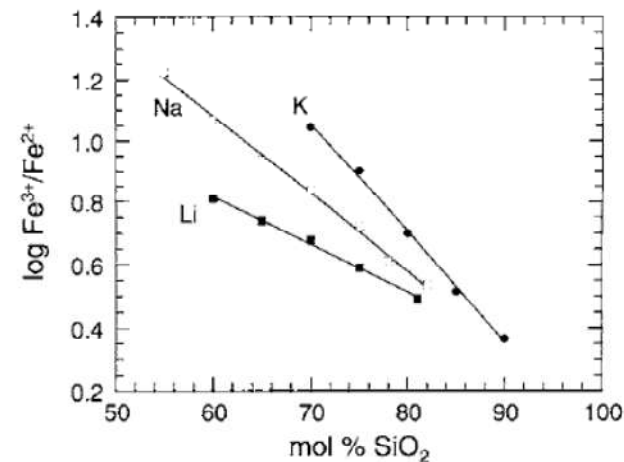
variations of $a_{O^{2-}}$ with composition !???!

Figure 10.16 - Iron redox ratio against K/(K+Al) for potassium aluminosilicates at constant 78 mol % SiO_2 [Dickenson and Hess, 1981]. Experiments made in air at 1400°C with a total of 2 wt % FeO.
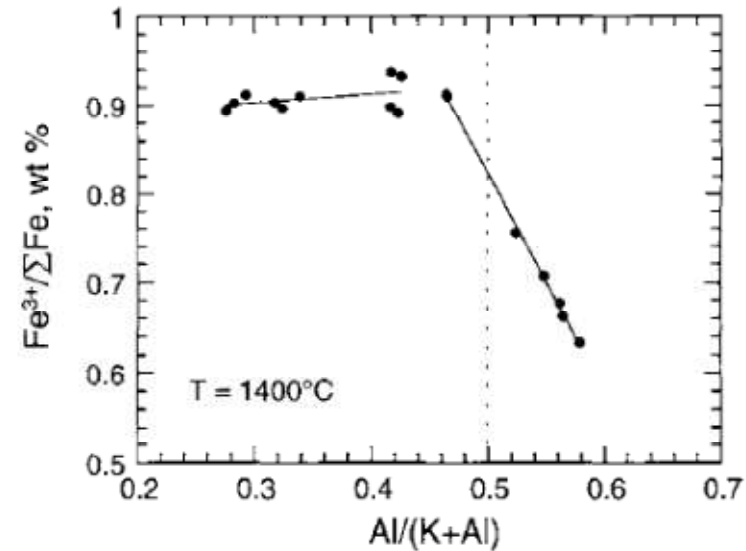
Empirical efforts….

$$\ln (x_{Fe_2O_3}/x_{FeO}) = a \ln f_{O_2} + b/T + c + \Sigma d_i x_i$$
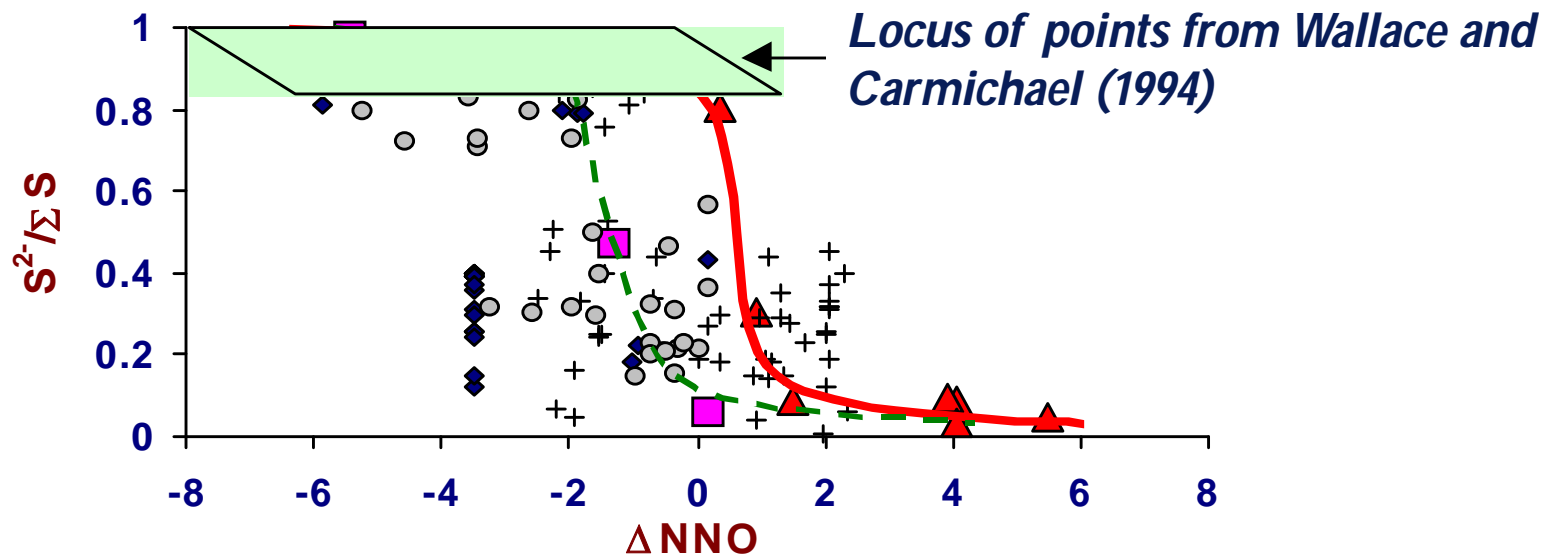
$$\ln (x_{Fe_2O_3}/x_{FeO}) = a \ln f_{O_2} + b/T + c + \Sigma d_i x_i$$
$$+ e [1 - T_0/T - \ln T/T_0] + f P/T + g (T-T_0)P/T + h P^2/T$$

$$\ln (x_{Fe^{3+}}/x_{Fe^{2+}}) = a \ln f_{O_2} + b/T + c + d(Al/(Al+Si)) + e(Fe^{3+}/Fe^{3+}+Si) + \Sigma f_i x_i$$

……..

Dealing with redox couples: an example from Ite literature

$$\log \frac{\left[S^{2-} \right]}{\left[SO_4^{2-} \right]} = -1.02 \log fO_2 - 25410/T + 10$$

$$S^{2-} + 2O_2 \Leftrightarrow SO_4^{2-}$$
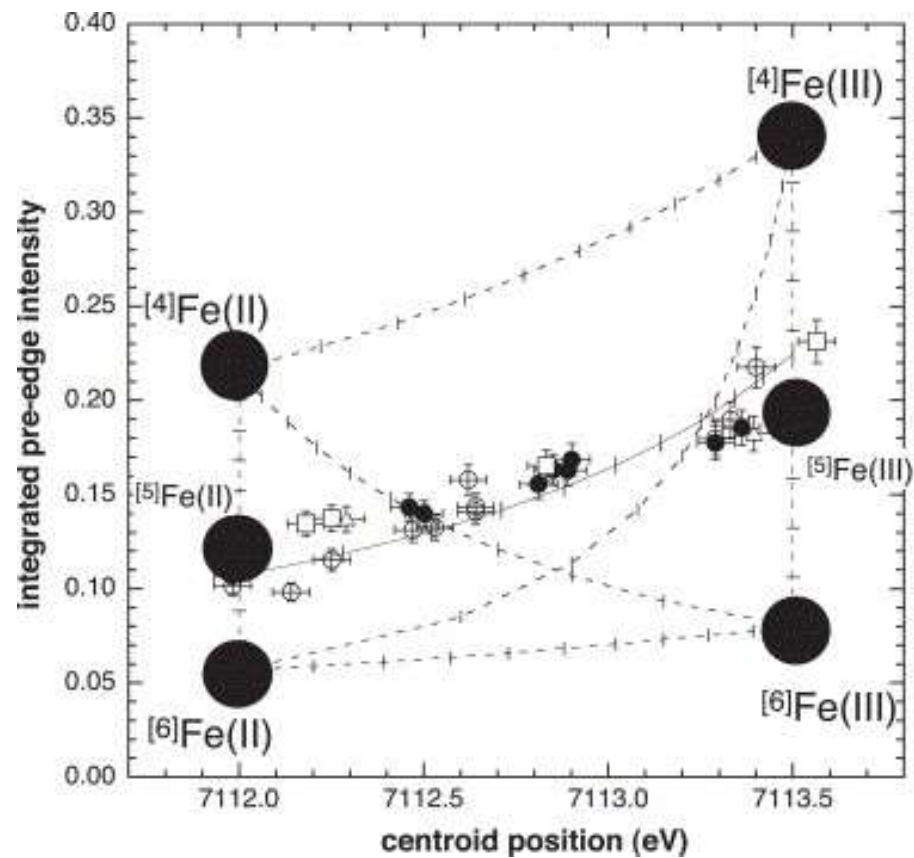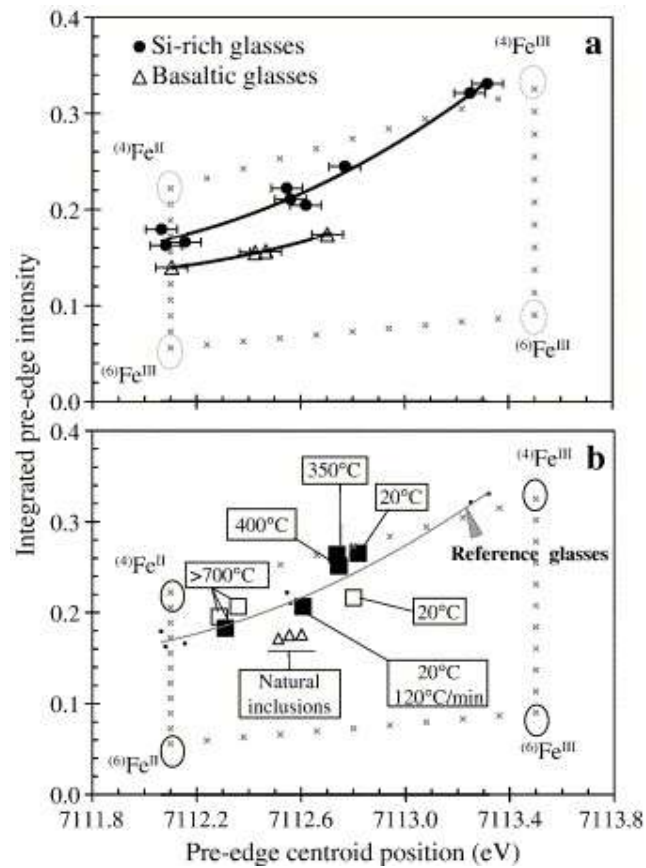

Locus of points from Wallace and Carmichael (1994)

- ◆ Douglas and Zaman (1969)
- ▲ Carroll and Rutherford (1988)
- ○ Zaman and Paul (1969)
- ■ Nagashima and Katsura (1973)
- + Clemente (1998)
- ● Katsura and Nagashima (1974)

$$\frac{nSO_4^{2-}}{nStot} = \frac{\lambda SK\alpha_{glass} - \lambda SK\alpha_{FeS}}{\lambda SK\alpha_{BaSO_4} - \lambda SK\alpha_{FeS}} = \frac{\Delta\lambda SK\alpha_{glass}}{\Delta\lambda SK\alpha_{BaSO_4}}$$
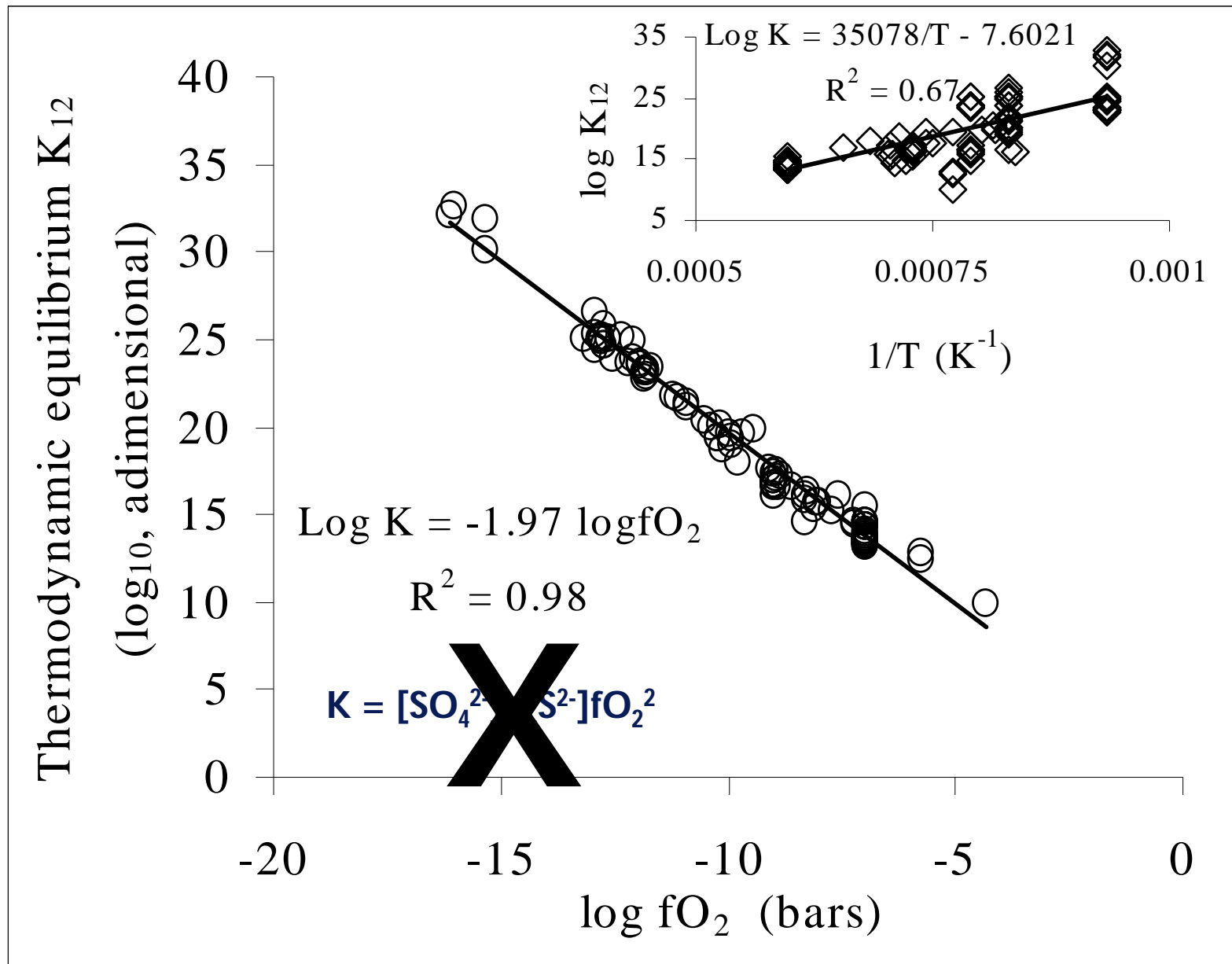
Moretti and Ottonello (2003), J. Non-Cryst. Sol.
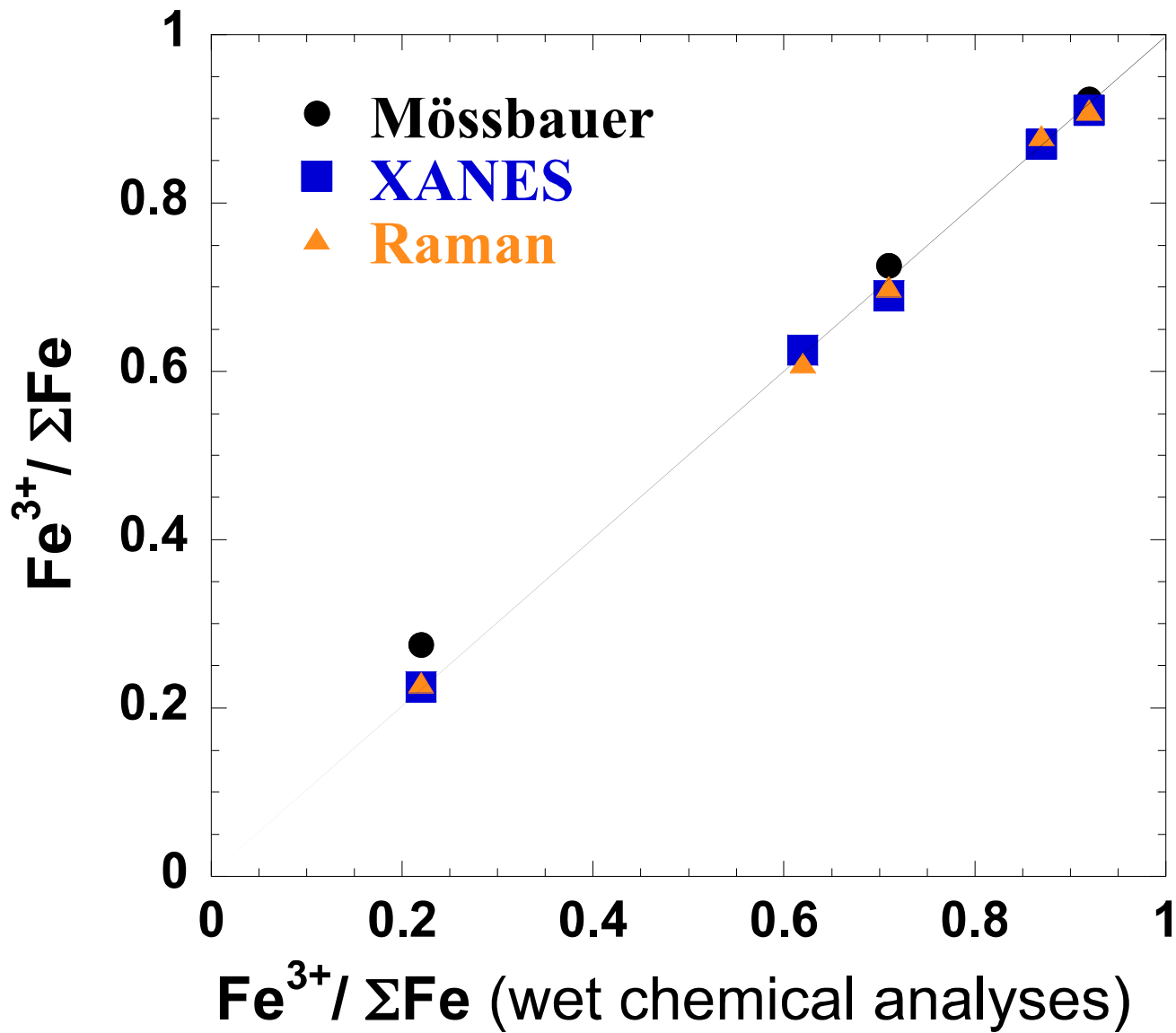
=> **Good compatibility between different techniques**

Magnien V., Neuville D.R., Cormier L., Mysen B.O. and Richet P. (2004) Kinetics of iron oxidation in silicate melts: A preliminary XANES study. Chem. Geol., 213, 253-263.
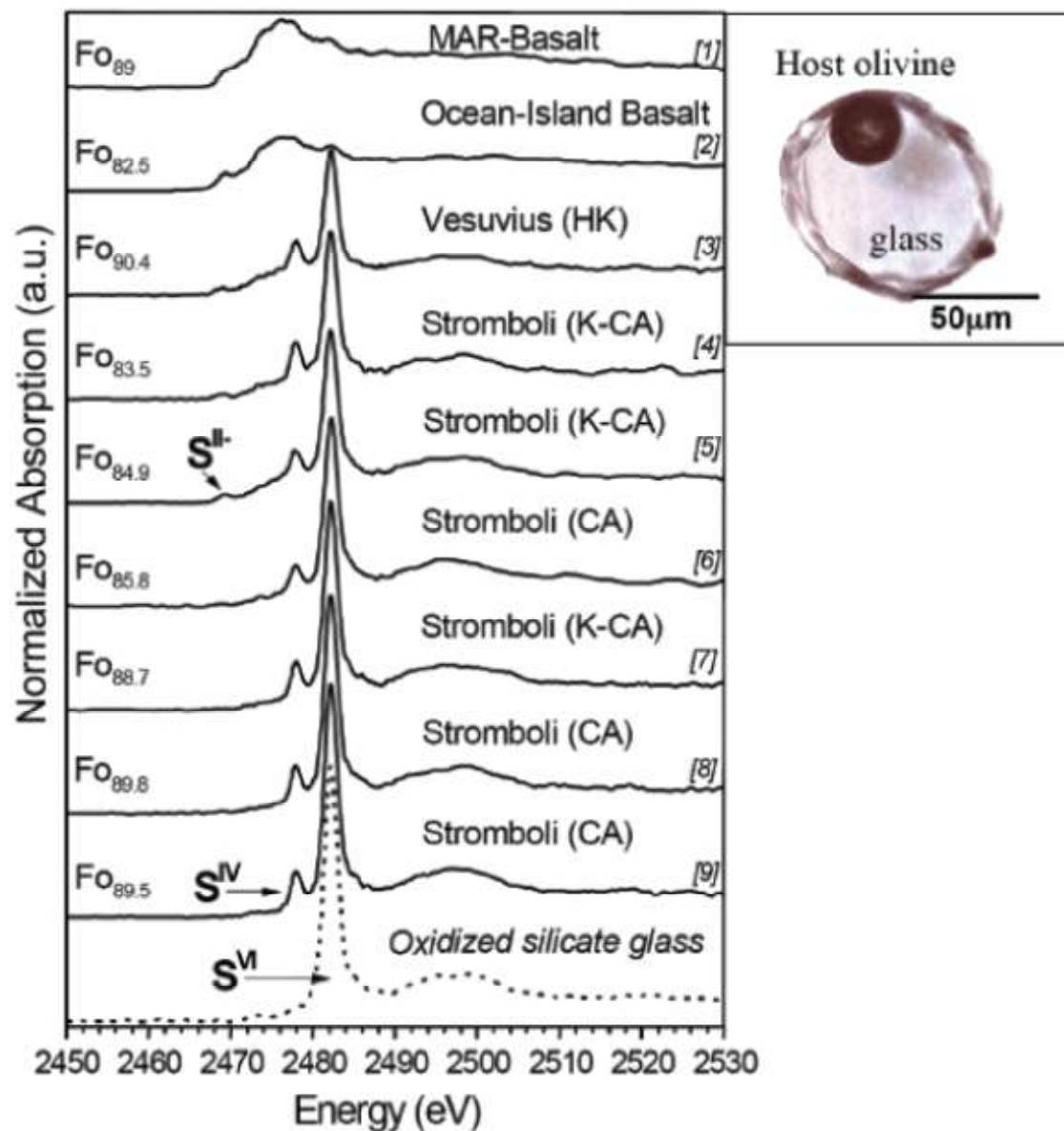
FIGURE 3 Micro–X-ray near-edge structure (XANES) spectra at the sulfur K-edge of the glass inclusions (1) to (9) and one oxidized silicate glass. Photomicrograph of an olivine-hosted glass inclusion. The silicate melt is trapped at high temperature during crystal growth and quenched as glass (From Métrich et al. 2002).

The questions…

-How do we write chemical reactions for silicate melts to account for COMPOSITIONAL dependences?

-Which 'syntax' do we use?

-Is the chemical syntax for describing chemical exchanges directly available from structural studies? Or is just an (useful) approximation of some major features?

Outer sphere ion pair

Inner sphere ion pair
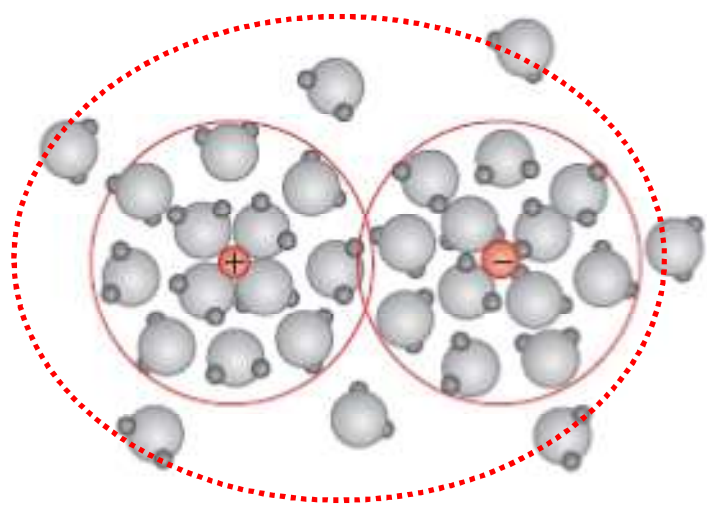
(complex)

Intact solvation shells
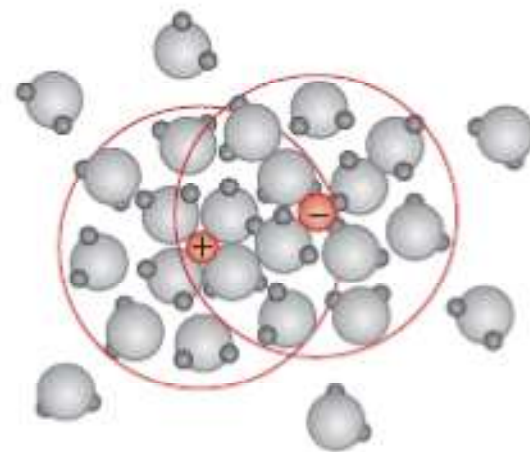
Partial disruption of
solvation shells
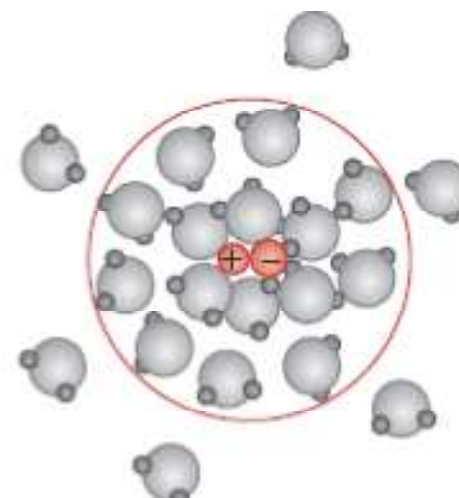
Disruption of solvation
shells

Figure 3.2 - Connectivity between oxygen coordination tetrahedra of Si with the octahedron of another cation M through nonbridging oxygens.
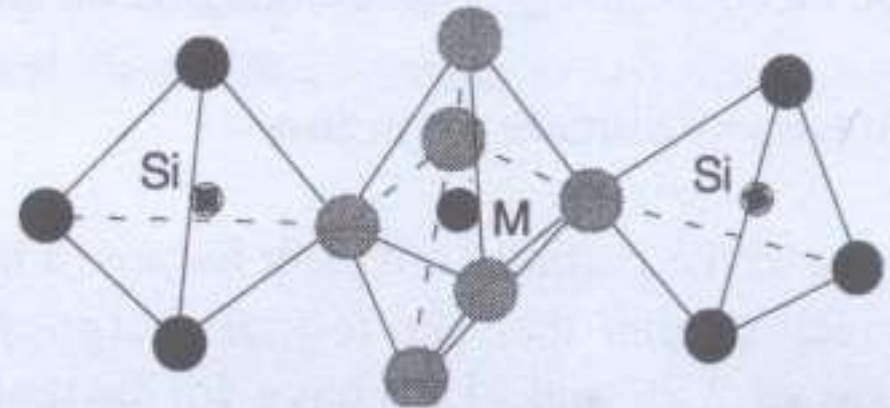
Mysen and Richet, 2005
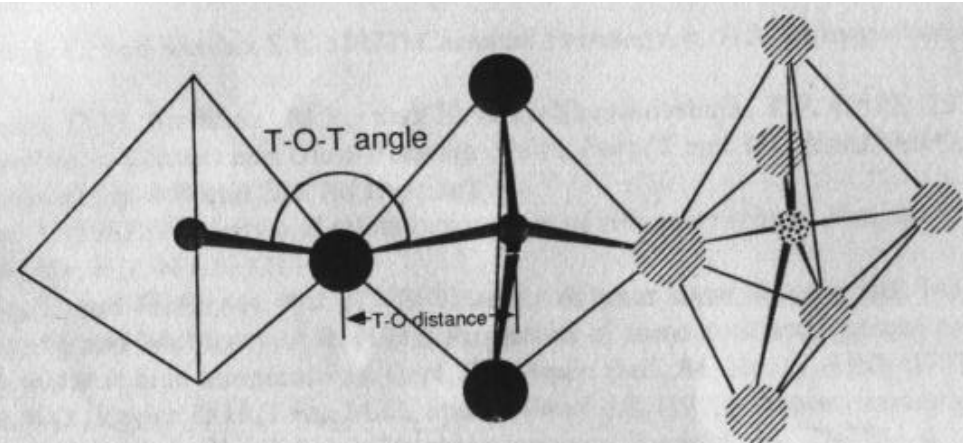
● Bridging oxygen

▨ Nonbridging oxygen

● Tetrahedral (network-forming) cation

▨ Network-modifying cation

Fig. 1. Schematic representation of the geometric relationships of bridging and nonbridging oxygen and network-forming and network-modifying cations.

TiO$_5$ TiO$_4$ SiO$_4$ Na   relatively polymerized area (Na-poor)
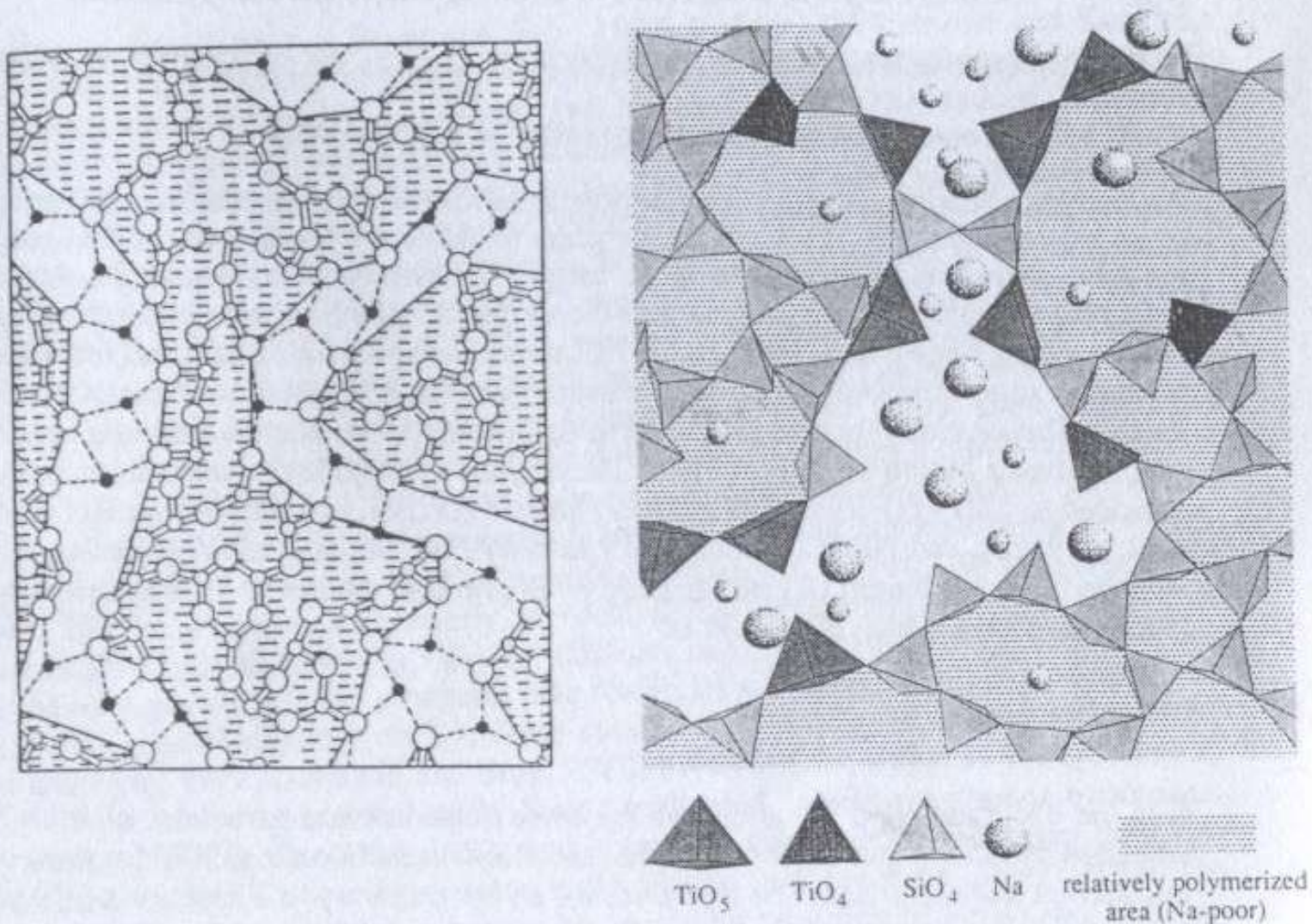
Figure 51 (left). Modified random network model for a "two-dimensional" oxide glass. Small open circles represent network-forming cations (C$_F$), small filled circles represent network-modifying cations (C$_M$), and large open circles represent oxygens (O). The boundaries are through the C$_F$-O (non-bridging) bonds and are intended to highlight percolation channels where C$_M$ cations are concentrated. (From Greaves, 1985.)

Depolymerization of Silicate Melts to accommodate volatiles (e.g. water)
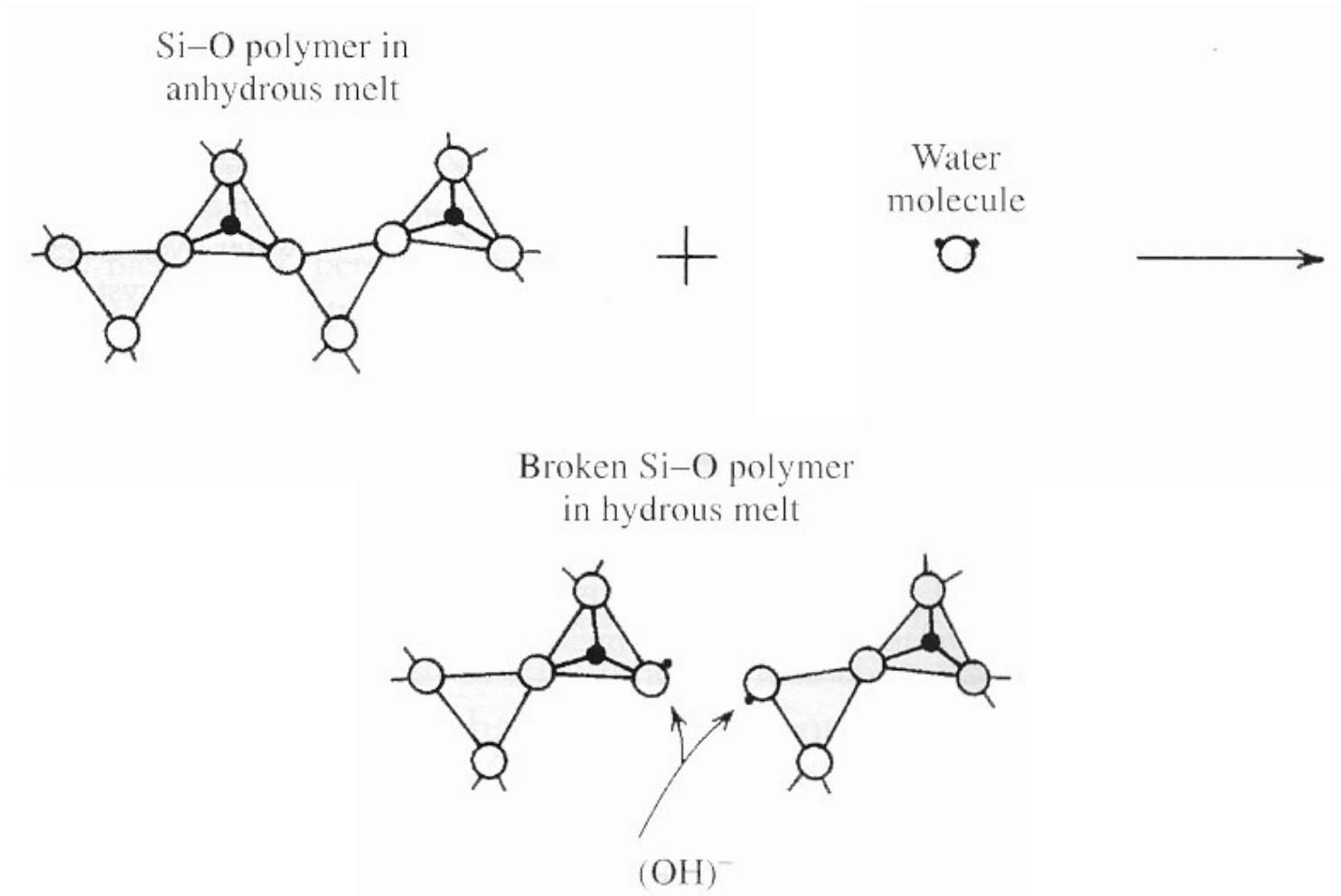
Mysen and Richet, 2005

Some observations…

We usually do not perceive the problem of the chemical syntax as long as:

-we interpret our own data and a **few** more

➔ Thus we tend to adopt the detected structural scenario and turn it into the chemical syntax

Some observations…

- But what happens if we want to find the general chemical mechanism and set models? (….the problem of many data from many compositions…)

- How "convert" structural findings into speciation hypotheses for general chemical mechanisms?

Acid-base exchanges

The dividing line between the Lewis acids and bases is not sharp a one, and its theoretical interpretation is obscure

→Strong role of the molecular structure (hence, bulk composition)
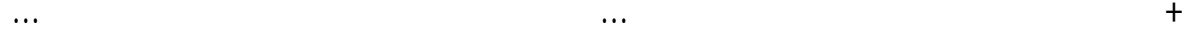
→Hard and soft categories…(atomic structures associated with hard acids and bases are rigid and impenetrable, whereas those associated with soft acids and bases are more readily deformable)

…it is not practical if we deal with chemical reactions

For example…

$$O^{2-} + SO_2 \leftrightarrow S^{2-} + ...$$

This **acid-base** and **redox** exchange synthesizes many (combined) reactions:

$SO_{2(g)} + 1/2O_{2(g)} + CaO_{(m)} \Leftrightarrow CaSO_{4(m)}$ +

$SO_{2(g)} + 1/2O_{2(g)} + H_2O_{(m)} \Leftrightarrow H_2SO_{4(m)}$ +

$SO_{2(g)} + 1/2O2(g) + 1/2SiO_{2(m)} \Leftrightarrow 1/2Si(SO_4)_{2(m)}$ +

...   ...   +

...   ...   +

...   .
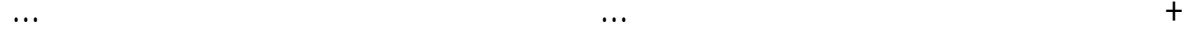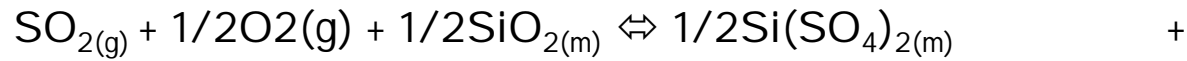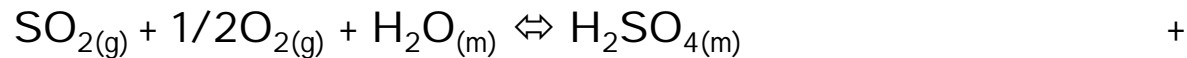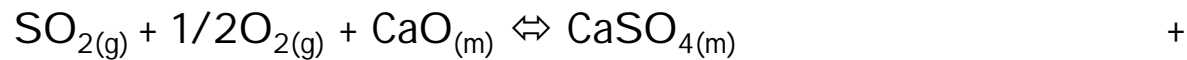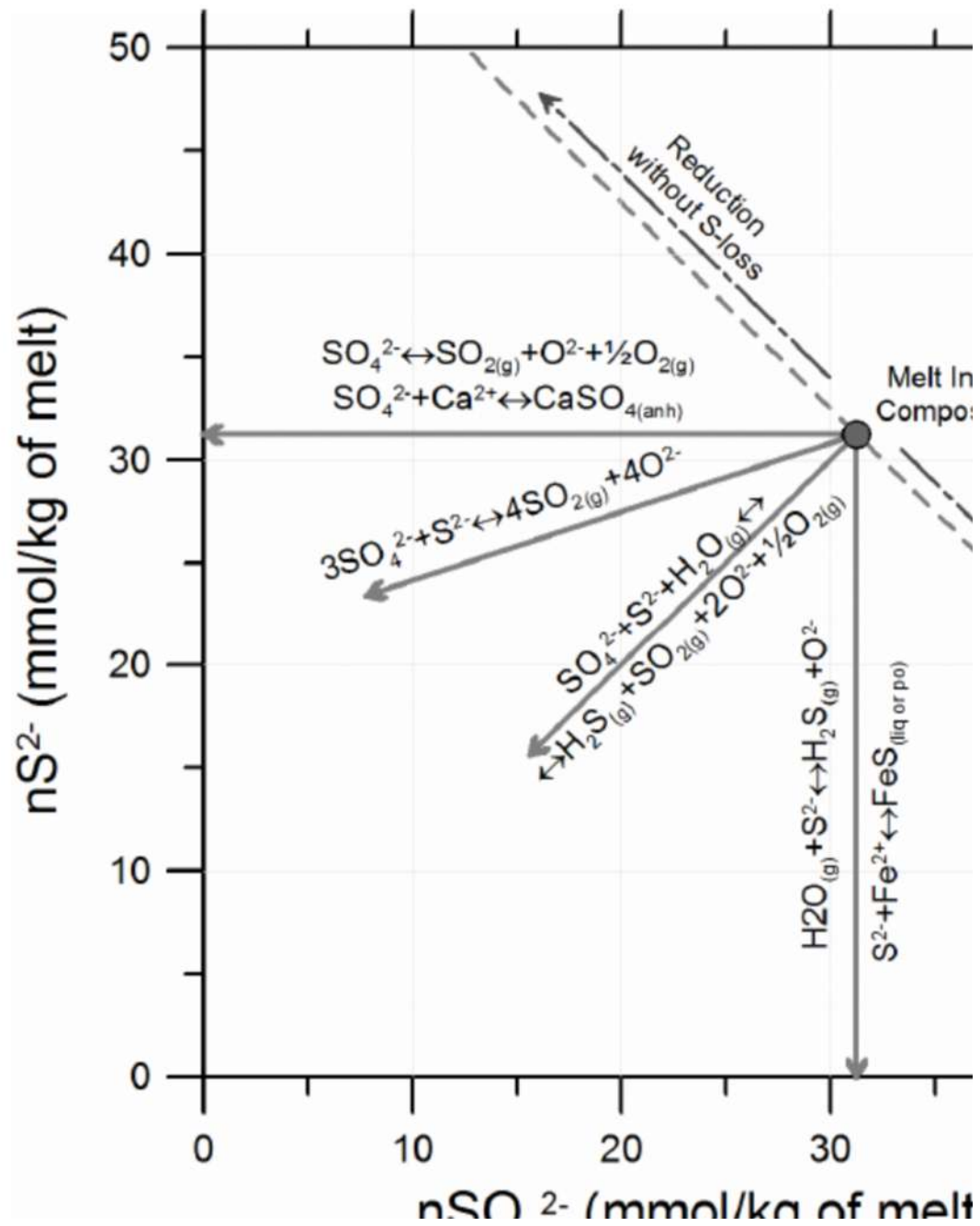
So we need ions…

- "The formation of ions sensu stricto in liquid water is due to the high dielectric constant of aqueous medium (efficient shielding of charge) as also manifested by the formation of hydration spheres.

- In contrast, none of these concepts is applicable to silicate melts. The dielectric properties are different, no volumetric electrostriction is known, electrostatic bond valences are generally greater to allow for such effects.

- The only and apparent similarity arises from adoption of analogous symbolic notation for melt species that uses negative charge, therefore, the thermodynamic identities look like ions"

So, we need ions to write chemical reactions…but…

- the connectivity of the silicate structure is such that cations and anions have actual charges lower than formal ones, and the residual charge distribution from bonding of bridging oxygen to silicon allows oxygen bonding with other cations.

- This makes the relative contribution of nonbridging and bridging oxygens to the oxygen coordination of the other cations poorly known (Mysen and Richet, 2005) and highlights the impossibility to readily distinguish solute and solvent like in aqueous solutions.

- The anionic framework of silicate melts, in fact, makes solute and solvents so intimately related that one cannot identify a solvation shell and identify directly, from structural studies, the complexes needed to define acid-base reactions.

$$2O^- \Leftrightarrow O^0 + O^{2-} \quad \text{Vs.} \quad 2Q^n \Leftrightarrow Q^{n-1} + Q^{n+1}$$

(Polymerization   Vs.   Connectivity)

Nevertheless…

…to understand what determines acid-base behavior and to write and inspect chemical reactions *we have to assume* an understanding of the bonding, structure, and properties of individual molecules also in melts (with its pros and cons…)

How deep need we to go with connections between structure and chemical thermodynamics ?

The "thermochemical knowledge" of a melt system does not seem to require the microstructural "complexity" that can be revealed by many spectroscopic investigations: the structural "characterization" exceeding that required for the **description of acid-base properties (e.g, in the Lux-Flood notation)** may be not useful.

Which acid-base 'syntax' to describe reactivity in melts?

In (essentially aprotic) silicate melts acid-base properties are expressed in terms of Lux-Flood formalism:

$$Acid + O^{2-} \Leftrightarrow Base \qquad (1)$$

"Reaction" 1 recalls the Bronsted-Lowry formalism for aqueous solutions:

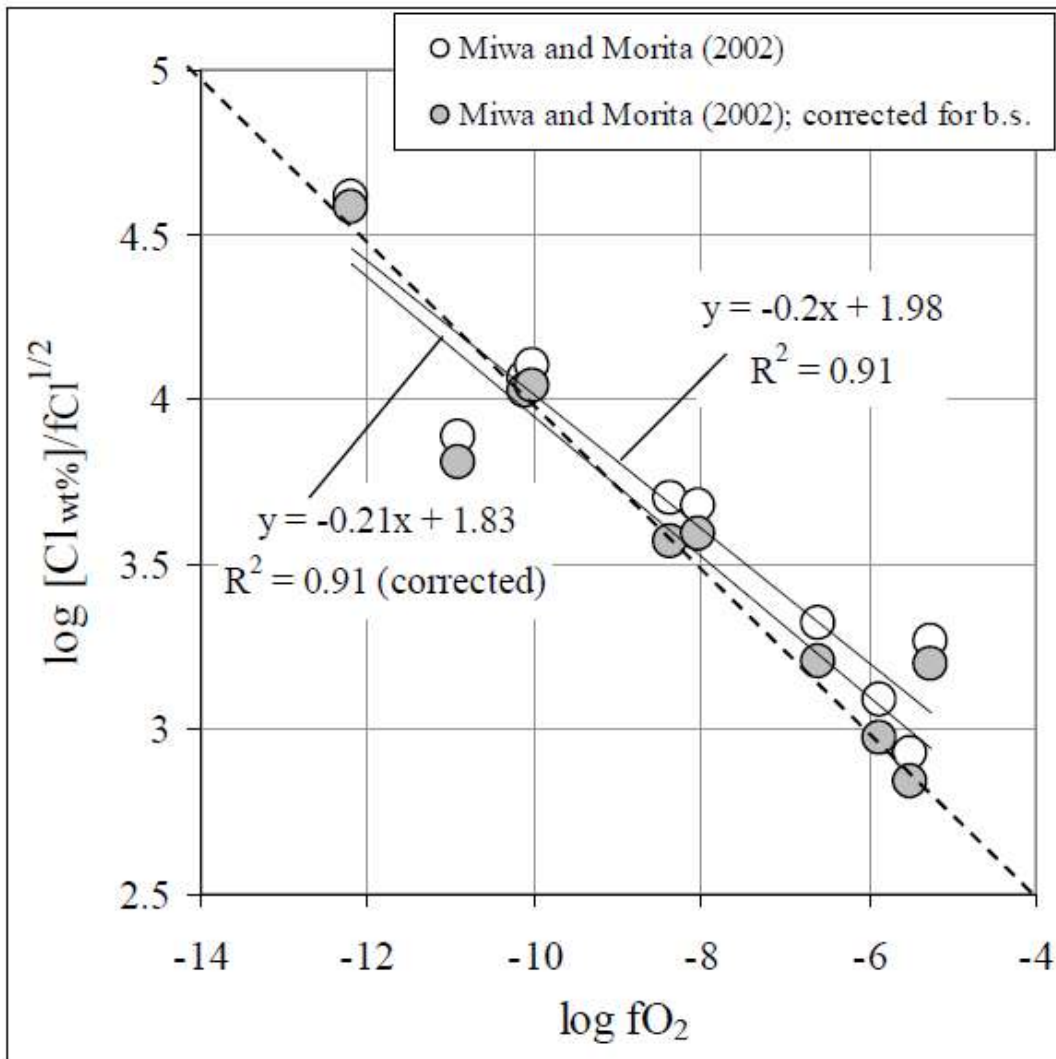$$Acid \Leftrightarrow Base + H^+ \qquad (2)$$

Which redox 'syntax' to describe reactivity in melts?

In aqueous solutions the electrode of reference is the "normal hydrogen electrode", whereas in silicate melts the reference electrode is the "normal oxygen electrode" ,i.e.:

$$1/2O_2 + 2e^- \Leftrightarrow O^{2-} \qquad (3)$$

Even if the main redox couple in oxide melts is given by iron, reaction (3) follows the syntax based on the O^{2-} exchange

$$C_{Cl^-} = [Cl_{wt\%}]PO_2^{1/4}/PCl_2^{1/2}$$

$$\tfrac{1}{2}O^{2-} + \tfrac{1}{2}Cl_{2,gas} \Leftrightarrow Cl^- + \tfrac{1}{4}O_{2,gas}$$

$$\tfrac{1}{2}Cl_2 + \tfrac{1}{2}Me^{v+}_{2/v}O \Leftrightarrow \tfrac{1}{4}O_2 + Me^{v+}_{1/v}Cl$$

$$\tfrac{1}{2}Cl_2 + e^- \Leftrightarrow Cl^- \qquad \text{[Chlorine electrode]}$$

$$\tfrac{1}{4}O_2 + e^- \Leftrightarrow O^{2-} \qquad \text{[Oxygen electrode]}$$

O^{2-} ?   Virtual or real ?

Bridging, non-bridging and free (O^{2-}) oxygen in Na_2O-SiO_2 glasses: An X-ray Photoelectron Spectroscopic (XPS) and Nuclear Magnetic Resonance (NMR) study

H.W. Nesbitt [a,*], G.M. Bancroft [b], G.S. Henderson [c], R. Ho [a], K.N. Dalby [a], Y. Huang [b], Z. Yan [b]

As has been proposed for $CaSiO_3$ glass and for sodic and potassic glasses containing La, we suggest that O^{2-} is present in sodic glasses at small concentrations. The O^{2-} content correlates with increased soda content and may be associated with, and instrumental in development of, three dimensional percolation channels in the glasses.
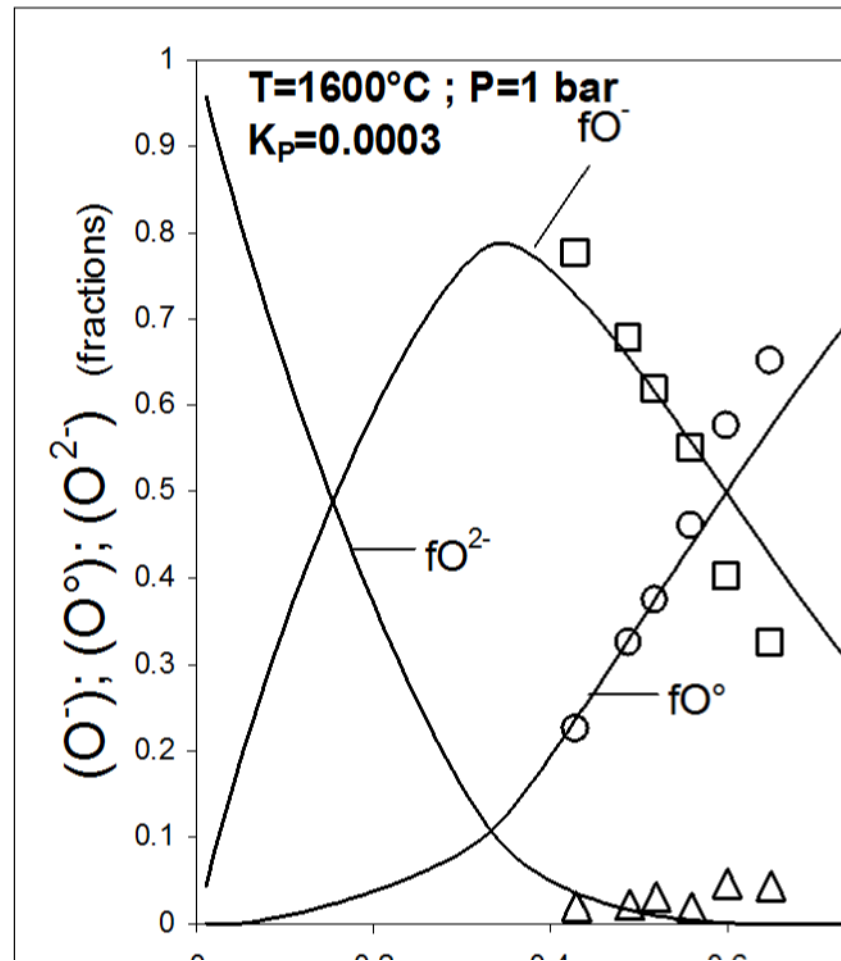
Calculated from data in Park and Rhee (2001)

5.3.1. Calculation of O-species distribution

The distribution of BO, NBO and O^{2-} in melts may be portrayed according to the reaction:

$$O^{\circ} + O^{2-} => 2O^{-} \tag{2a}$$

where O° represents BO, O^{2-} represents "free" oxygen and O^{-} represents NBO. The equivalent reaction employing neutral entities is:

$$SiO_2 + 2Na_2O => Na_4SiO_4. \tag{2b}$$

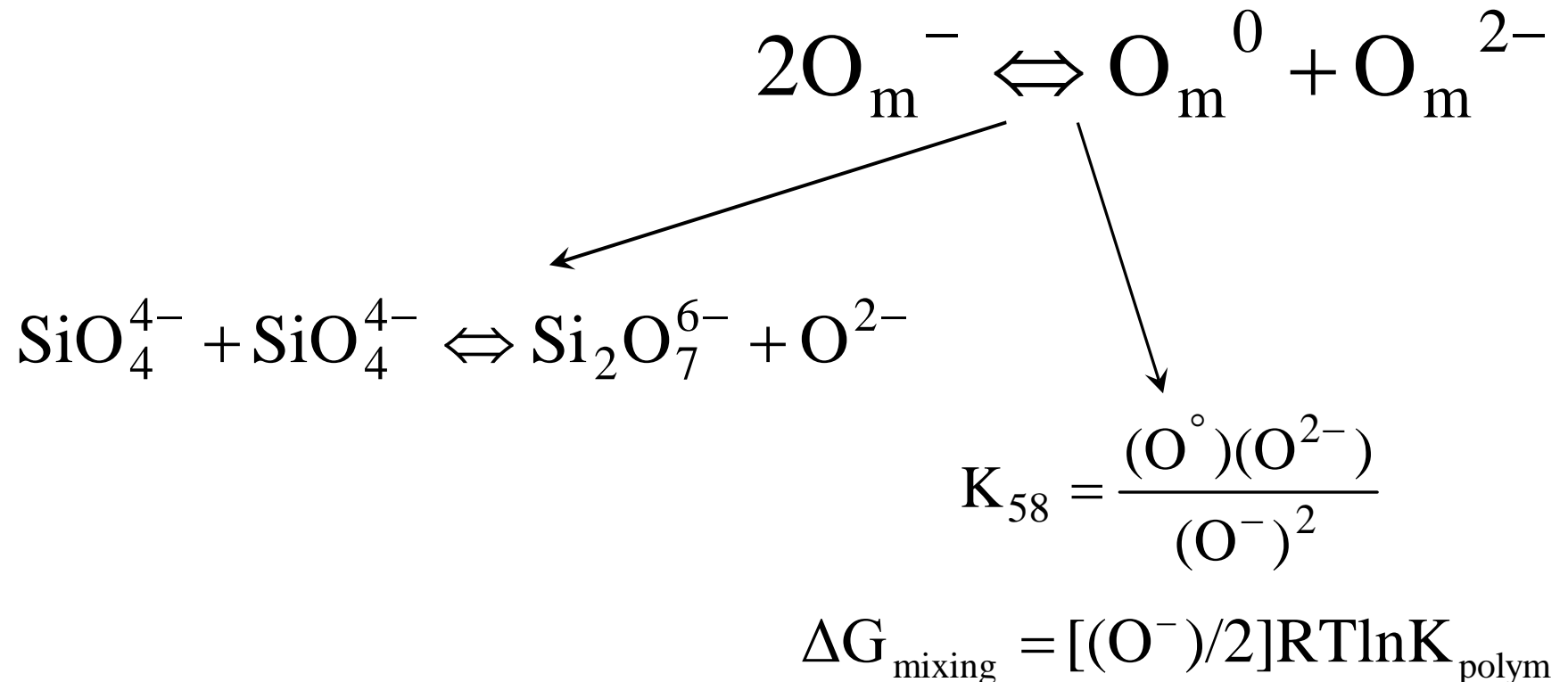The mass action equation associated with reaction (2a) is:

$$K_3 = (O_{NBO})^2 / [(O_{BO})(O_{MO})] \tag{3}$$

Nesbitt et al. (2011)

➔ **Free**-oxygen = oxide ion...**attached** to some metal cation

Polymeric nature of anion matrix: Toop-Samis and Masson models

In polymeric models for silicate melts, it is postulated that, <u>at each composition, for given P-T values, the melt is characterized by an equilibrium distribution of several ionic species of oxygen, metal cations and ionic polymers of monomeric units SiO_4^{4-}</u>.

$$2O_m^- \Leftrightarrow O_m^{\,0} + O_m^{\,2-}$$

$$SiO_4^{4-} + SiO_4^{4-} \Leftrightarrow Si_2O_7^{6-} + O^{2-}$$

$$K_{58} = \frac{(O^\circ)(O^{2-})}{(O^-)^2}$$

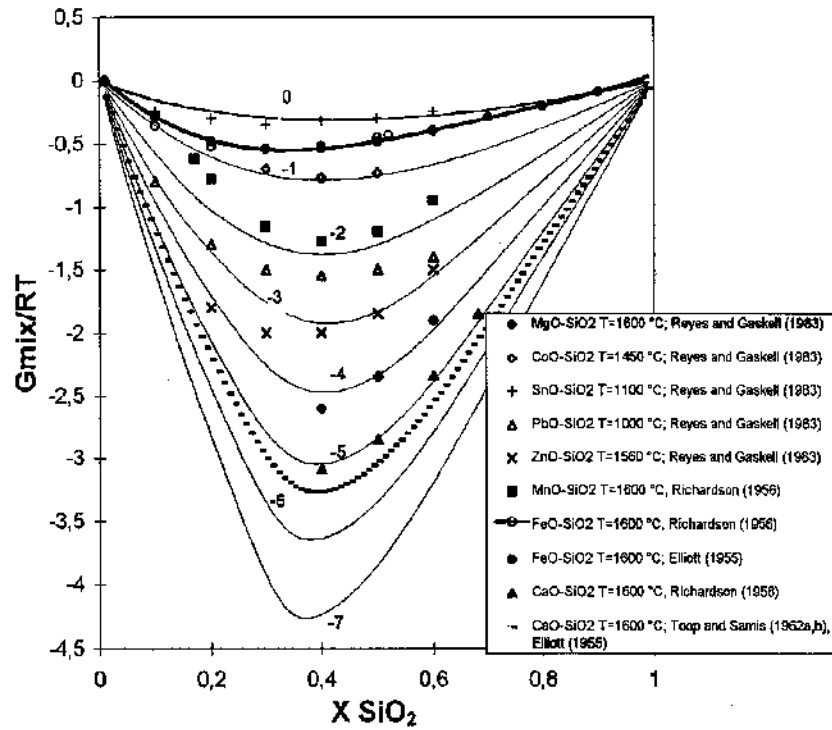$$\Delta G_{mixing} = [(O^-)/2]RTlnK_{polym}$$

Theory: the polymeric model

On the basis of simple mass balances we can link the three oxygen species to the melt composition and therefore to the melt compositions

$$\left(O^0\right) = \frac{4N_{SiO_2} - \left(O^-\right)}{2}$$

$$\left(O^{2-}\right) = \left(1 - N_{SiO_2}\right) - \frac{\left(O^-\right)}{2}$$

$$\left(O^-\right)^2\left(4K_2 - 1\right) + \left(O^-\right)\left(2 + 2N_{SiO_2}\right) + 8N_{SiO_2}\left(N_{SiO_2} - 1\right) = 0$$

Kp=(O°)(O²⁻)/(O⁻)²

Modifiers - Formers

$$\Delta G^{mixing} = \frac{(O^-)}{2} RT \ln K_{polym}$$

$$K_{polym} = \exp\left[4.662 \times \left(\sum_i X_{M_i^{v+}} \gamma_{M_i^{v+}} - \sum_j X_{T_j^{\eta+}} \gamma_{T_j^{\eta+}} \right) - 1.1445 \right]$$

Ottonello et al., Chem. Geol. (2001)

Even simple interaction parameters along limiting binaries cannot be reduced to fitting coefficients of mathematical minimization routines, but must be formally linked to the intrinsic atomistic properties of the interacting ions and molecules

In a chemically complex melt or glass the ability to transfer fractional electronic charges from the ligands to the central cation depends in a complex fashion on the melt or glass structure, which affects the polarization state of the ligand itself. Nevertheless, the mean polarization state of the various ligands (mainly oxide ions O^- and O^{2-} in natural silicate melts) and their ability to transfer fractional electronic charges to the central cation are conveniently represented by the "*optical basicity*" of the medium, i.e. ratio h/h^*, where h is Jørgensen's (1962) function of the ligand in the polarization state of interest, and h^* is the same function relative to the ligand in an unpolarized state (mainly free O^{2-} ions in an oxidic medium; Duffy and Ingram, 1971):

$$\Lambda = \frac{h}{h^*} = \frac{1-\beta}{1-\beta^*} = \frac{v_{free} - v_{glass}}{v_{free} - v^*}$$

with $v_{free} = {}^1S_0 \rightarrow {}^3P_1$ absorption band of the free p-block cation;
$v_{glass} = {}^1S_0 \rightarrow {}^3P_1$ absorption band measured in the glass;
$v^* = {}^1S_0 \rightarrow {}^3P_1$ absorption band in a free O^{2-} medium.

The reciprocal of optical basicity Λ of a cation (i.e. "*basicity moderating parameter*" γ of Duffy and Ingram, 1973) represents the tendency of an oxide forming metal M to reduce the localized donor properties of oxide ions, and is related to the optical basicity of the medium by:

$$\gamma_M = \frac{Z_M \times r_M}{|Z_O| \times \Lambda_{MO}}$$

where Z_M = formal oxidation number of cation in MO

Z_O = formal oxidation number of oxide ion in MO

r_M = stoichiometric ratio between number of cations and number of total oxide ions in the medium.

Table I. Optical basicity Λ and basicity moderating parameter of the central cation γ according to various sources. Pauling's and Sanderson's electronegativities (Pauling, 1932, 1960; Sanderson, 1967) are also listed. Λ, γ, χ_S: adimensional; χ_P: eV (from Ottonello et al., 2001).

Oxide	Λ						γ		χ_P	χ_S
	(1)	(2)	(3)	(4)	(5)	(6)	(6)	(7)		
H_2O			0.40			0.39	2.56	2.50	2.15	3.55
Li_2O						1.00	1.00		1.0	0.74
B_2O_3			0.42			0.42	2.38		2.0	2.84
Na_2O		1.15	1.15	1.15	1.15	1.15	0.87	0.87	0.9	0.70
MgO	0.78	0.78	0.78	0.78	0.78	0.78	1.28	1.28	1.2	1.99
Al_2O_3	0.60	0.60	0.60	0.61	0.59	0.59	1.69	1.67	1.5	2.25
SiO_2	0.48	0.46	0.48	0.48	0.48	0.48	2.09	2.09	1.8	2.62
TiO_2		0.65		0.61	0.61	0.58	1.72	1.54	1.6	1.60
Cr_2O_3	0.70					0.58	1.72		1.6	1.88
MnO	0.94-1.03	0.98		0.90	0.59	0.59	1.69	1.69	1.5	2.07
FeO	0.86-1.08	1.03	1.00	1.03	0.51	0.48	2.09	1.354	1.8	2.10
Fe_2O_3	0.73-0.81	0.77		1.21	0.48	0.48	2.09	2.09	1.8	2.10
CoO						0.51	1.96	1.96	1.7	2.10
NiO						0.48	2.09	2.09	1.8	2.10
Cu_2O						0.43	2.30	2.30	1.9	2.60
ZnO		0.82-0.98				0.58	1.72	1.72	1.6	2.84
SrO	1.10					1.03	0.97		1.0	1.00
SnO						0.48	2.09	2.09	1.8	3.10
BaO	1.15	1.15		1.15	1.15	1.12	0.89		0.9	0.78
PbO						0.48	2.09	2.09	1.8	3.08

depolymerizing role of water has been overrated with respect to its actual acid-based properties in melts.

(1) Duffy (1992); (2) Young et al. (1992); (3) Duffy and Ingram (1974a,b); (4) Sosinsky and Sommerville (1986); (5) Gaskell (1982); (6) Ottonello et al. (2001); eq. (4.19) (note that Λ ≈ γ⁻¹); (7) Ottonello et al. (2001); obtained by non linear minimization of FeO thermo-dynamic activity data in multicomponent melts.
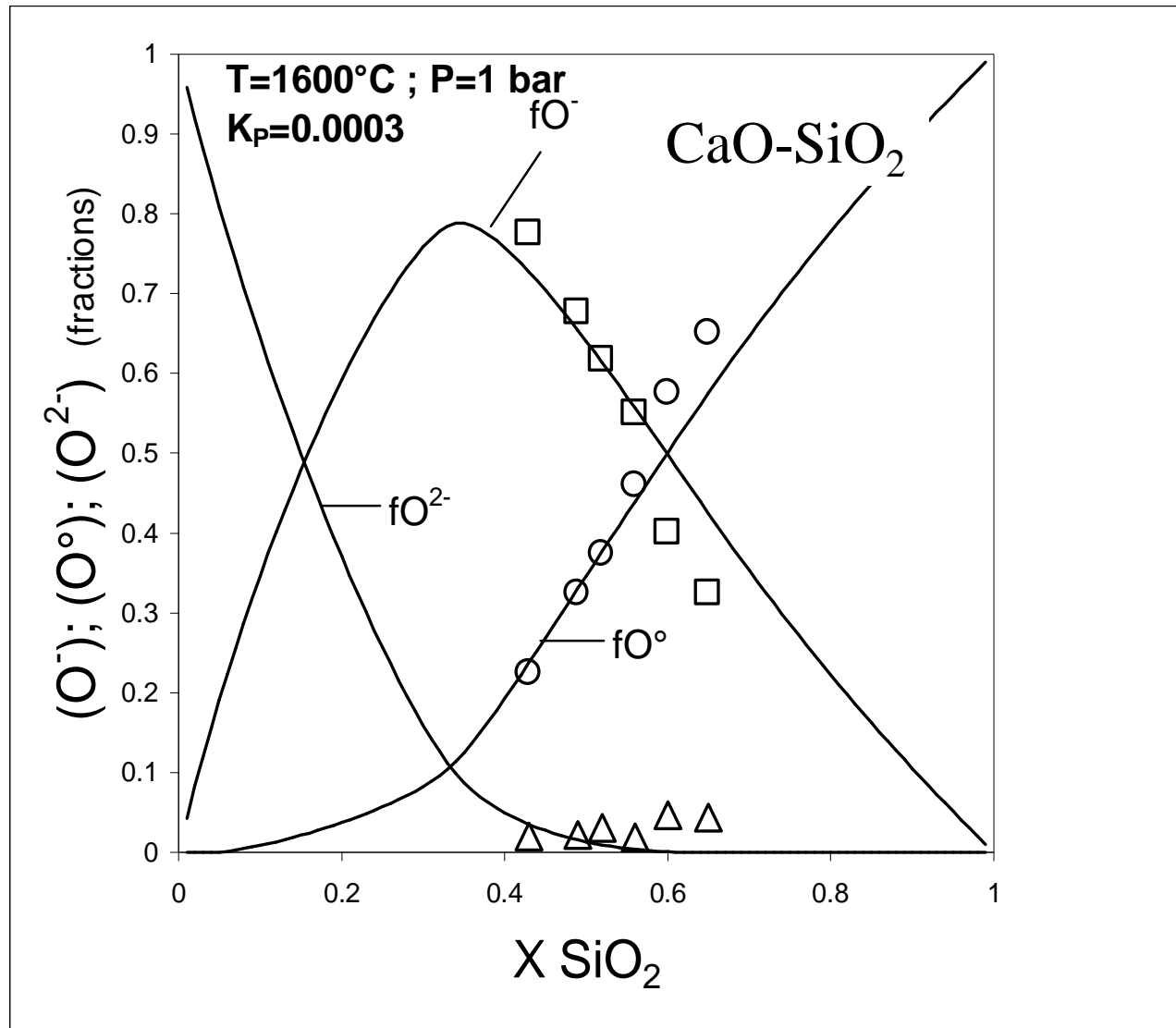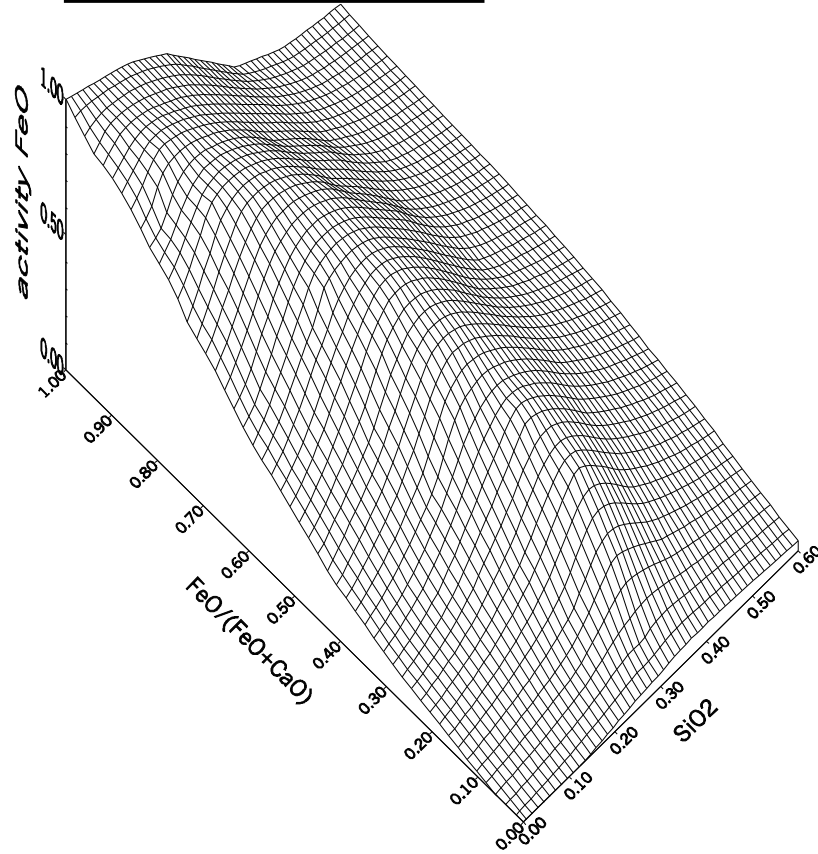
Ottonello and Moretti (2004) J. Phys. Chem. Solids
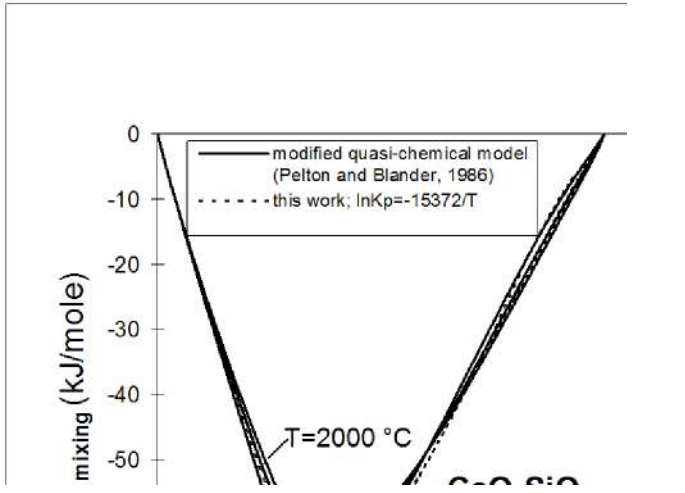
Ottonello et al., 2001
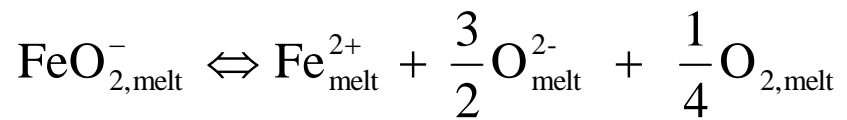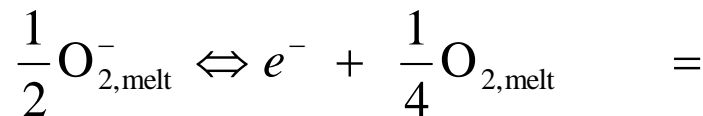
Hybrid Polymeric Model

T = 1600°C

activity FeO

FeO/(FeO+CaO)

SiO2

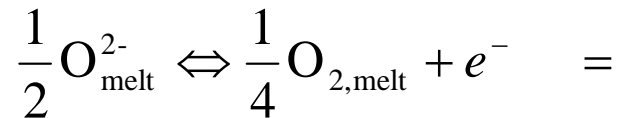$$\Delta G_{mixing} = \Delta G_{chemical} + \Delta G_{strain} = \frac{\left(O^-\right)}{2} RT \ln K_{18} + \frac{3RT}{2\overline{v}_{Si}}\left(\frac{x}{a}\right)^2 \qquad \Delta G_{mixing} = \frac{\left(O^-\right)}{2}\left(\Delta H_{18} - T\Delta S_{18} - T\eta\right)$$

Back to basics: amphoteric behavior of trivalent iron

$$FeO + 1/4O_2 \Leftrightarrow FeO_{1.5}$$

In the above reaction the redox potential is expressed by the oxygen fugacity . But how does the electron transfer take place?

(From the Fraser's approach to Europium)

$Fe^{3+}_{melt} + e^- \Leftrightarrow Fe^{2+}_{melt}$ +

$\frac{1}{2}O^{2-}_{melt} \Leftrightarrow \frac{1}{4}O_{2,melt} + e^-$ =

$\frac{}{}$

$Fe^{3+}_{melt} + \frac{1}{2}O^{2-}_{melt} \Leftrightarrow Fe^{2+}_{melt} + \frac{1}{4}O_{2,melt}$

$FeO^-_{2,melt} + e^- \Leftrightarrow Fe^{2+}_{melt} + 2O^{2-}_{melt}$ +

$\frac{1}{2}O^-_{2,melt} \Leftrightarrow e^- + \frac{1}{4}O_{2,melt}$ =

$\frac{}{}$

$FeO^-_{2,melt} \Leftrightarrow Fe^{2+}_{melt} + \frac{3}{2}O^{2-}_{melt} + \frac{1}{4}O_{2,melt}$
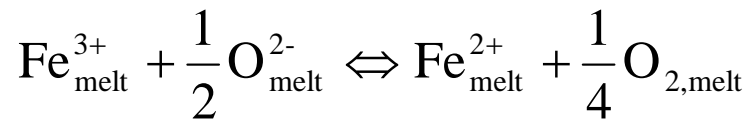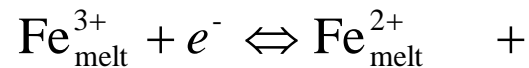
That's the way electron transfer operates. It is not evident from the equilibrium involving macroscopic components: to get that you must adopt the ionic notation.

Iron redox model

The message:

1. **Silicate melts are polymerized liquids**

2. **Polymeric units are highly reactive**

Polymerization and redox state are intimately interrelated. This melt affects properties, including oxidation state, volatile solubility *et cetera.*

$$\left(\frac{Fe^{II}}{Fe^{III}}\right) = \frac{n_{Fe^{II}}}{n_{Fe^{III}}} = \frac{[Fe^{2+}]\sum cations}{[FeO_2^-]\sum anions + [Fe^{3+}]\sum cations}$$

$$\left(\frac{Fe^{II}}{Fe^{III}}\right) = \frac{1}{K_1 f_{O_2}^{1/4}} \times \frac{a_{O^{2-}}^{1/2} K_4 \sum cations}{K_2^{1/2} a_{O^{2-}}^2 \sum anions + K_3^{1/2} \sum cations}$$

Ratio of activities   *Ratio of activity coefficients*
$(a_{FeO}/a_{FeO1.5})$ $(g_{FeO1.5}/g_{FeO})$

Fig. 4.10: Thermodybamic activity of stoichiometric ferrous oxide FeO in equilibrium with pure iron metal at T=1600K and various aO₂
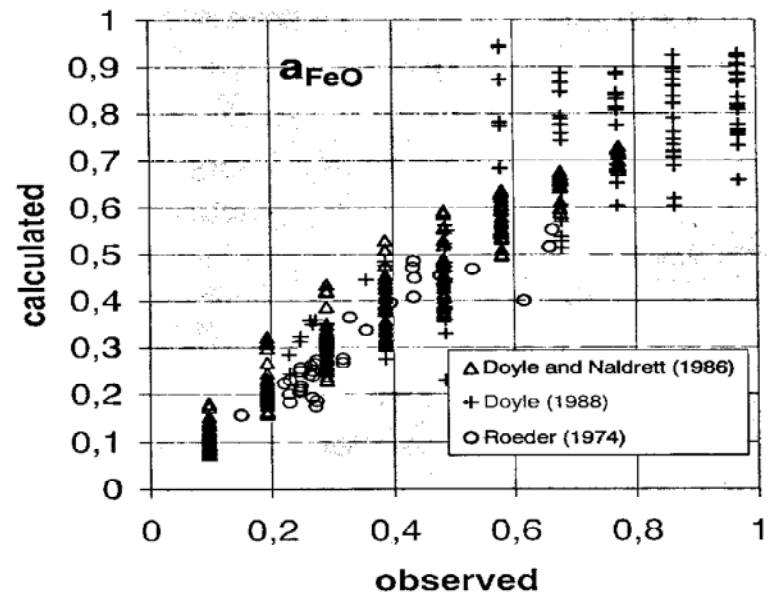
Fig. 4.12: Computed versus measured activity of ferrous oxide components in melts equilibrated with metallic iron at various T anf fO2 conditions and 1 bar pressure
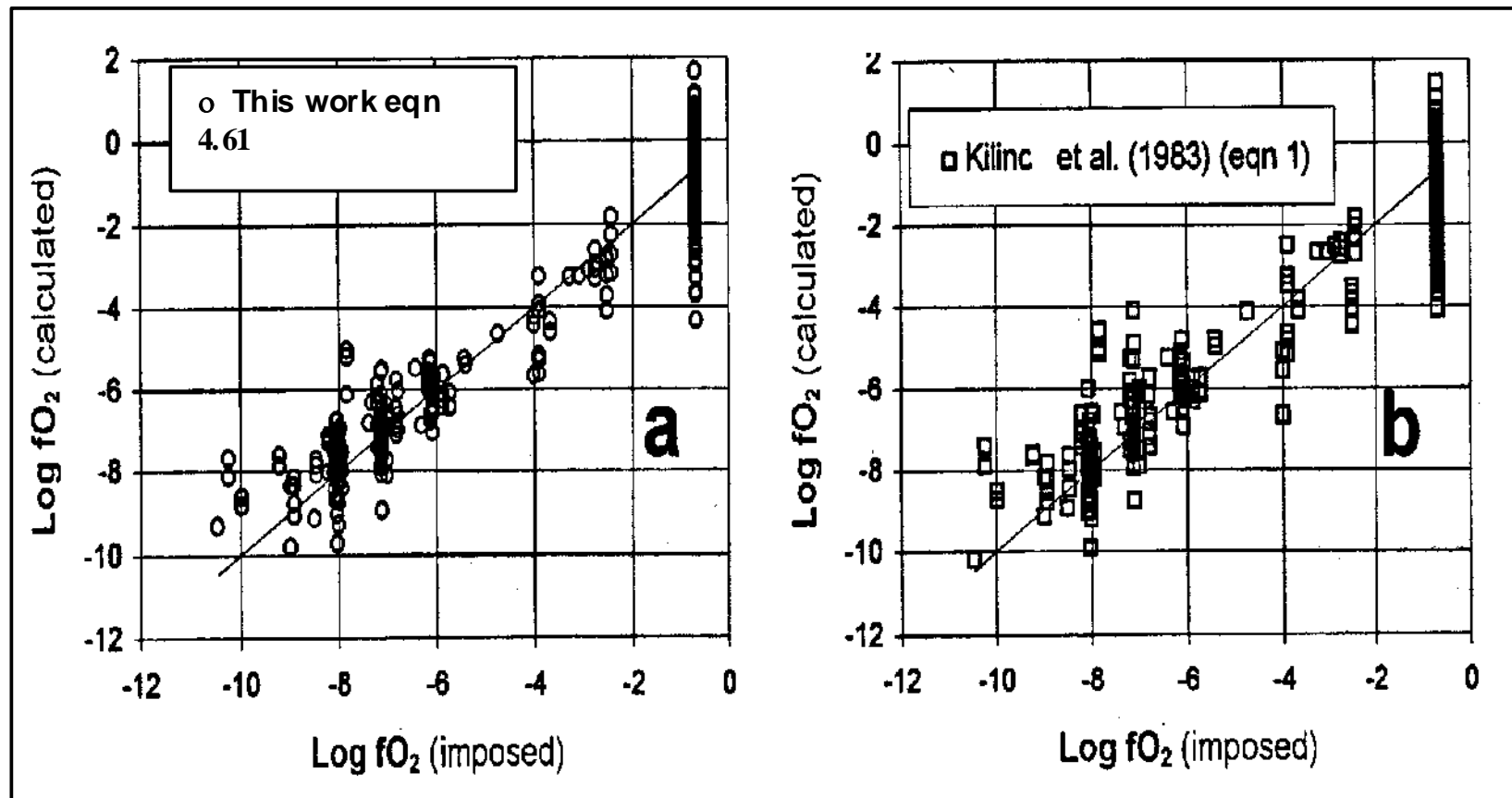
Fig. 4.14: fO2 estimates based on thermochemical model (eqn. 4.61) (4.13) and those based on Sack equation 4.86 (b). The dataset is the same used for model calibration, in both cases
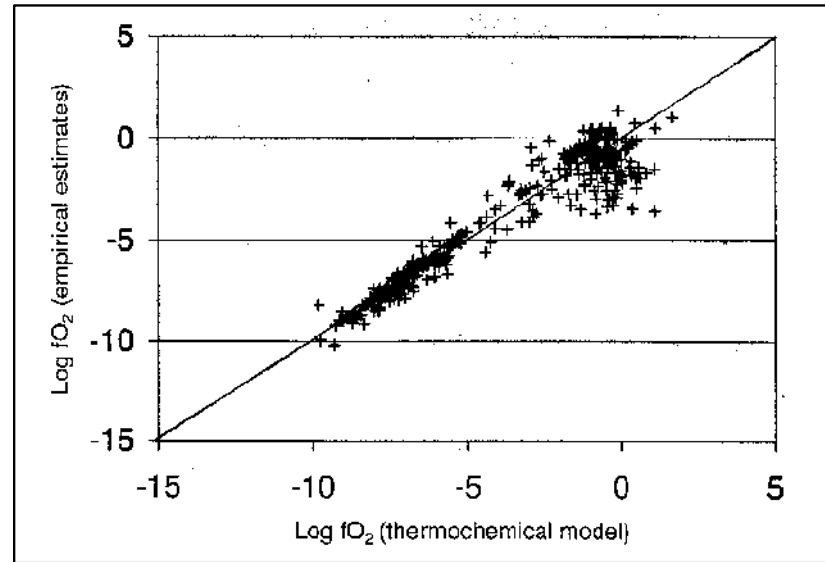
Fig. 4.15: Comparison between fO_2 estimates based on thermochemical model and estimates of the Kilinc equation. Dataset is the same adopted in constraining iron equilibria in molten systems.
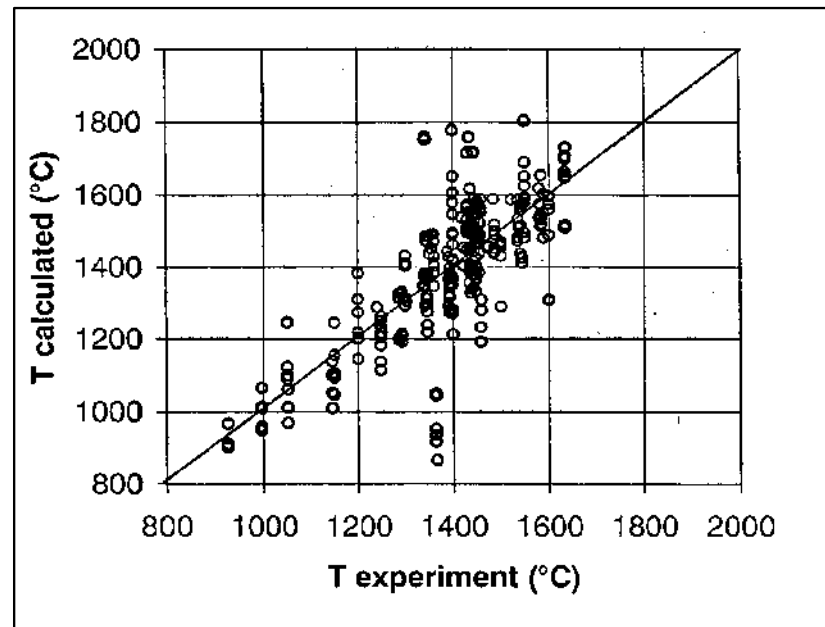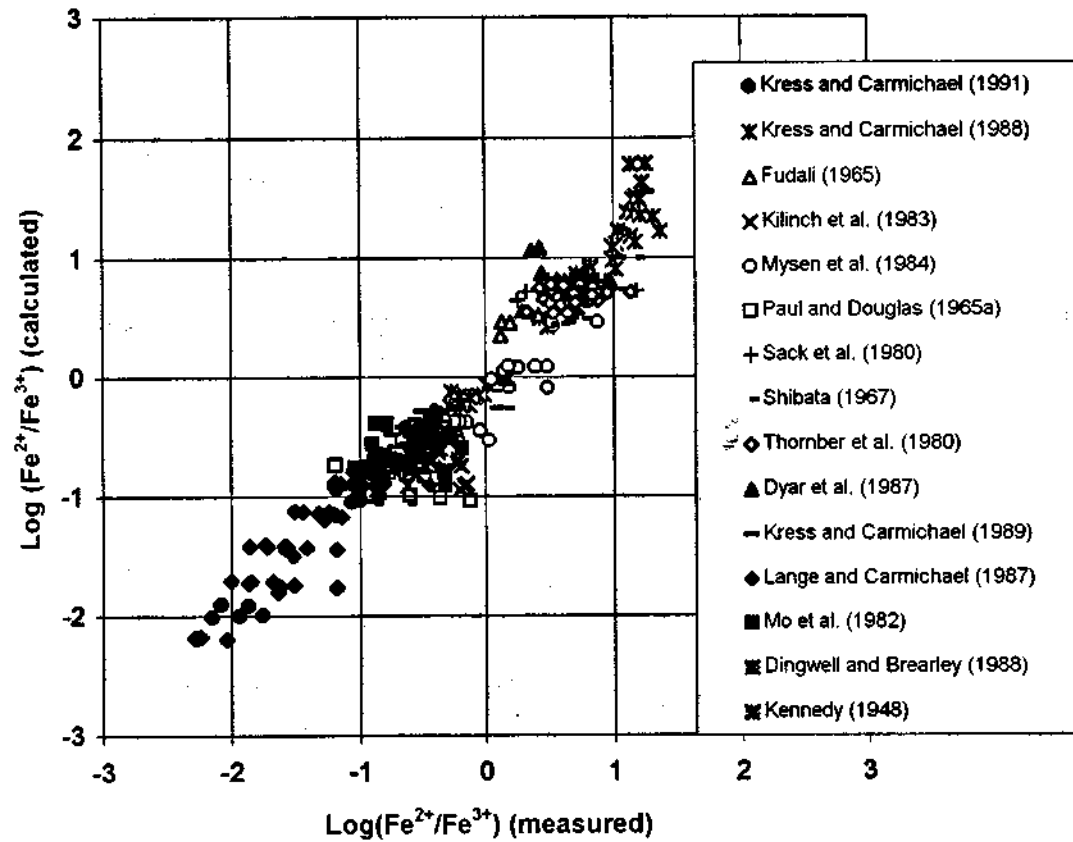
Fig. 4.13: Iron redox ratio in quenched melts and glasses equilibrated with a fO2 buffered atmosphere at various T conditions.
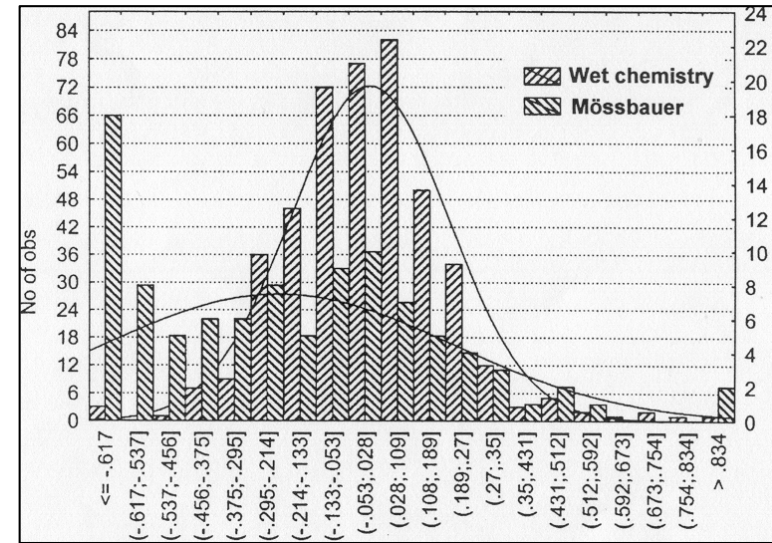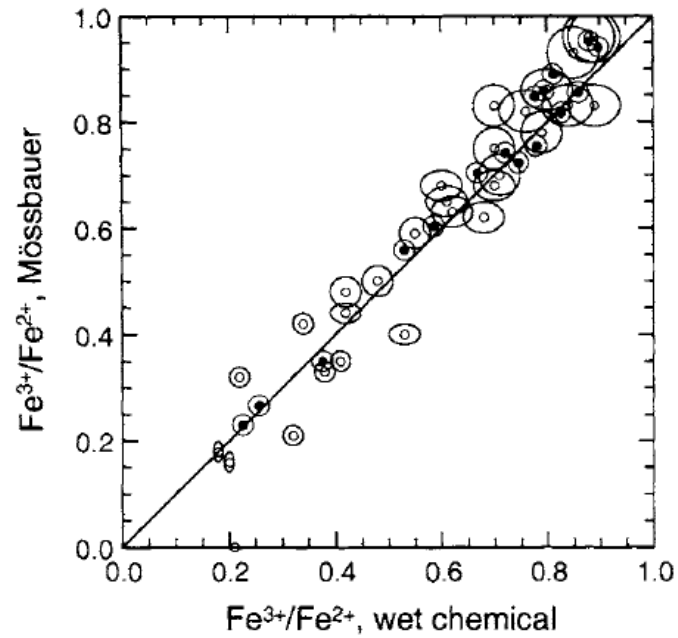
Fig. 4.19: Statistics of residuals for the Mossbauer and wet chemistry data subsets. The distribution of residuals for wet chemistry subset (444 samples) is normal, centered on x = 0.0003. The distribution of residuals for the Mossbauer
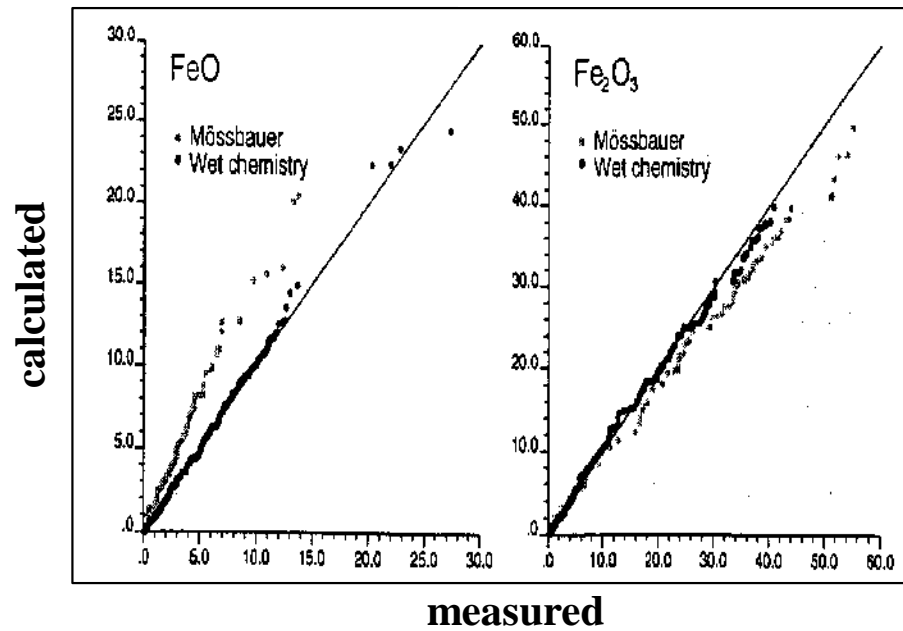
Fig. 4.20: Quantile-quantile representation of the observed Vs calculated FeO and Fe2O3 wt% amounts in the two subsets.

Let us introduce the underlined amphoteric behavior of water, i.e. an acidic dissociation:

$$H_2O + O^{2-} \Leftrightarrow 2OH^-$$
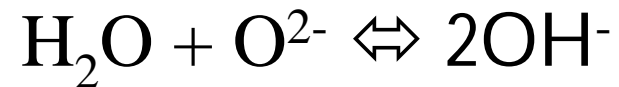
Which can be coupled to the basic dissociation (see Fraser):

$$2H^+ + O^{2-} \Leftrightarrow H_2O$$

By subtracting:

$$H^+ + O^{2-} \Leftrightarrow OH^-$$
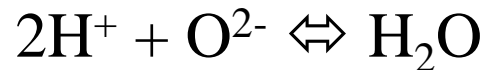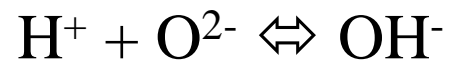
$$K = \frac{n_{O^{2-}}}{n_{OH^-}} \cdot \frac{n_{H^+}^{TOT} - n_{OH^-}}{\sum cations} \qquad n_{H^+}^{IN} + n_{OH^-} = 2 \cdot n_{H_2O}$$
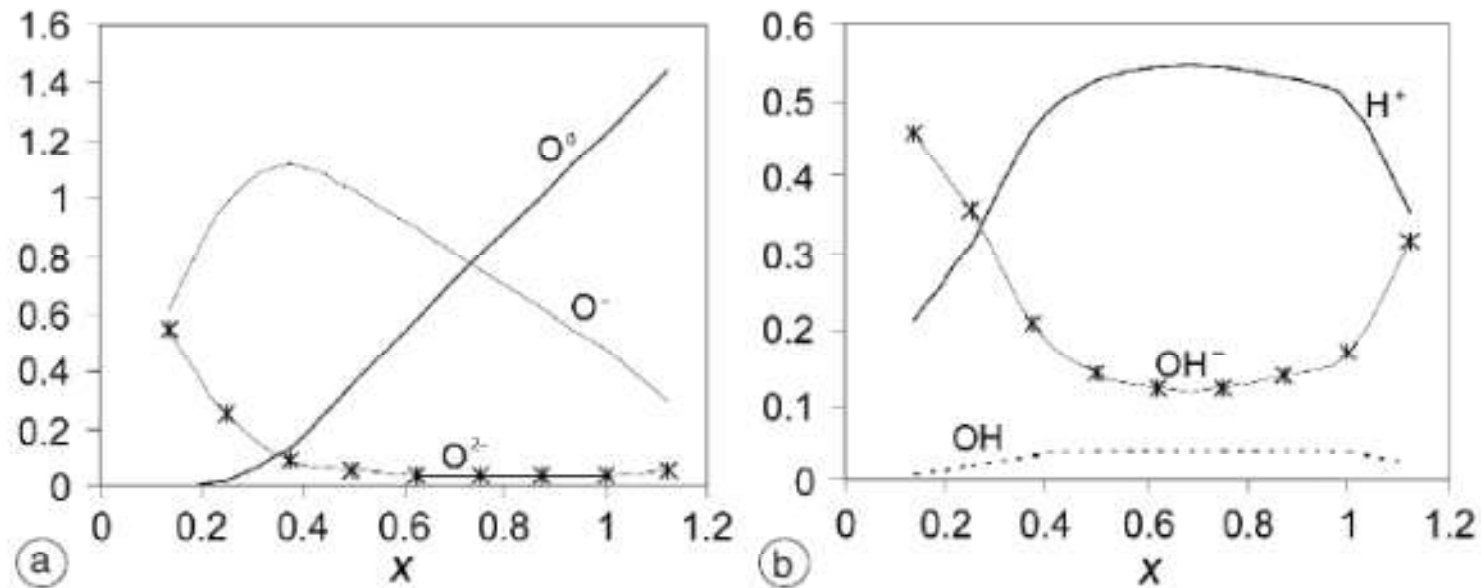
Fig. 7a,b. Relative proportions of oxygens of the Fincham-Richardson (1954) notation (a) plotted against the compositional parameter in the binary join $Na_{5-4x}Al_xSi_{3x}O_8$. Water-derived species dissolved in the same compositional range have been plotted in b). Note the comparable amount of OH and OH^- for the albitic composition ($x=1$).

Moretti (2005, AoG)

At parity of water content, high free hydroxyl concentration is expected in more basic melts, in agreement with Xue and Kanzaki (2004), Behrens et al. (2004) for water diffusivities etc…

Iron redox ratio in hydrous silicate melts is also origin of controversies. Current hypotheses about the role of water on the Fe^{III}/Fe^{II} value are:

-Water does not affect ferric to ferrous ratio.

-Water causes a decrease of the ferric to ferrous ratio.

-Water causes an increase of the ferric to ferrous ratio.

==> Parameterization of the ferric to ferrous ratio should consider the "impact" of water on melt acid-base properties and then polymerization together with the effect of pressure on the previous reactions.

New experimental evidences
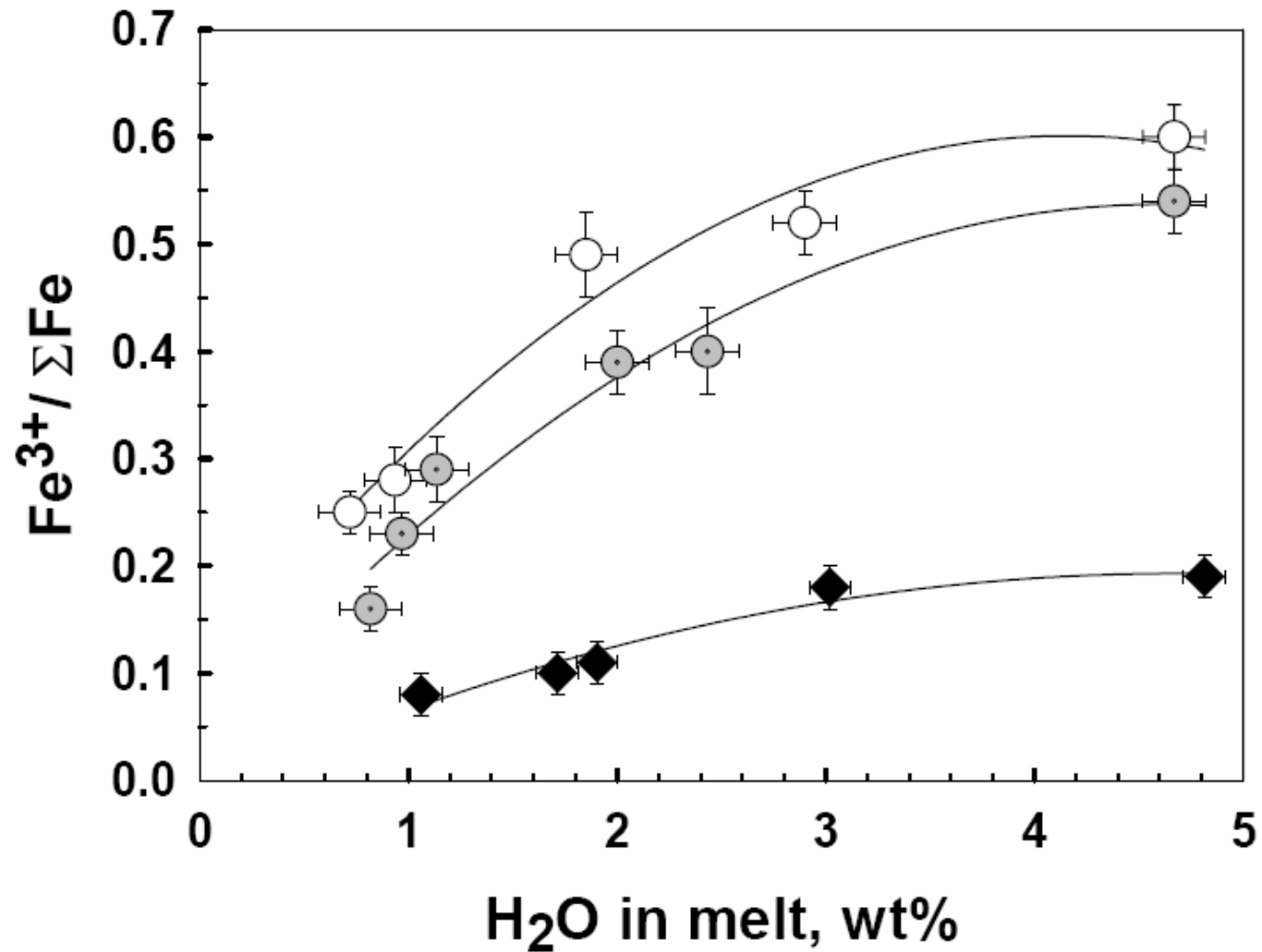
Botcharnikov *et al.* **(GCA, 2005)**

QFM + const *redox buffer holding on each line*

Model comparison
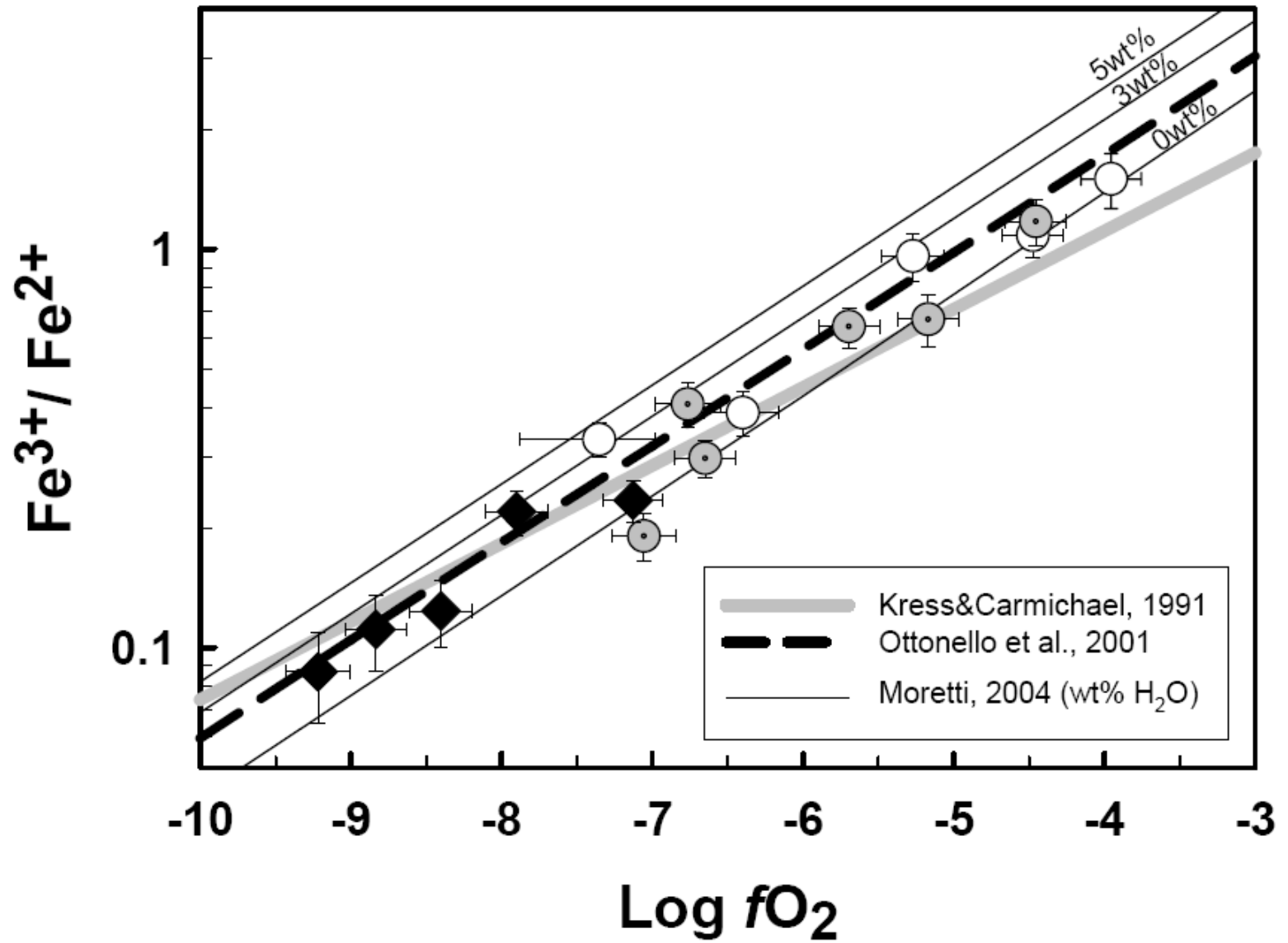
Botcharnikov et al. (2005)

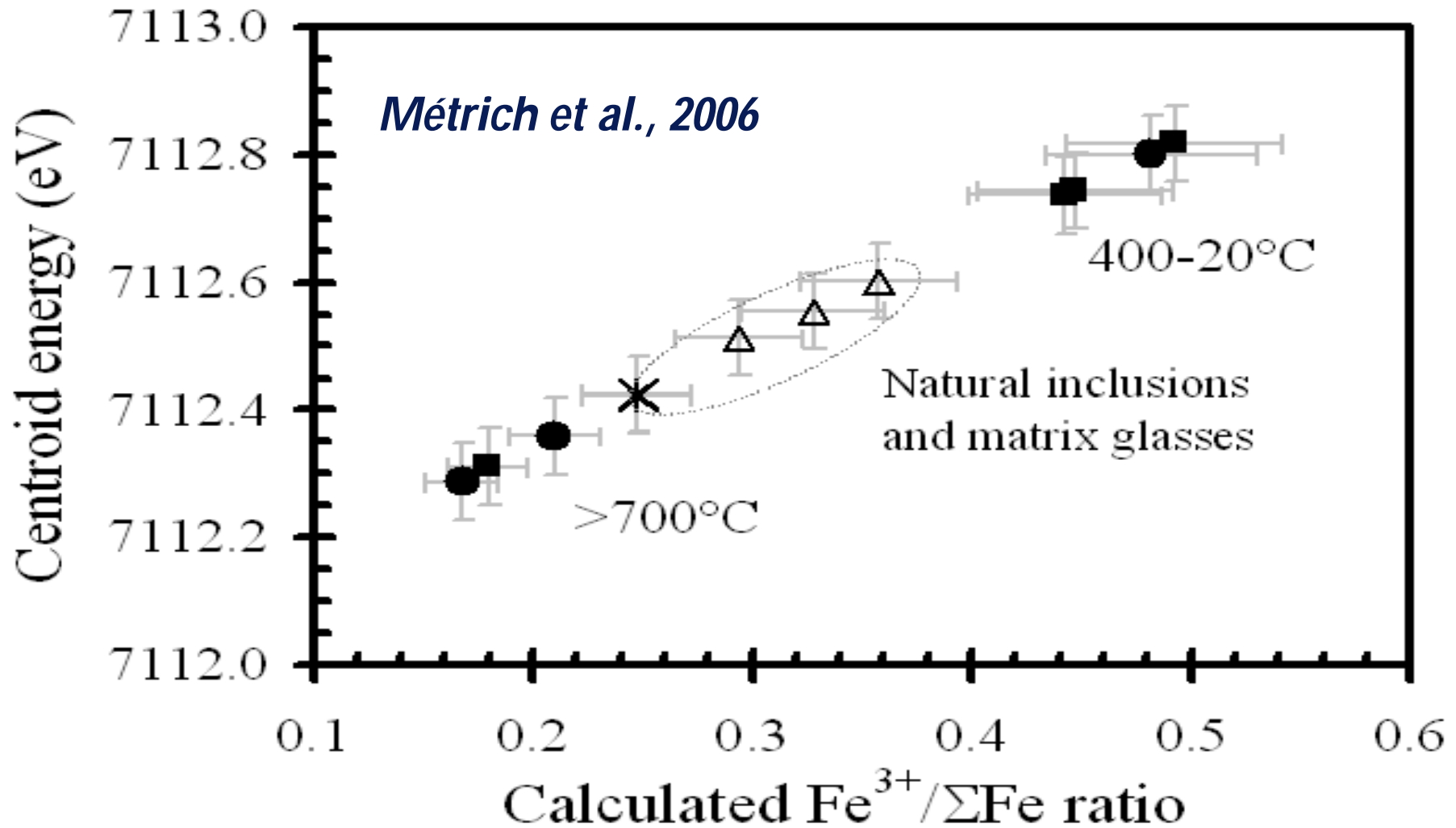About the effect of water on the iron oxidation state of melts…

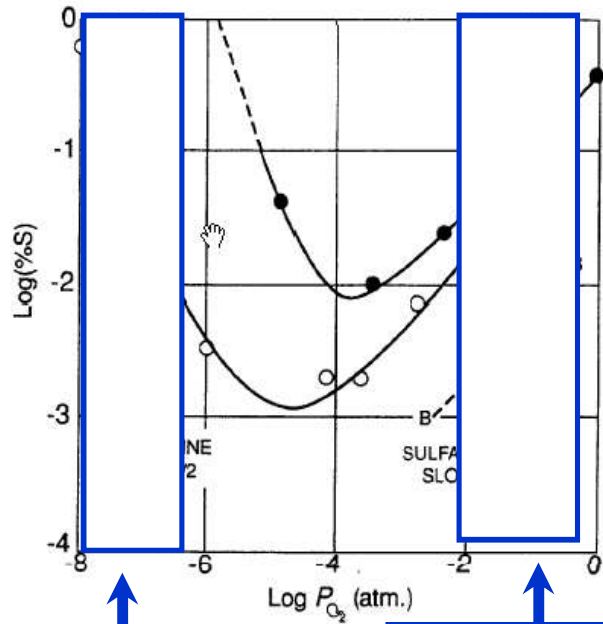Redox models simply relating Fe^{2+}/Fe^{3+} to fO_2 are not applicable !
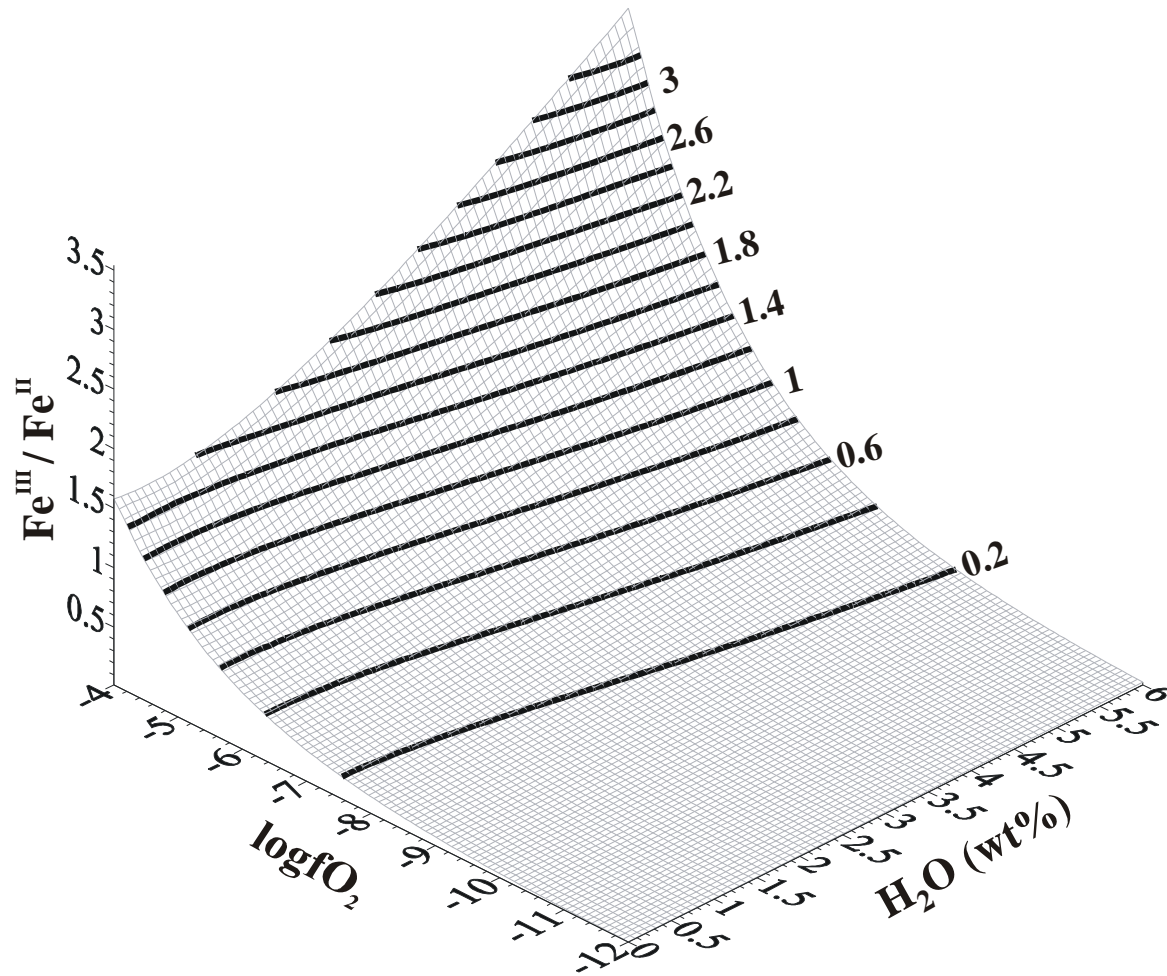
Moretti (in prep.)

Iron redox model: unexpected features

We can explain, for example, the increase of oxidation with decreasing T. This depends on oxygen fugacity, that is, on
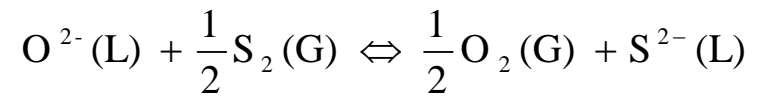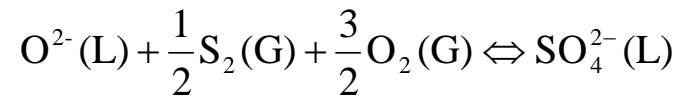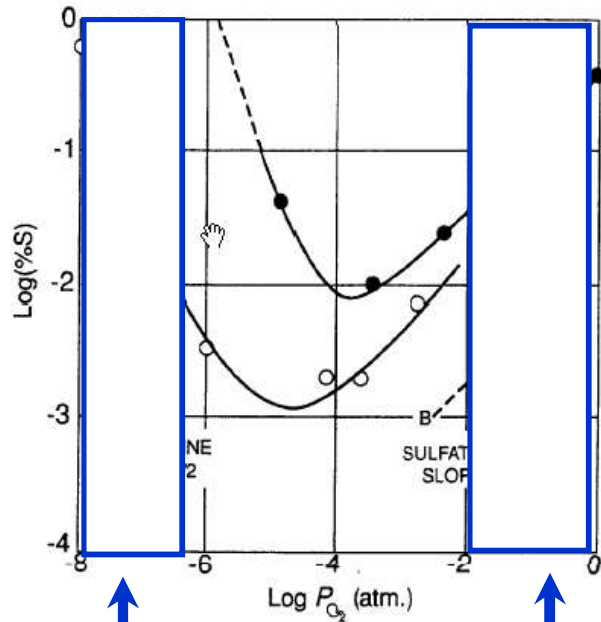
Log(%S) vs Log P_{O_2} (atm.)

S as sulphide

S as sulphate

Sulfide equilibrium:

$$O^{2-}(L) + \frac{1}{2}S_2(G) \Leftrightarrow \frac{1}{2}O_2(G) + S^{2-}(L)$$

Sulfate equilibrium:

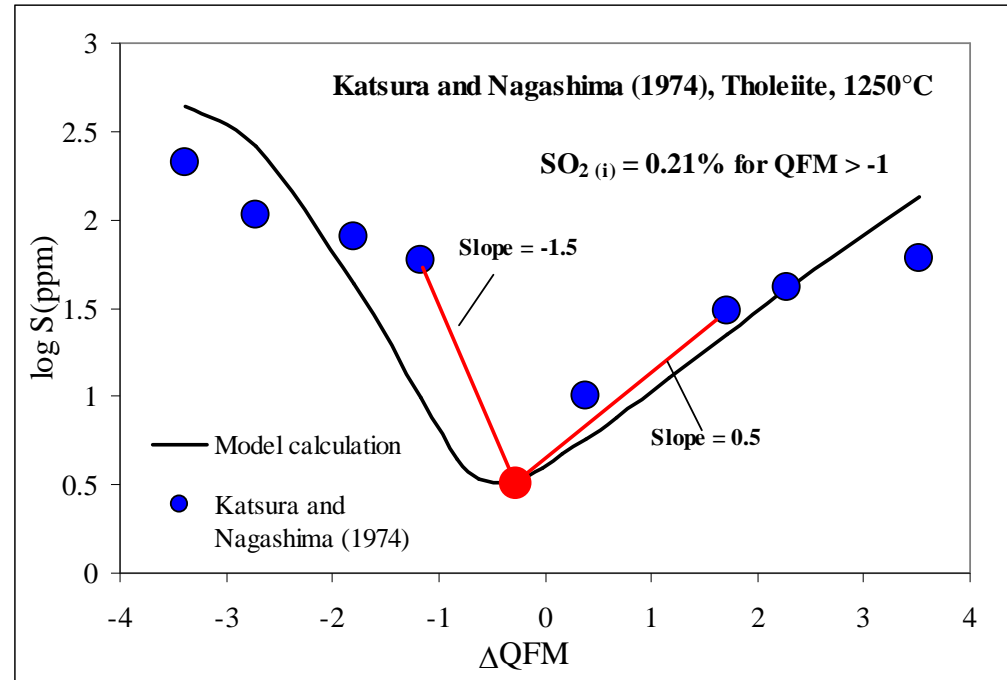$$O^{2-}(L) + \frac{1}{2}S_2(G) + \frac{3}{2}O_2(G) \Leftrightarrow SO_4^{2-}(L)$$

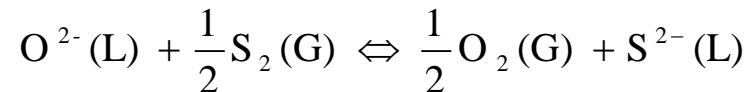# S solubility: the Conjugated-Toop-Samis (CTSFG) model *(Moretti and Ottonello, 2005)*
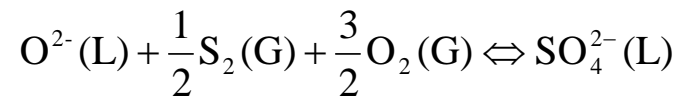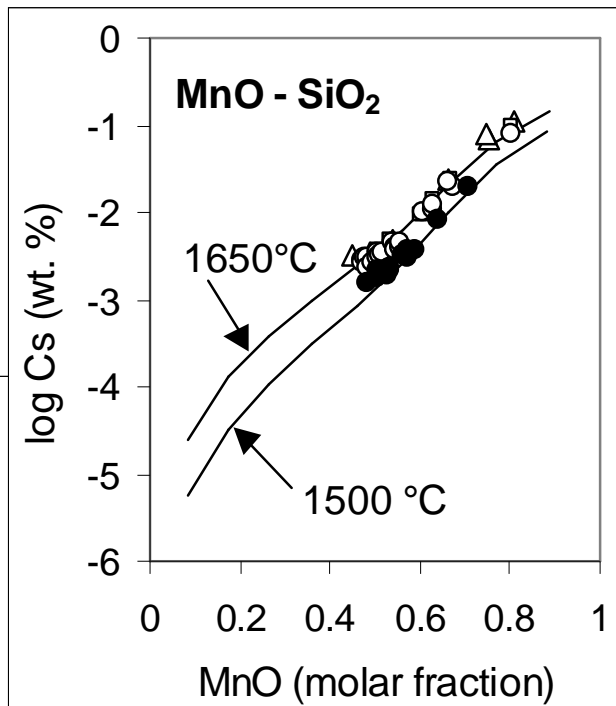

S as sulphide

S as sulphate

Moretti and Ottonello (2004) Submitted to GCA

Sulfide equilibrium:

$$O^{2-}(L) + \frac{1}{2}S_2(G) \Leftrightarrow \frac{1}{2}O_2(G) + S^{2-}(L)$$

Sulfate equilibrium:

$$O^{2-}(L) + \frac{1}{2}S_2(G) + \frac{3}{2}O_2(G) \Leftrightarrow SO_4^{2-}(L)$$

CaO-SiO₂ panel: y-axis log Cs (wt%), x-axis CaO (molar fraction), curves labeled 1650 °C and 1500 °C.

MnO - SiO₂ panel: y-axis log Cs (wt. %), x-axis MnO (molar fraction), curves labeled 1650°C and 1500 °C.

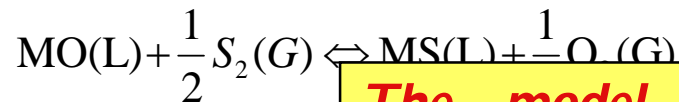**MnO - Al₂O₃** panel: y-axis log Cs (wt.%), x-axis MnO (molar fraction), labeled 1650 °C.
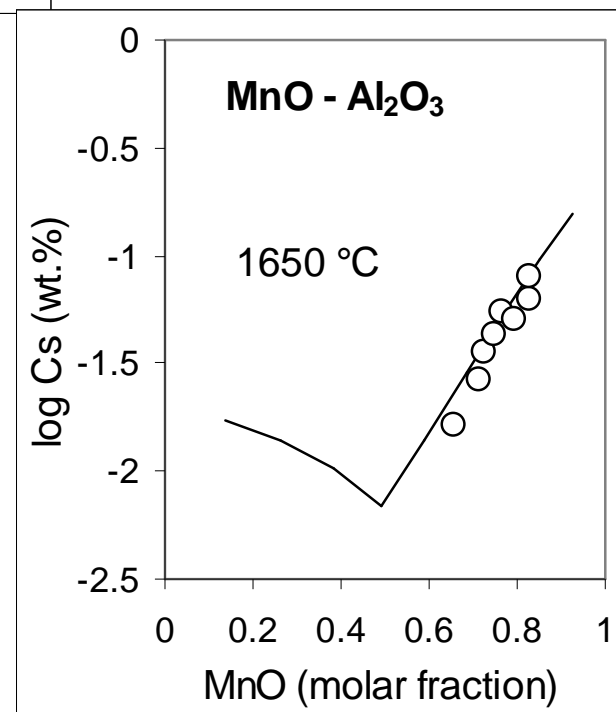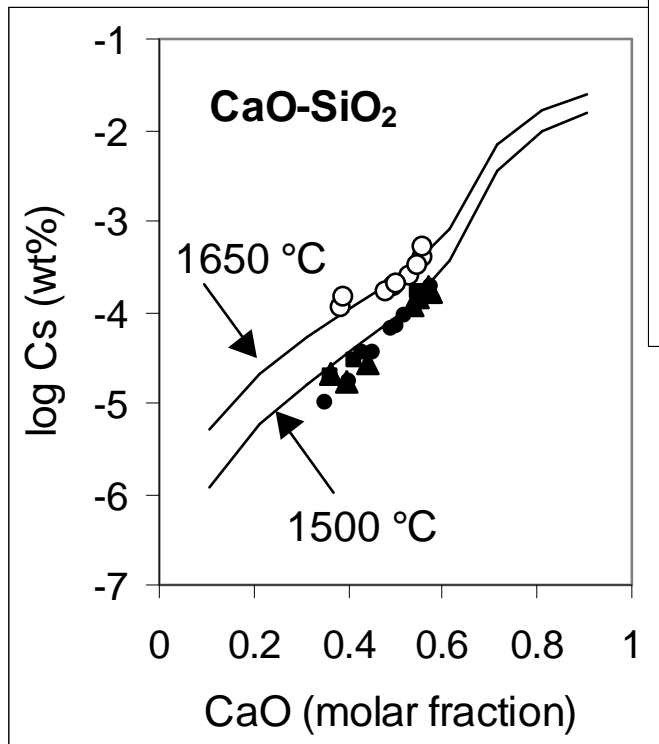
Moretti and Ottonello, 2003

Theory of the S solubility model (CTSFG)

$$C_{S^{2-}} = [S]_{wt\%} \left(\frac{f_{O_2}}{f_{S_2}} \right)^{\frac{1}{2}}$$

$$C_{SO_4^{2-}} = [S]_{wt\%}\, f_{O_2}^{-\frac{3}{2}} f_{S_2}^{-\frac{1}{2}}$$

Sulfide-metal oxide reactions:

$$MO(L) + \frac{1}{2}S_2(G) \Leftrightarrow MS(L) + \frac{1}{2}O_2(G)$$

$$k_{M_iO\text{-}M_iS} = \frac{a_{M_iS}}{a_{M_iO}} \left(\frac{f_{O_2}}{f_{S_2}} \right)^{\frac{1}{2}} = \text{ex}\ldots$$

Sulfate-metal oxide reactions:

$$MO(L) + \frac{1}{2}S_2(G) + \frac{3}{2}O_2(G) \Leftrightarrow MSO_4(L)$$

$$k_{M_iO\text{-}M_iSO_4} = \frac{a_{M_iSO_4}}{a_{M_iO}}\, f_{O_2}^{-\frac{3}{2}} f_{S_2}^{-\frac{1}{2}} = \exp\left(a_i'' + \frac{b_i''}{T} - \frac{\Delta v_L}{RT}(P-1) \right)$$
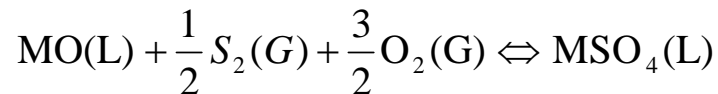
Gas-liquid reactions: **Flood and Grjotheim** (1952) thermochemical cycle:

$$\ln k_{S^{2-},SO_4^{2-}} = \sum_{i=1}^{N_{OX}} N_i^{v+} \ln C^{anneal}\, k_{MO-(S^{2-},SO_4^{2-}),i}$$

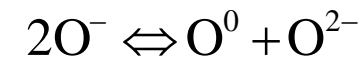$$N_i^{v+} = \frac{v_i^+ n_i}{\sum\limits_{i=1}^{N_{OX}} v_i^+ n_i}$$

where N^{n+} represent *electrically equivalent* ... omputed ... ationic or ... ts)

Pincham and Richardson (1954):

$$2O^- \Leftrightarrow O^0 + O^{2-}$$

O^- are singly bonded (or non-bridging) oxygens

• **O^0 are doubly bonded (or bridging) oxygens**

• **O^{2-} are free oxygens**

The Toop-Samis (extended) model is applied

The model computes $C^{anneal.}$ (entropies of annealing). $k_{MO\text{-}(S2\text{-},SO42\text{-})}$ constants are from independent thermodynamic compilations when available.

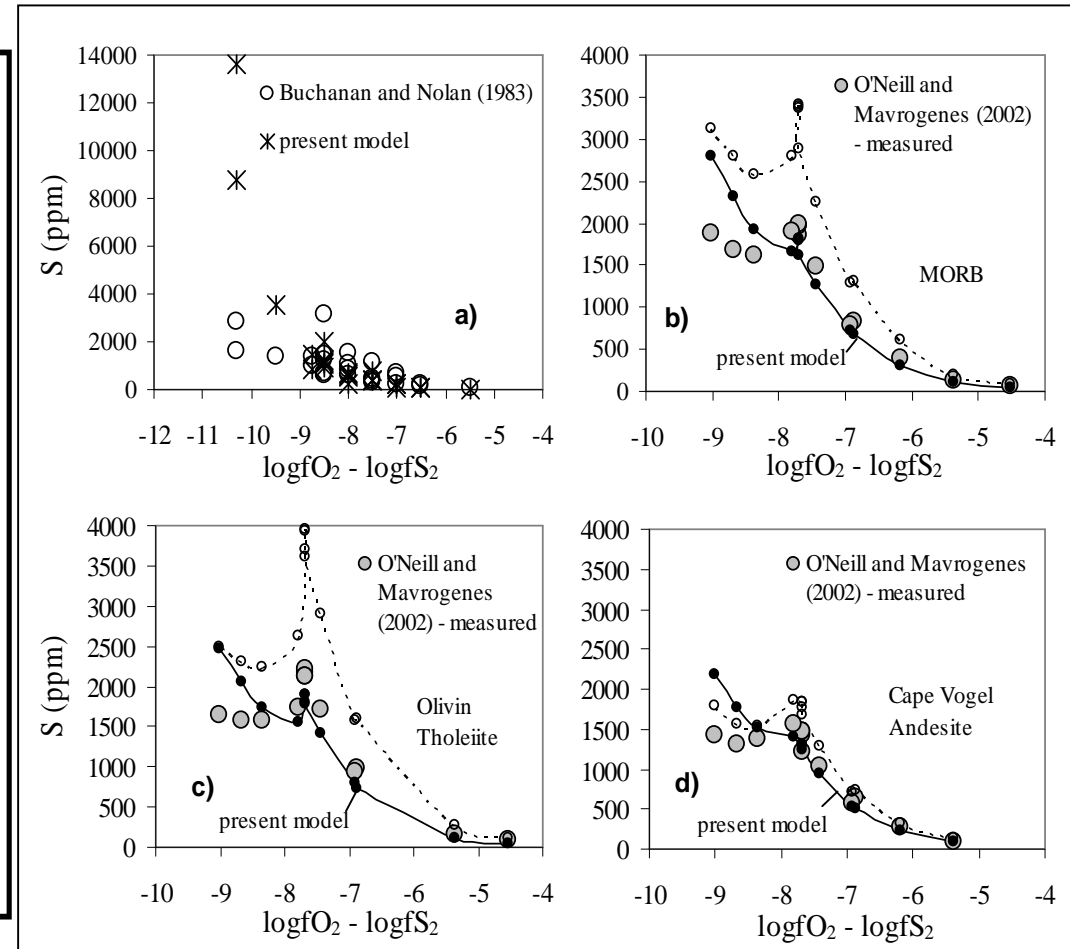# The S solubility (CTSFG) model: verification and check of the simplex and its features

Simple metallurgical slags (log Cs contouring)

SiO_2-Al_2O_3-CaO, T = 1500°C

Natural-like melts (sulfur content)
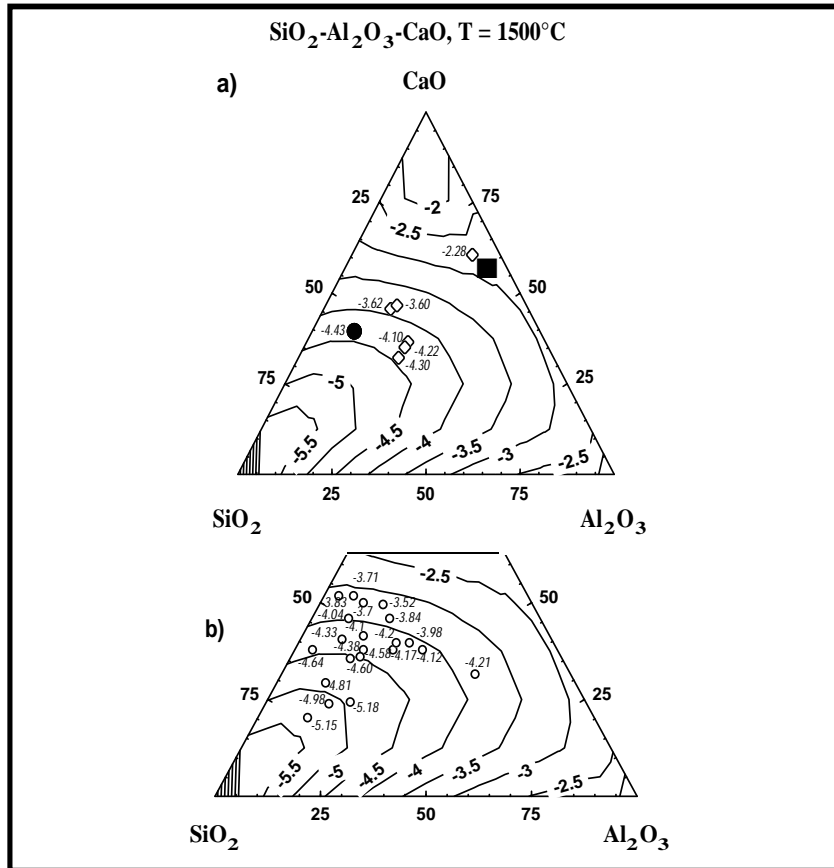
Moretti and Ottonello (2003), Metall. Mat. Trans. B   *Moretti and Ottonello (2005)*

S solubility at P: considering volumes for systems in which they have never been determined !

$$\ln K'^{P-T}_{O-S,M} = \boxed{\phantom{1\text{-bar }\ln K}} \Big/ T - \frac{1}{RT}\int_{1}^{P}\left(\Delta V_m + \Delta V_g\right)dP$$
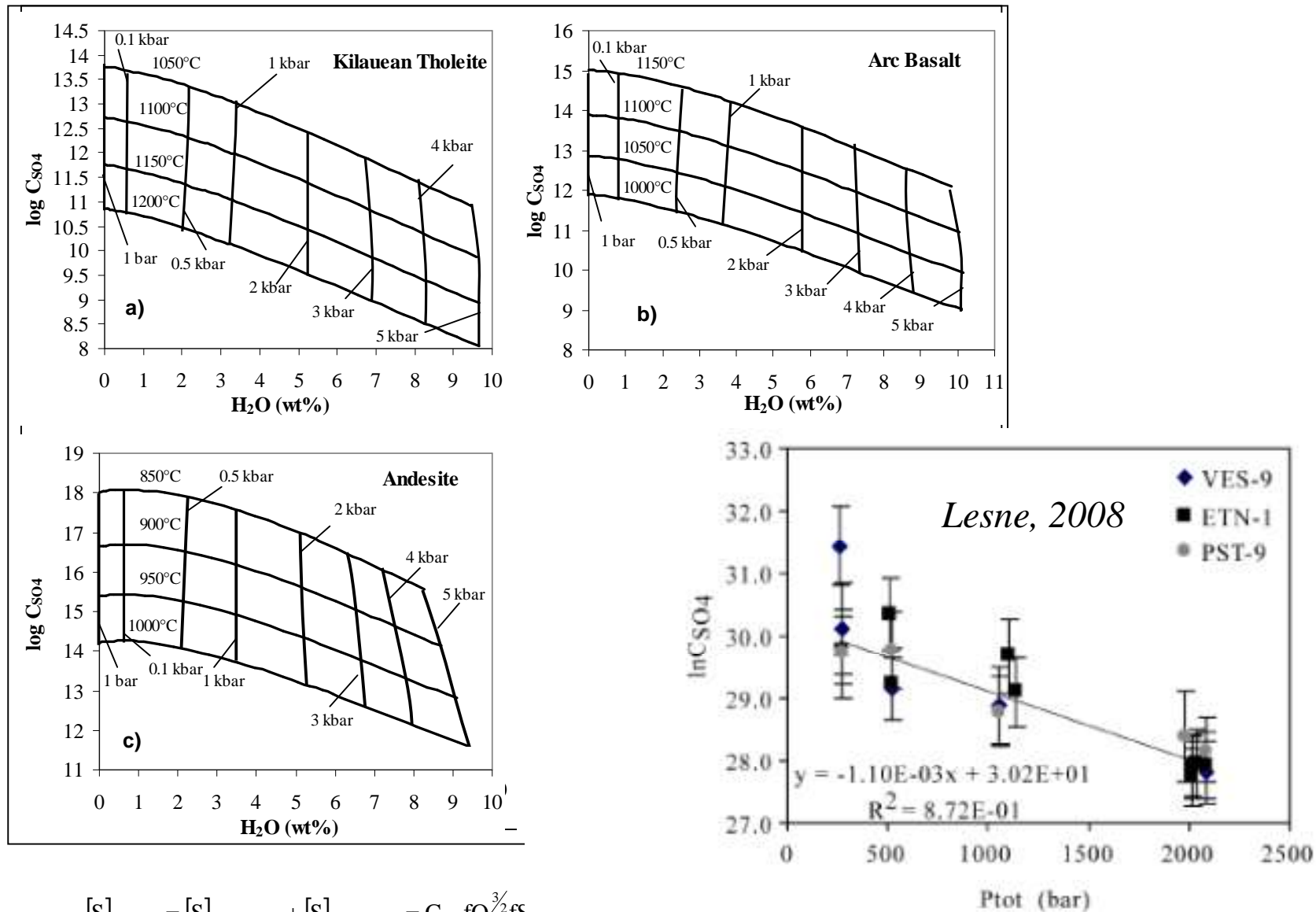
1-bar lnK

$$V_{M\,2/\upsilon^+\,SO_4} = V_{M\,2/\upsilon^+\,O} + V_{SO_3}$$

*Our value for the (partial) molar volume of V_{SO_3} is **57.71 cm³/mol** at 1673K... must be checked experimentally (no data at present)*

$$\Delta V_{SO_4\text{-}S_2} = V_{M\,2/\upsilon^+\,SO_4} - V_{M\,2/\upsilon^+\,S} = 41 \;\; (\text{cm}^3/\text{mol})$$
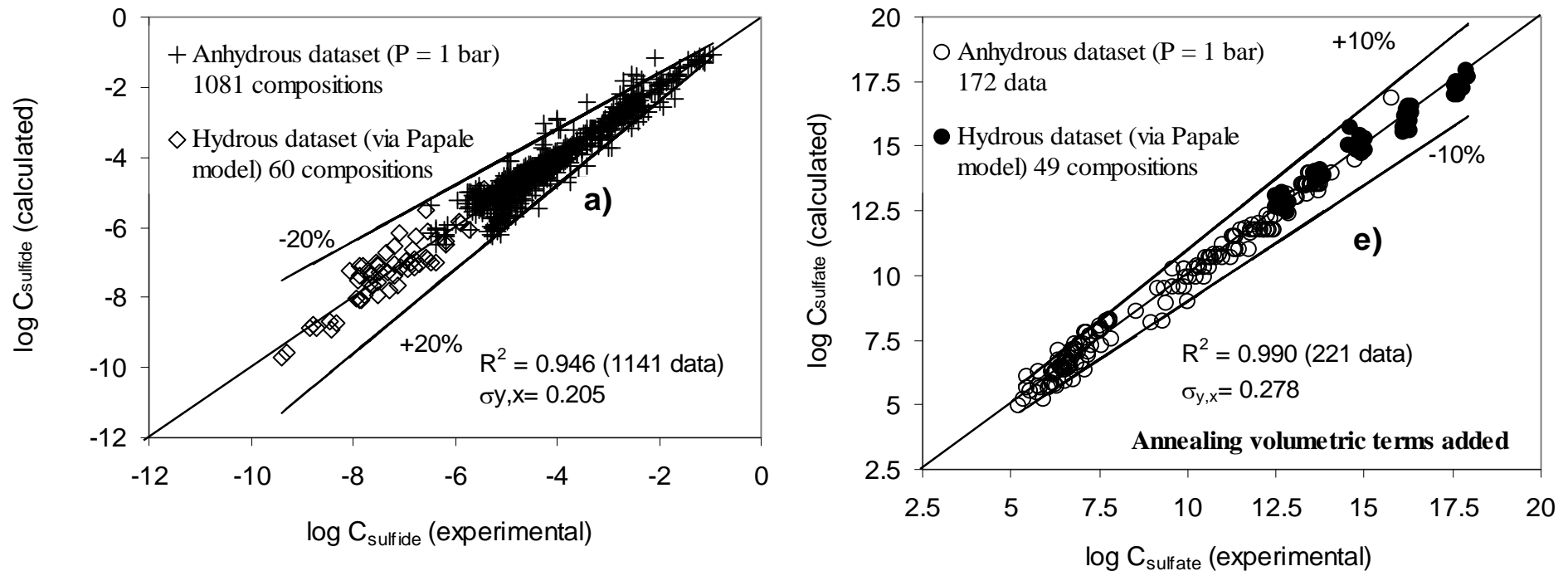
The CTSFG solubility model: features of the sulfide and sulfate capacity surfaces

$$[S]_{wt\%,tot} = [S]_{wt\%,sulfide} + [S]_{wt\%,sulfate} = C_{S^{6+}} fO_2^{3/2} fS$$

Figure III.10: $\ln C_{SO4}$ calculated as explained in the text, versus total pressure.

The CTSFG model for sulfur: bulk performance and suggestions for experimentalists

Plot a) — log C$_{sulfide}$ (calculated) vs log C$_{sulfide}$ (experimental):
+ Anhydrous dataset (P = 1 bar) 1081 compositions
◇ Hydrous dataset (via Papale model) 60 compositions
-20%
+20%
R^2 = 0.946 (1141 data)
σy,x = 0.205

Plot e) — log C$_{sulfate}$ (calculated) vs log C$_{sulfate}$ (experimental):
○ Anhydrous dataset (P = 1 bar) 172 data
● Hydrous dataset (via Papale model) 49 compositions
+10%
-10%
R^2 = 0.990 (221 data)
σy,x = 0.278
Annealing volumetric terms added

Moretti and Ottonello (2005)

Limits

- *Most data are at 1 bar ! => more data at pressure are needed*

- *Few data for sulfate solubility (high fO$_2$) even at 1 bar !*

- *Lack of experimental data on partial molar volumes of sulfide and sulfate liquid species*

- *Need of fS$_2$ probes for high-P pressure vessel experiments*
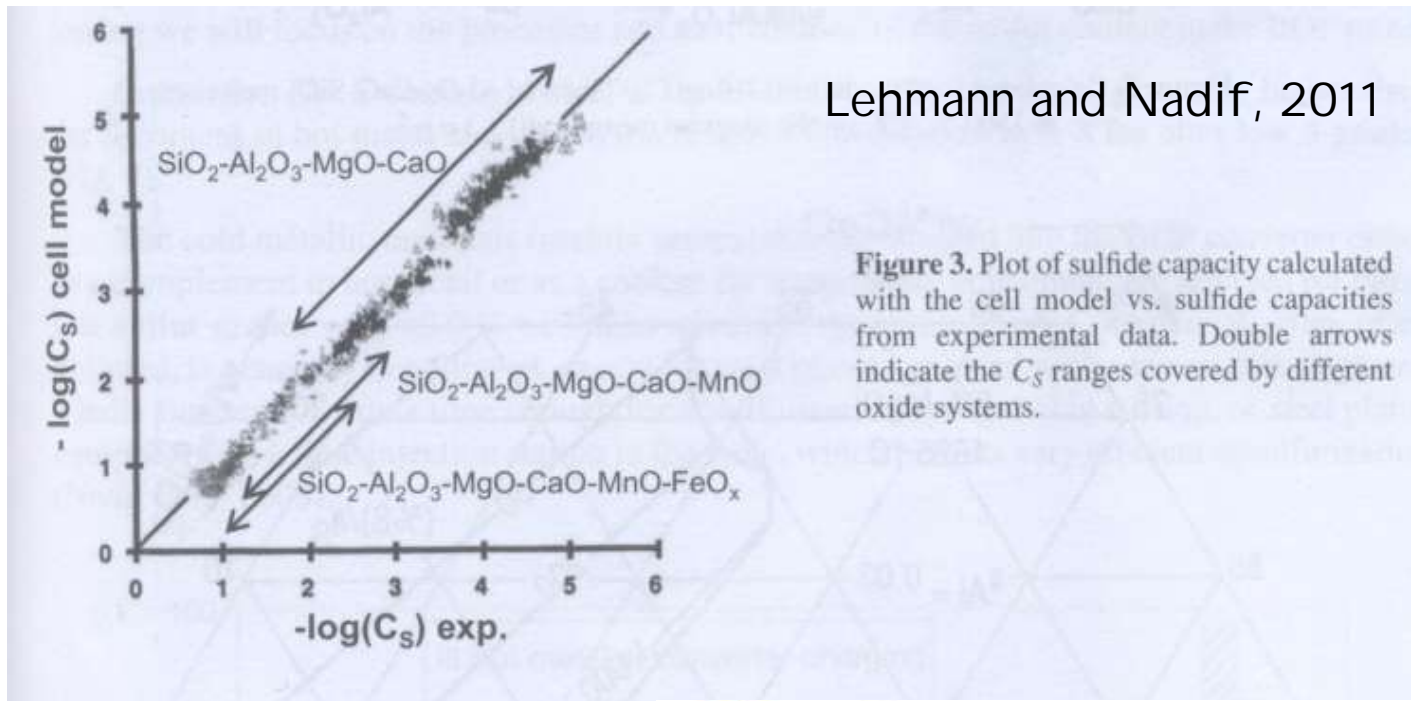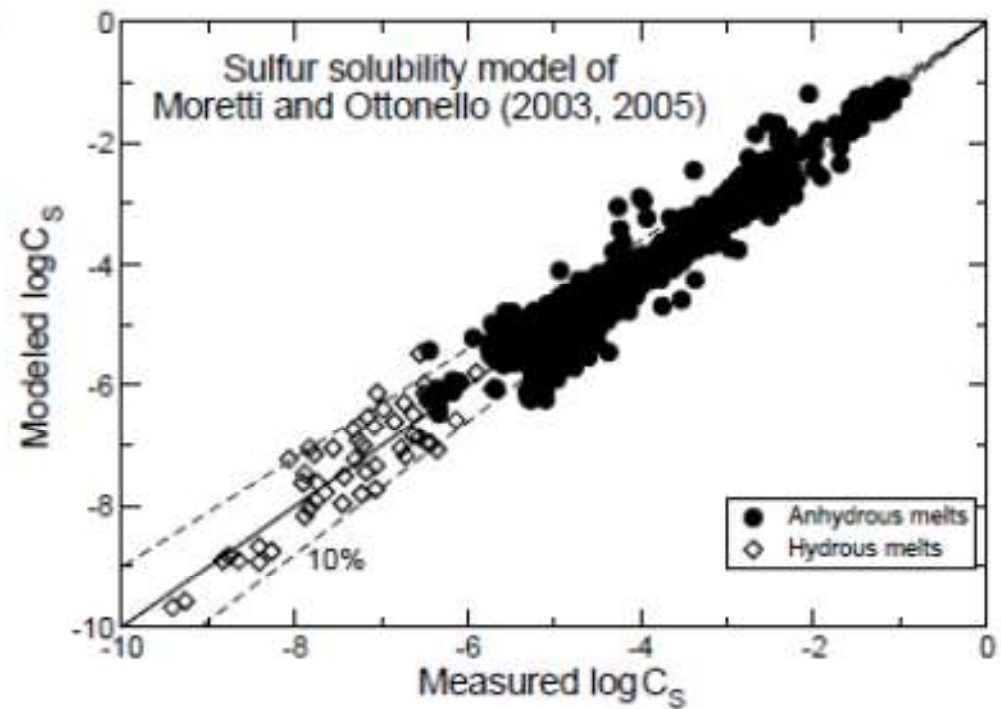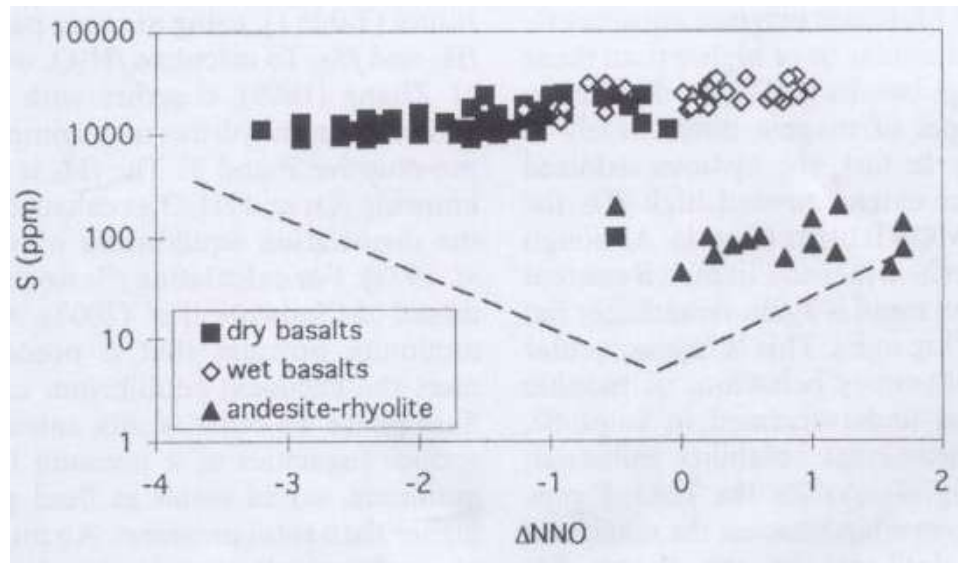
Lehmann and Nadif, 2011

Figure 3. Plot of sulfide capacity calculated with the cell model vs. sulfide capacities from experimental data. Double arrows indicate the C_S ranges covered by different oxide systems.
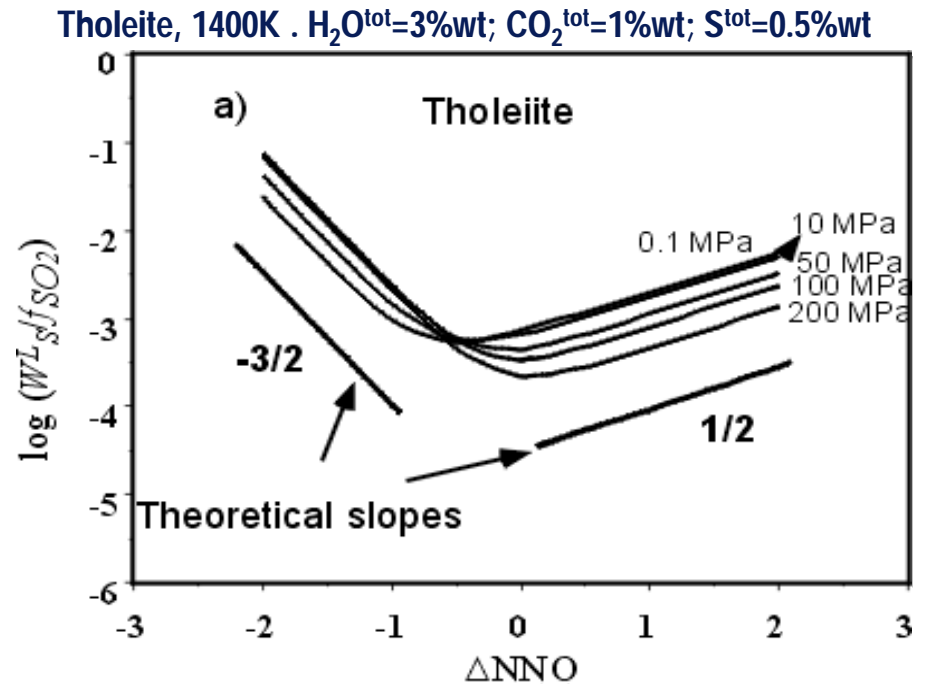
(a)

Sulfur solubility model of Moretti and Ottonello (2003, 2005)

Are complex approaches really needed for data interpretation?

Tholeite, 1400K . H_2O^{tot}=3%wt; CO_2^{tot}=1%wt; S^{tot}=0.5%wt
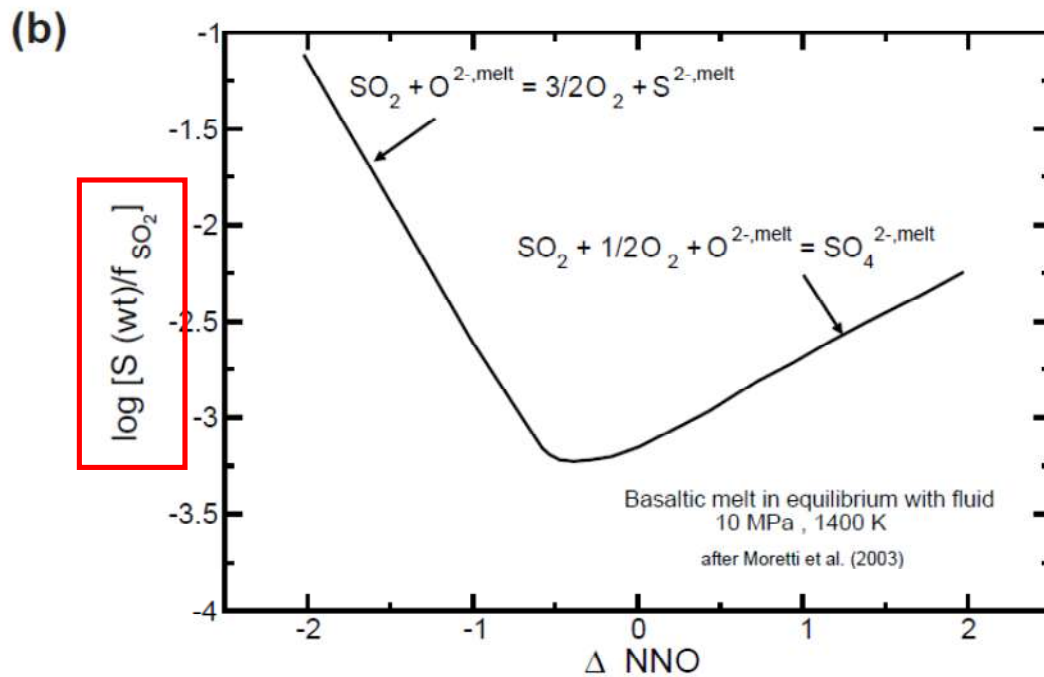
Scaillet and Pichavant (2003) Geol. Soc. Spec. Publ. 213

Moretti et al. (2003) Geol. Soc. Spec. Publ. 213

Mass partitioning in Nature is non-linear. The expected linearity required by theory (stoichiometry in this case) is embodied, not cancelled. "Complex" models may reveal it.
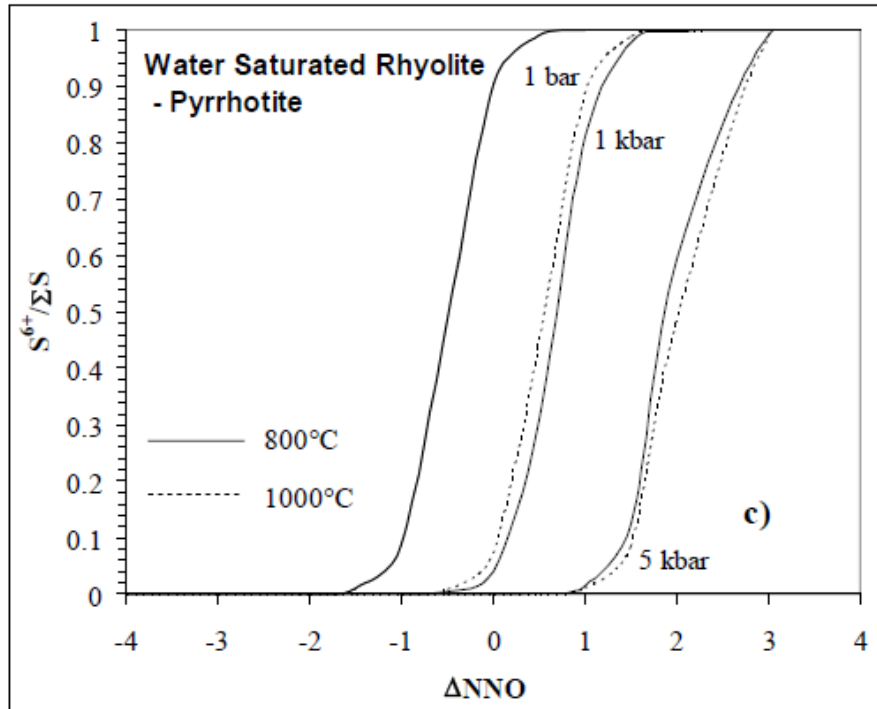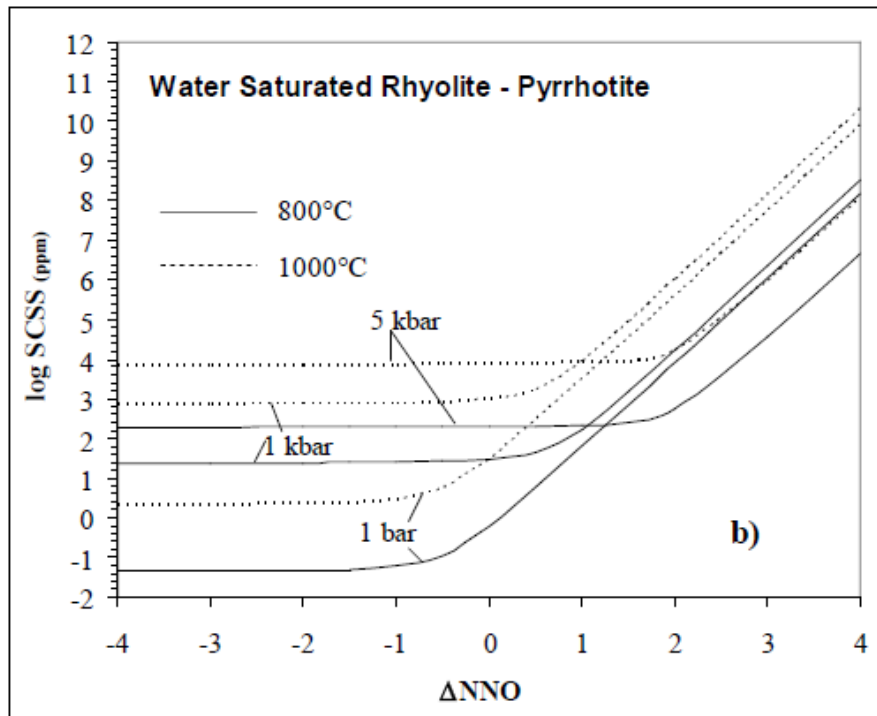
(a)

S (ppm) vs Δ NNO

S^{Total}

S^{4+}

S^{2-}

Basaltic melt in equilibrium with fluid
10 MPa, 1400 K
after Moretti et al. (2003)

<= Non linear behavior

(b)

$\log [S\,(wt)/f_{SO_2}]$ vs Δ NNO

$SO_2 + O^{2-,melt} = 3/2\,O_2 + S^{2-,melt}$

$SO_2 + 1/2\,O_2 + O^{2-,melt} = SO_4^{2-,melt}$

Basaltic melt in equilibrium with fluid
10 MPa , 1400 K
after Moretti et al. (2003)
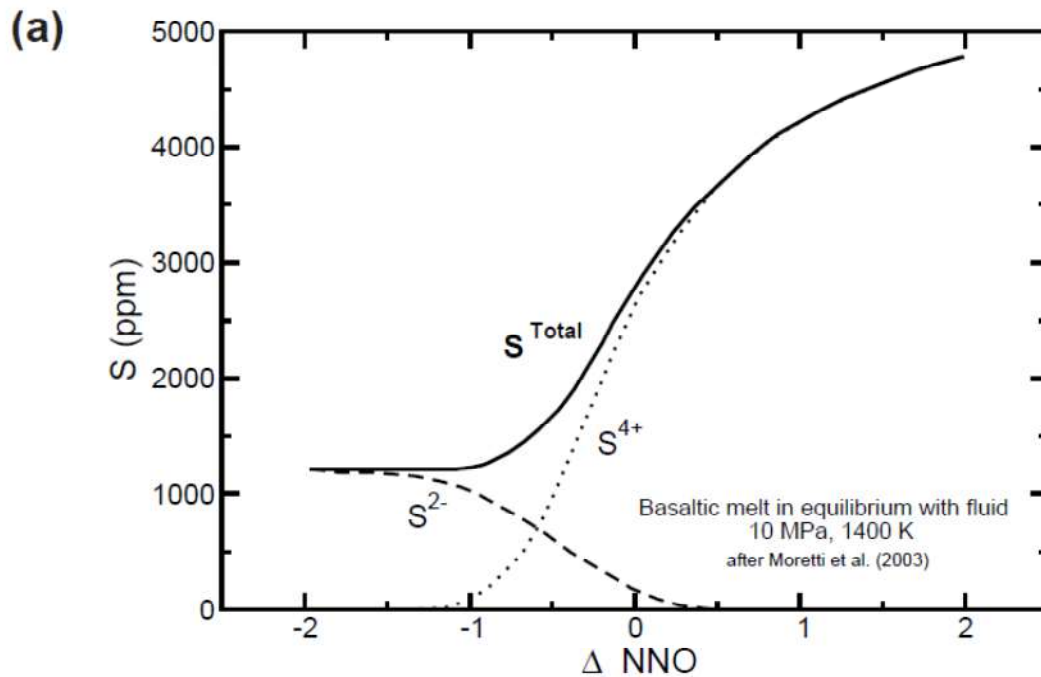
<= Linear (stoichiometric) behavior
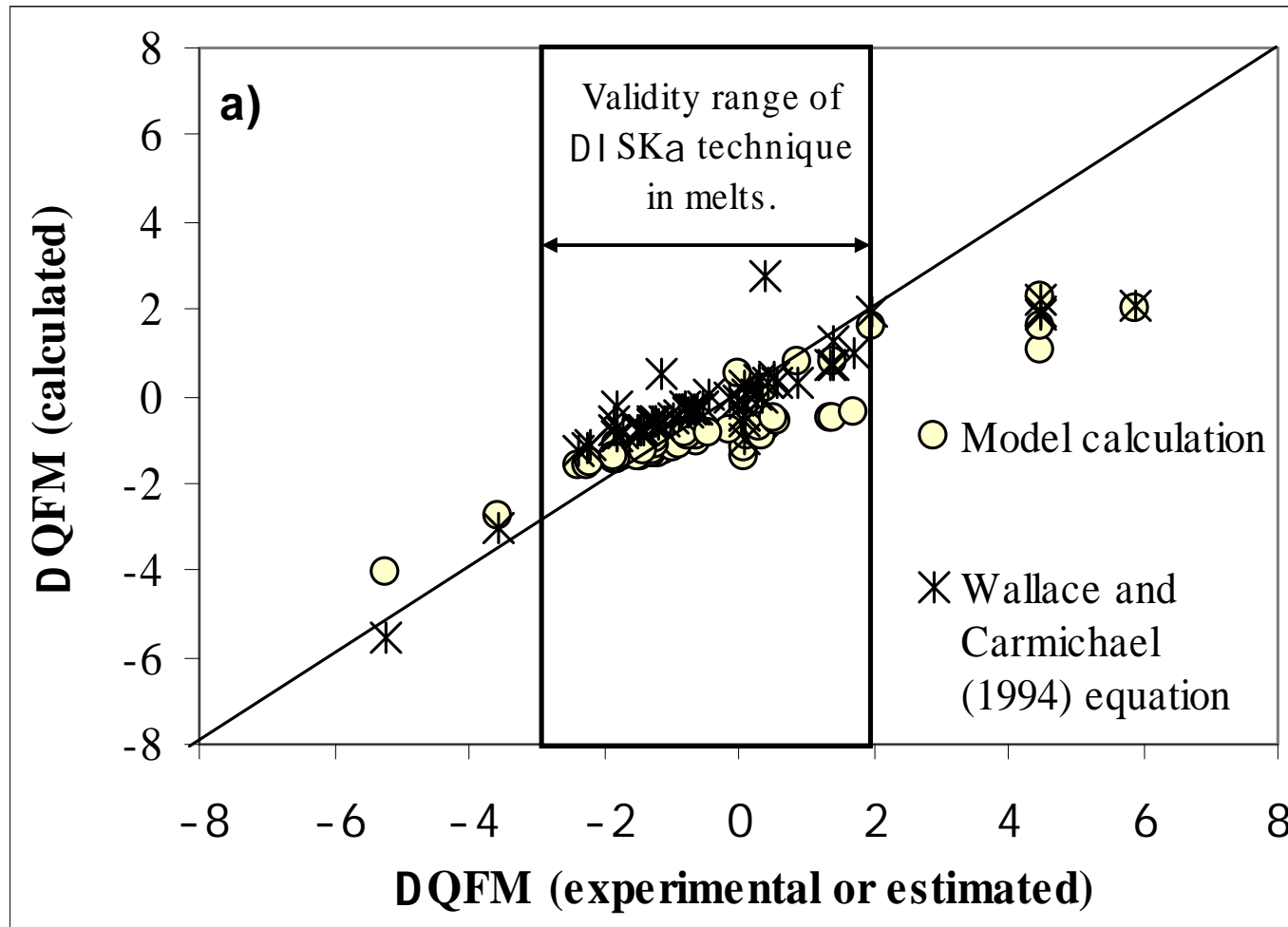
Moretti et al. (2003)

Baker & Moretti (2011)

STRONG ROLE OF COMPOSITION (e.g. H_2O content) ON SULFUR SPECIATION !
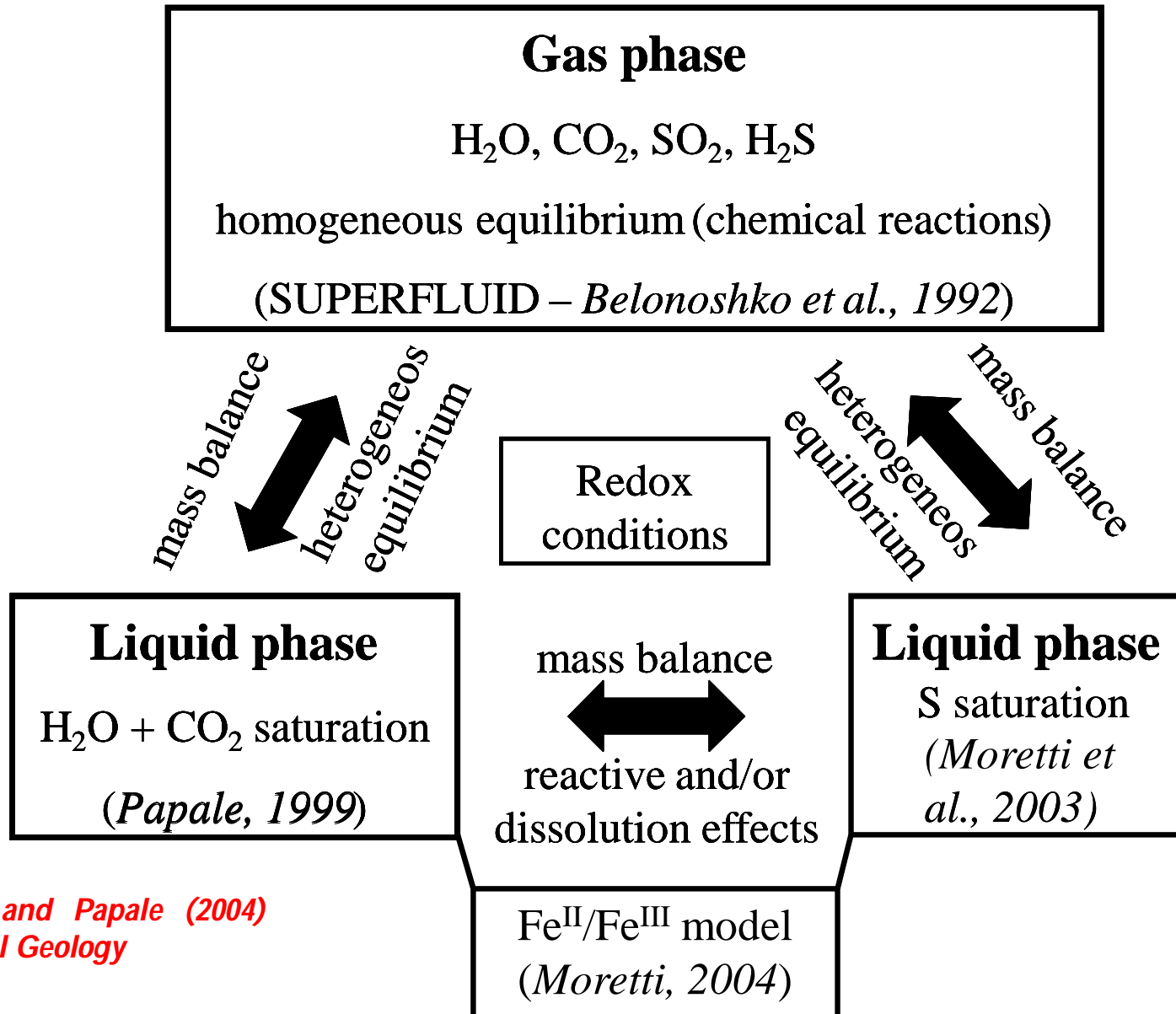
Never forget this!

Baker & Moretti (2008)

Application to S speciation and fO₂ determination

... the $S^{2-} + 2O_2 \Leftrightarrow SO_4^{2-}$ equilibrium computed by the CTSFG model is then applied to an __independent__ set of data:

a)

Validity range of DISKa technique in melts.

✳ 2.7

○ Model calculation

✳ Wallace and Carmichael (1994) equation

DQFM (calculated) (y-axis: 8, 6, 4, 2, 0, -2, -4, -6, -8)

DQFM (experimental or estimated) (x-axis: -8, -6, -4, -2, 0, 2, 4, 6, 8)

The H_2O-CO_2-H_2S-SO_2 saturation model

Gas phase

H_2O, CO_2, SO_2, H_2S

homogeneous equilibrium (chemical reactions)

(SUPERFLUID – *Belonoshko et al., 1992*)

mass balance

heterogeneos equilibrium

heterogeneos equilibrium

mass balance

Redox conditions

Liquid phase

$H_2O + CO_2$ saturation

(*Papale, 1999*)

mass balance

reactive and/or dissolution effects

Liquid phase

S saturation

(*Moretti et al., 2003*)

Moretti and Papale (2004) Chemical Geology

Fe^{II}/Fe^{III} model

(*Moretti, 2004*)

Theory of the revised and extended H_2O-CO_2 saturation model *(Papale et al., 2006)*

- Fully non-ideal
- Fluid phase of any composition in the system H_2O+CO_2
- Liquid phase of any composition from two/three components to natural (12 components)

Equilibrium equations

$$P^G = P^L = P$$

$$T^G = T^L = T$$

$$f_{H_2O}^G = f_{H_2O}^L \Rightarrow \phi_{H_2O} y_{H_2O} P = \gamma_{H_2O} x_{H_2O} f_{H_2O}^{oL}$$

$$f_{CO_2}^G = f_{CO_2}^L \Rightarrow \phi_{CO_2} y_{CO_2} P = \gamma_{CO_2} x_{CO_2} f_{CO_2}^{oL}$$

Mass balance equations

$$y_{H_2O} + y_{CO_2} = 1$$

$$\frac{x_{H_2O}^T - x_{H_2O}}{y_{H_2O} - x_{H_2O}} = \frac{x_{CO_2}^T - x_{CO_2}}{y_{CO_2} - x_{CO_2}}$$

The revised H₂O-CO₂ saturation model (Papale et al., 2006)

Excess Gibbs free energy of the liquid: $G^E = N \sum_{i=1}^{n-1} \sum_{j=i+1}^{n} x_i x_j w_{ij}$

Activity coefficients:

$$\left(\frac{\partial G^E}{\partial n_i} \right)_{P,T,n_{j \neq i}} = RT \ln \gamma_i$$

Water:

$$RT \ln \gamma_{H_2O} = (1 - x_{H_2O}) x$$

> **The model computes H₂O₍ₘ₎-oxides interaction parameters and CO₂₍ₘ₎-oxides interaction parameters. All other oxide-oxide interactions are from Ghiorso et al. (1983)**

$$- x_{CO_2}$$

$$= (1 - x_{H_2O} - x_{CO_2}) \sum_{i \neq H_2O,CO_2 = 1} \sum_{j \neq H_2O,CO_2 = i+1} x_i x_j w_{ij} \quad (22)$$

Carbon dioxide:

$$RT \ln \gamma_{CO_2} = (1 - x_{CO_2}) x_{H_2O} w_{H_2OCO_2} - x_{H_2O} (1 - x_{H_2O} - x_{CO_2}) \sum_{i \neq CO_2 = 1}^{n} x_i' w_{H_2Oi}^{(0)}$$

$$+ (1 - x_{CO_2})(1 - x_{H_2O} - x_{CO_2}) \left[\sum_{i \neq H_2O = 1}^{n} x_i' w_{CO_2i}^{(0)} + \ln \frac{P}{P^o} \sum_{i \neq H_2O = 1}^{n} x_i' w_{CO_2i}^{(1)} \right]$$

$$- (1 - x_{H_2O} - x_{CO_2})^2 \sum_{i \neq H_2O,CO_2 = 1}^{n-1} \sum_{j \neq H_2O,CO_2 = i+1}^{n} x_i' x_j' w_{ij} \quad (23)$$
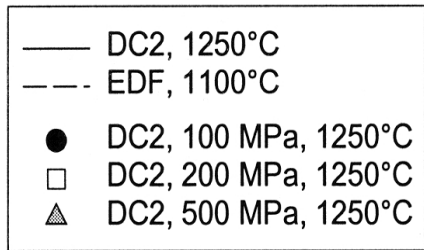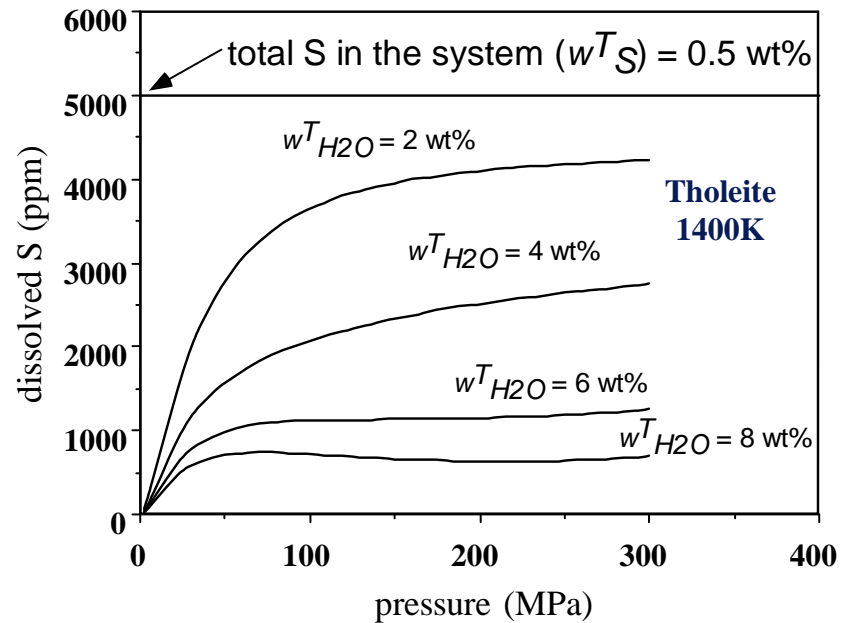
Tamic et al., 2001
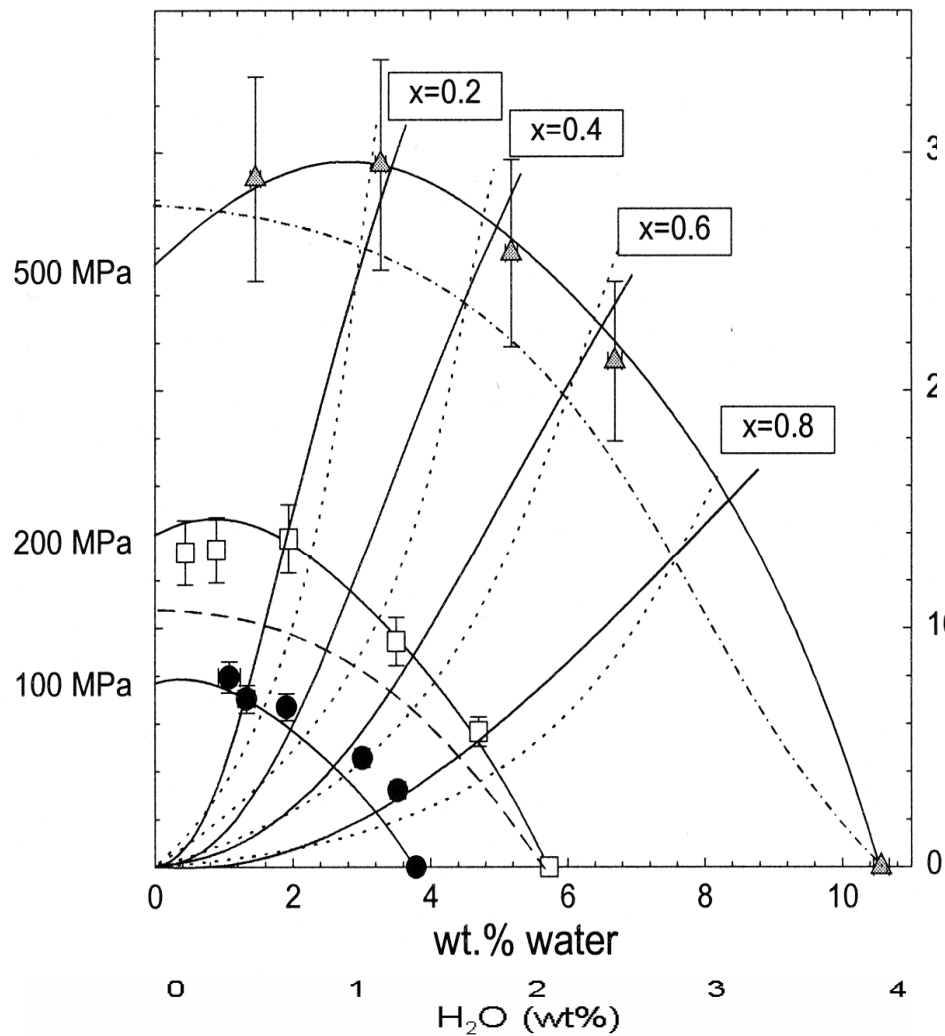
Rhyolite (comp. from Blank et al. 1993)
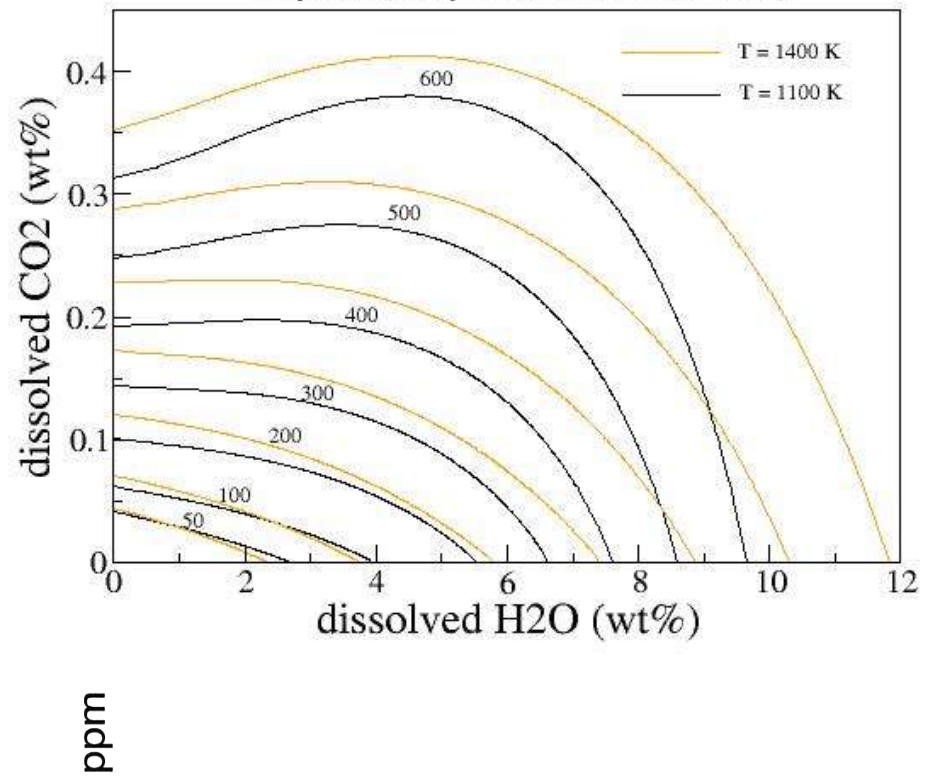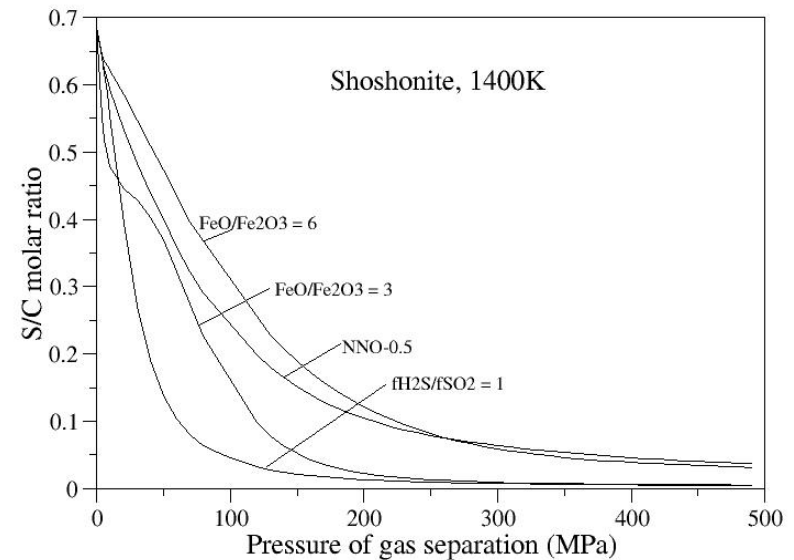
(Papale et al., 2006)

Volatile mixed "solubility"
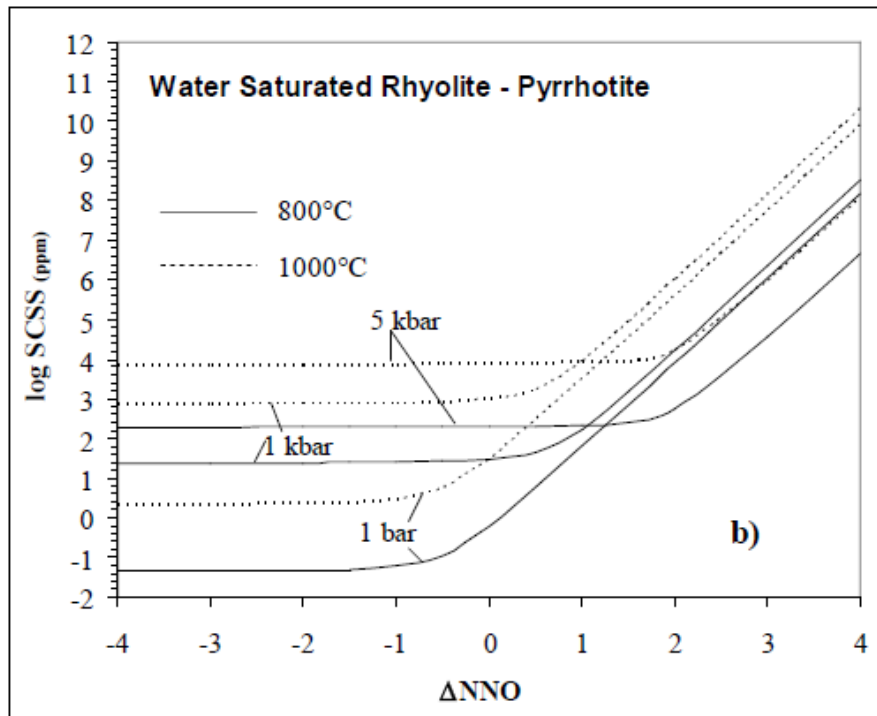

(applicable to glass inclusions)

Moretti et al. (2003) Geol. Soc. Spec. Publ. 213
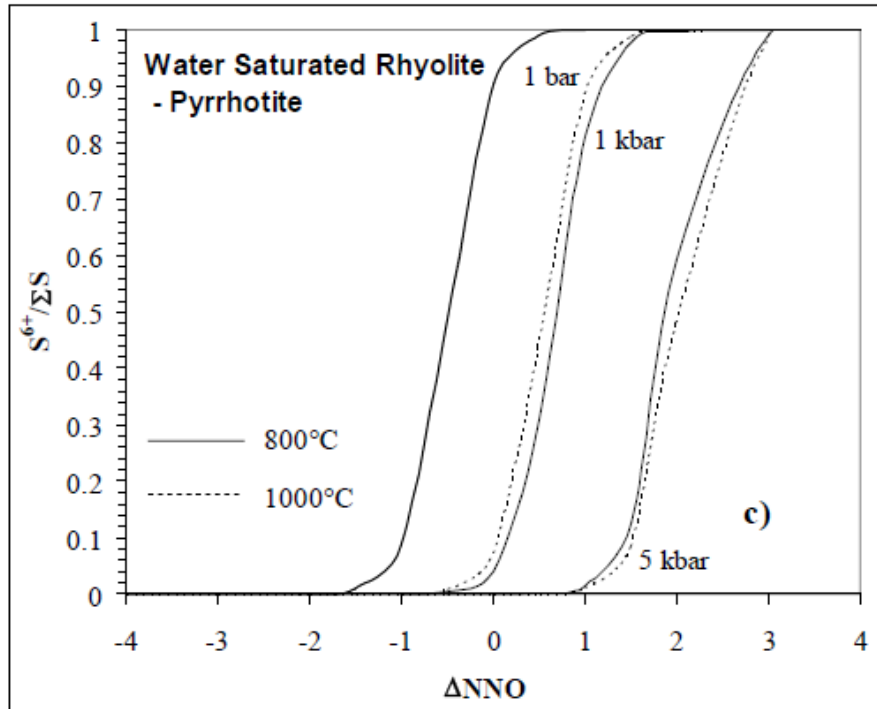
Single-step volatile separation

(applicable to the geochemical sensing of volcanoes)
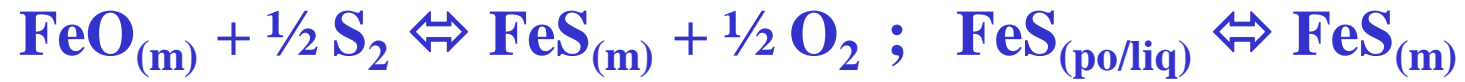
Papale and Moretti, work in progress

Water Saturated Rhyolite - Pyrrhotite

STRONG ROLE OF COMPOSITION (e.g. H_2O content) ON SULFUR SPECIATION !

Never forget this!

Baker & Moretti (2008)

$$FeO_{(m)} + \tfrac{1}{2} S_2 \Leftrightarrow FeS_{(m)} + \tfrac{1}{2} O_2 \; ; \;\; FeS_{(po/liq)} \Leftrightarrow FeS_{(m)}$$

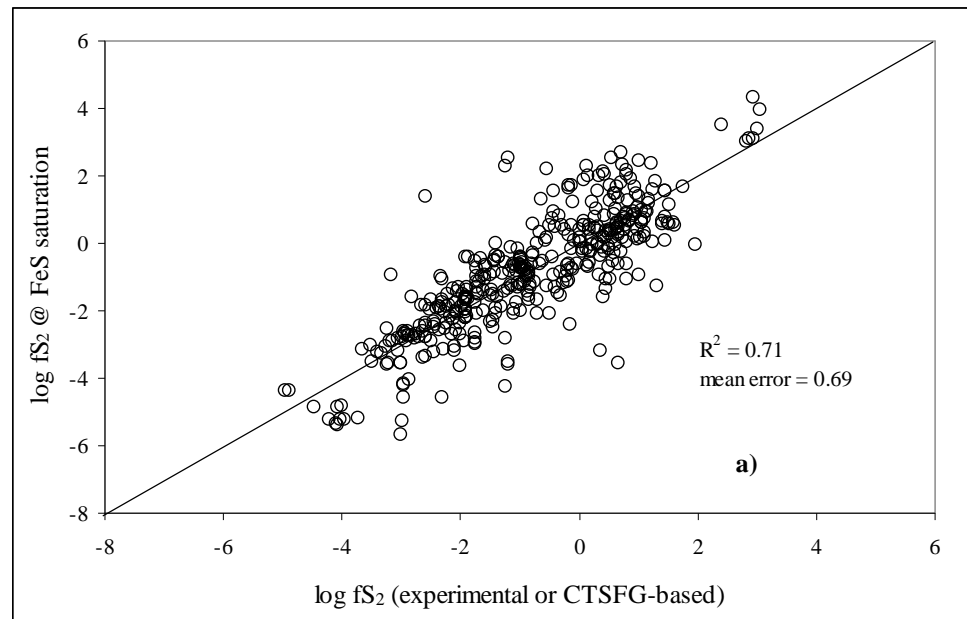**a_{FeO} and a_{FeS} from "built-in" polymeric modeling and Flood and Grjotheim thermochemical cycle**
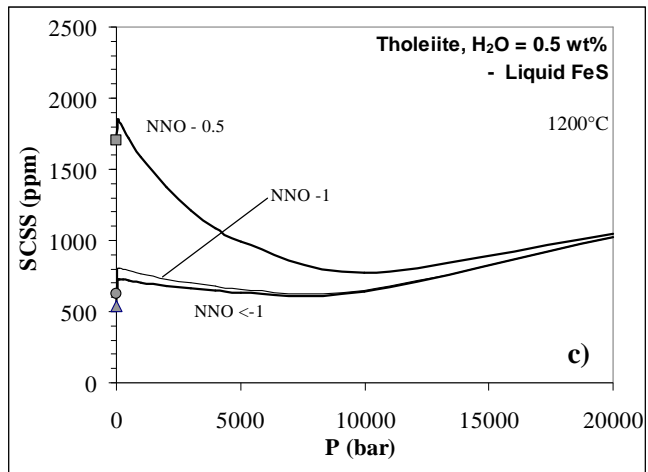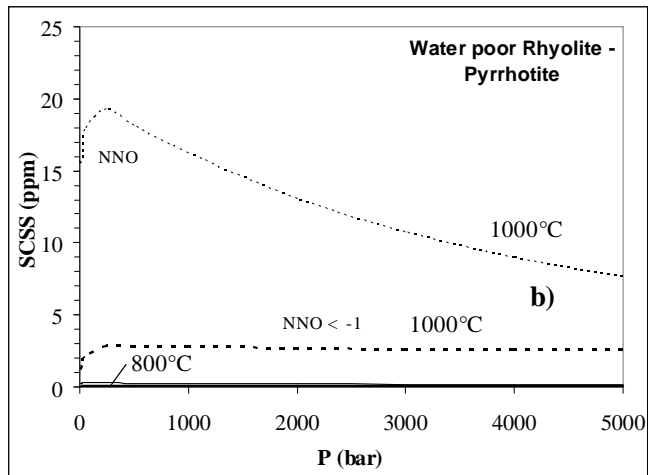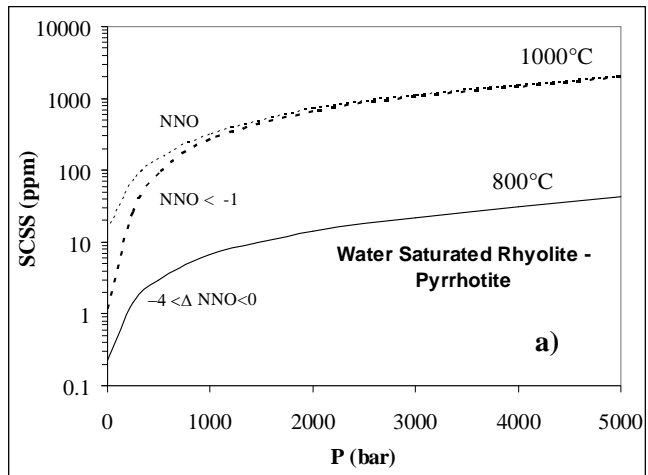
a)

b)

c)
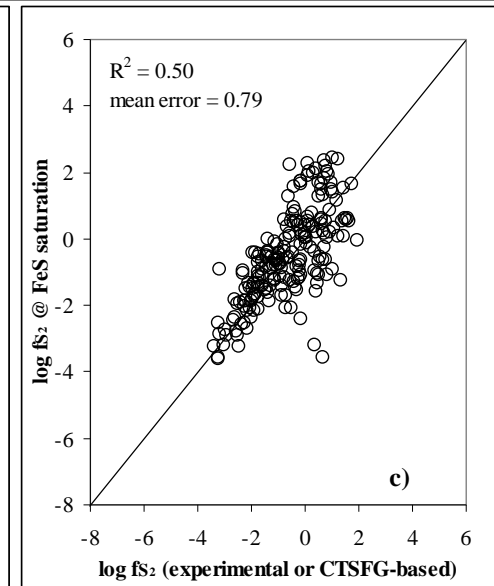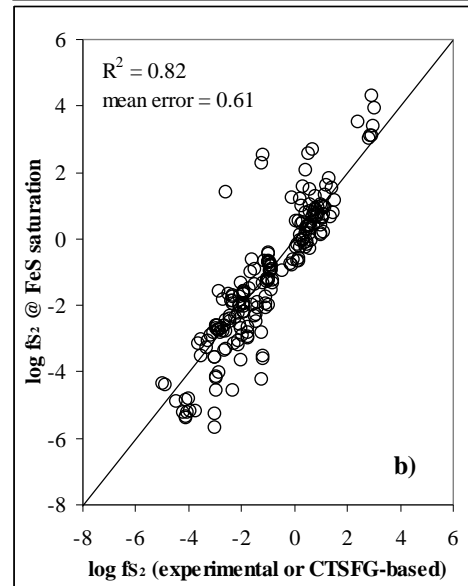
Table 7. Ranges of coloring ions concentrations (in wt% of oxide) and redox pairs ratios (in %) in SLS container glasses produced in Italy (data from SSV).

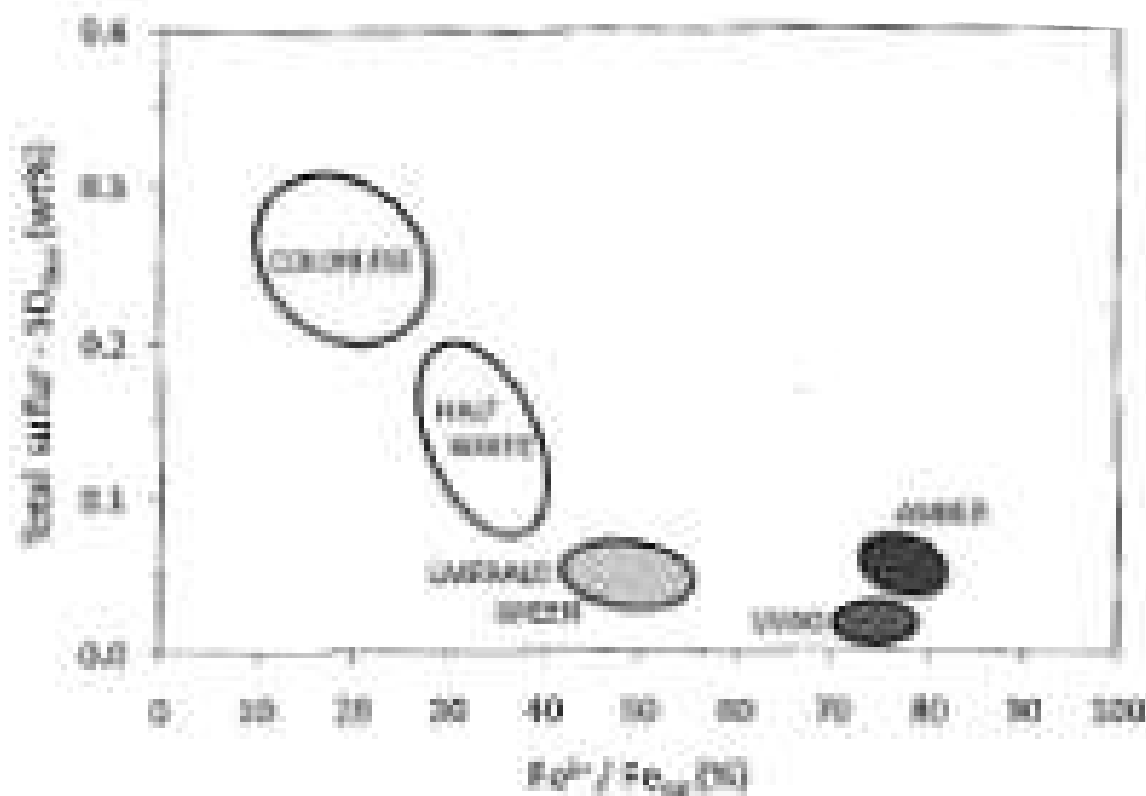| Glass type	$Fe_2O_{3,tot}$	$SO_{3,tot}$	Cr_2O_3	Fe^{2+}/Fe_{tot}	S^{2-}/S_{tot}
Colorless	0.015-0.07	0.20-0.30	—	1 -30	—
Half white	0.1-0.2	0.08-0.20	traces	30 40	—
Emerald green	0.4-0.6	0.04-0.05	0.15 0.25	43 56	—
Yellow green UVAG	0.4-1.0	0.01-0.03	0.06 0.13	70 80	75 90
Amber	0.3-0.5	0.04-0.06	0.03 0.06	74 82	85 95

Figure 7. Typical ranges of total retained sulfur and Fe^{2+}/Fe_{tot} ratio for different container glass types produced in Italy (data from SSV).

Fe-S mutual interactions

We can also study the mutual redox exchanges between more redox couples (when existing…) such as Fe, Ni, S and so on… But even when studying mutual interactions, O^{2-} and therefore oxygen species via Toop-Samis equilibrium, intervene through the normal oxygen electrode (see Moretti and Ottonello, 2003 JNCS). For example, if you consider Fe and S redox equilibria you should write the following ionic equilibria:
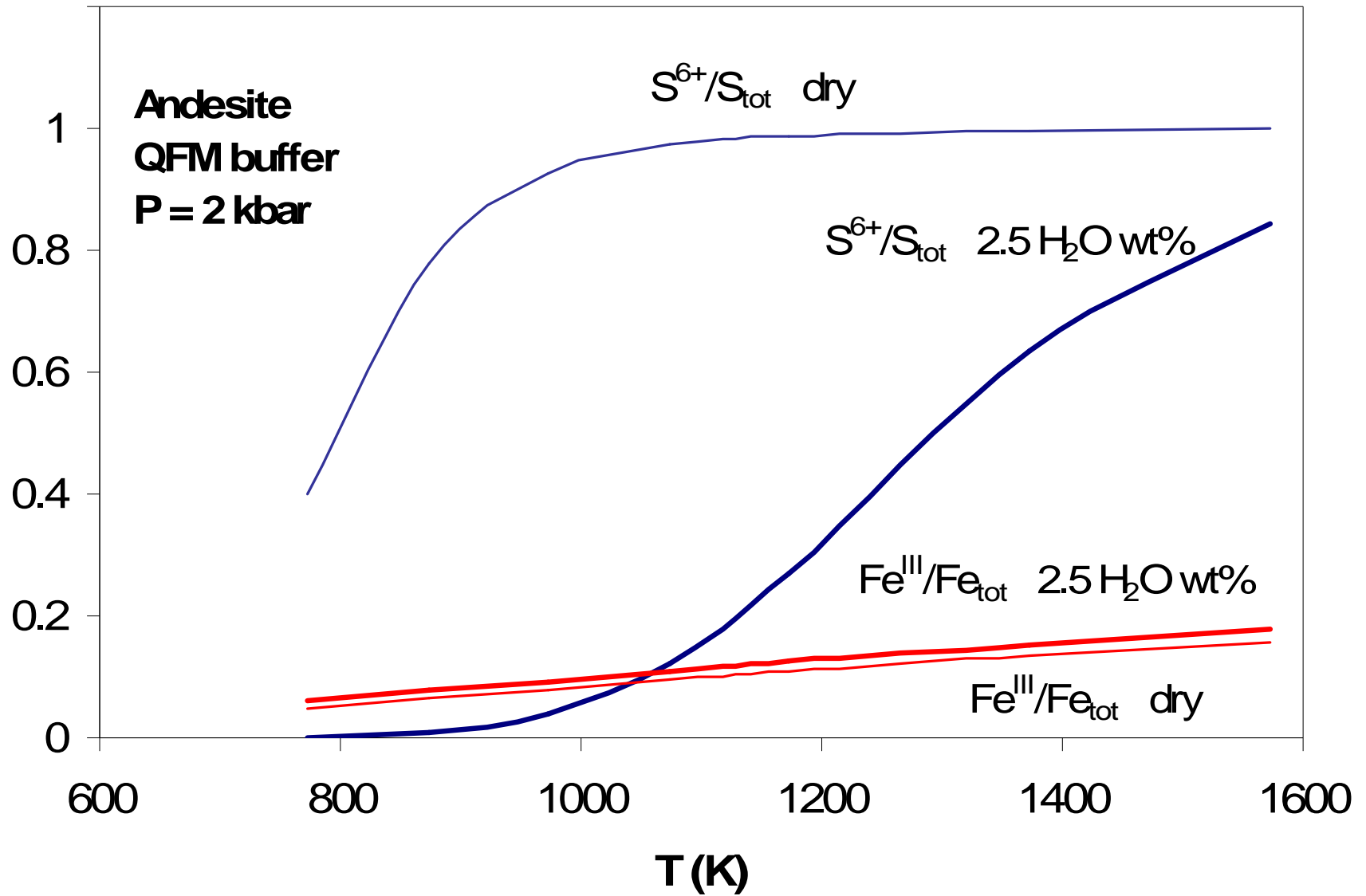
$$8Fe^{3+}_{melt} + S^{2-}_{melt} + 4O^{2-}_{melt} \Leftrightarrow 8Fe^{2+}_{melt} + SO^{2-}_{4,melt}$$

$$SO^{2-}_{4,melt} + 8Fe^{2+}_{melt} + 12O^{2-}_{melt} \Leftrightarrow S^{2-}_{melt} + 8FeO^{-}_{2,melt}$$

If you write:

$$SO^{2-}_{4,melt} + 8FeO \Leftrightarrow S^{2-}_{melt} + 4Fe_2O_{3,melt}$$

so that O^{2-} cancel out, you make a very huge mistake, since you are mixing different notations, confusing species with components and therefore mixing up standard states!

Remind that the basis of redox reactions in melts is the "normal oxygen electrode"

Fe-S mutual interactions

Andesite
QFM buffer
P = 2 kbar

S^{6+}/S_{tot} dry

S^{6+}/S_{tot} 2.5 H_2O wt%

Fe^{III}/Fe_{tot} 2.5 H_2O wt%

Fe^{III}/Fe_{tot} dry

T (K)

Remember, it is the following connection:

acid-base properties => polymerization
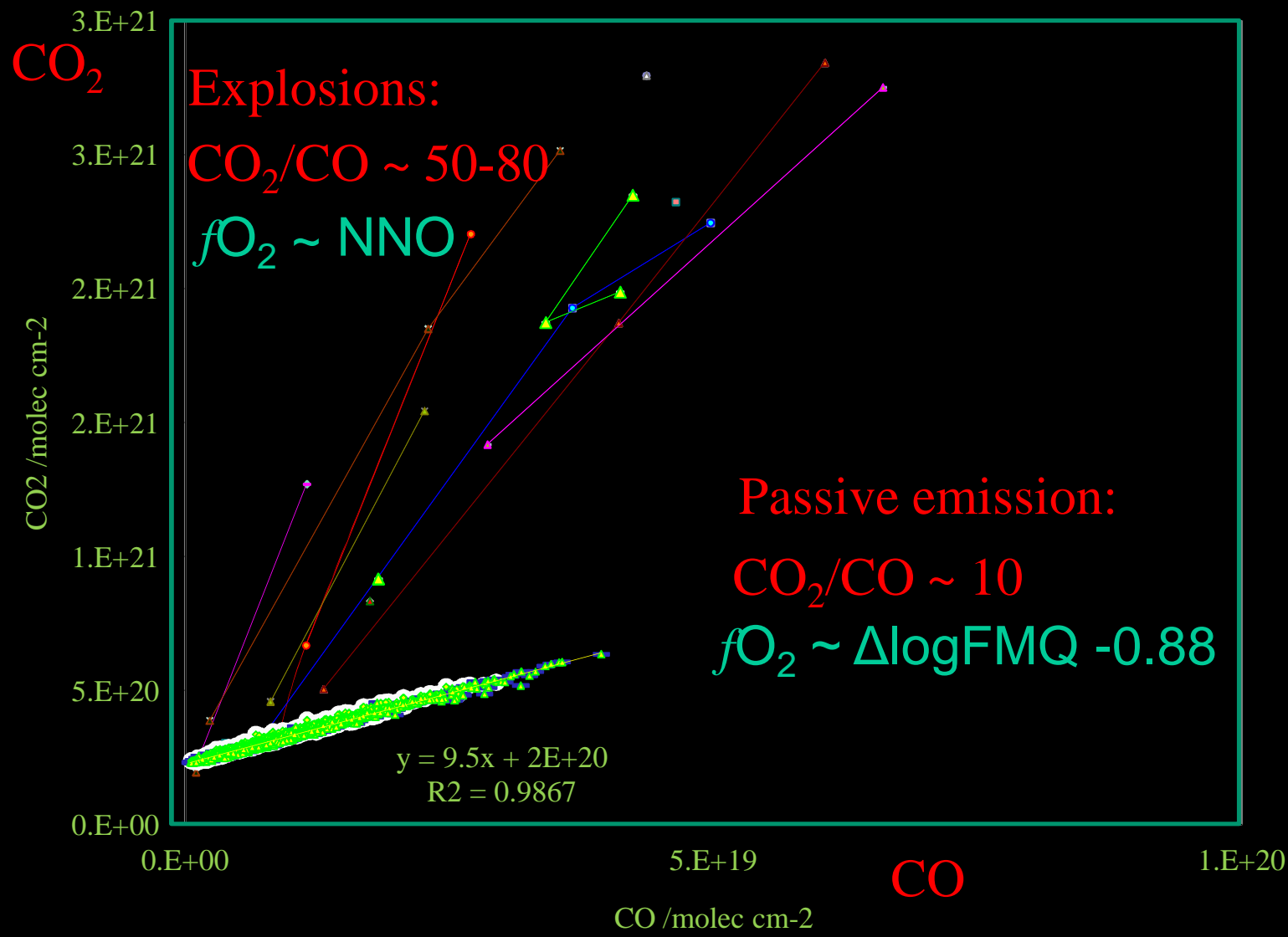
polymerization => redox state

redox state => solubilities
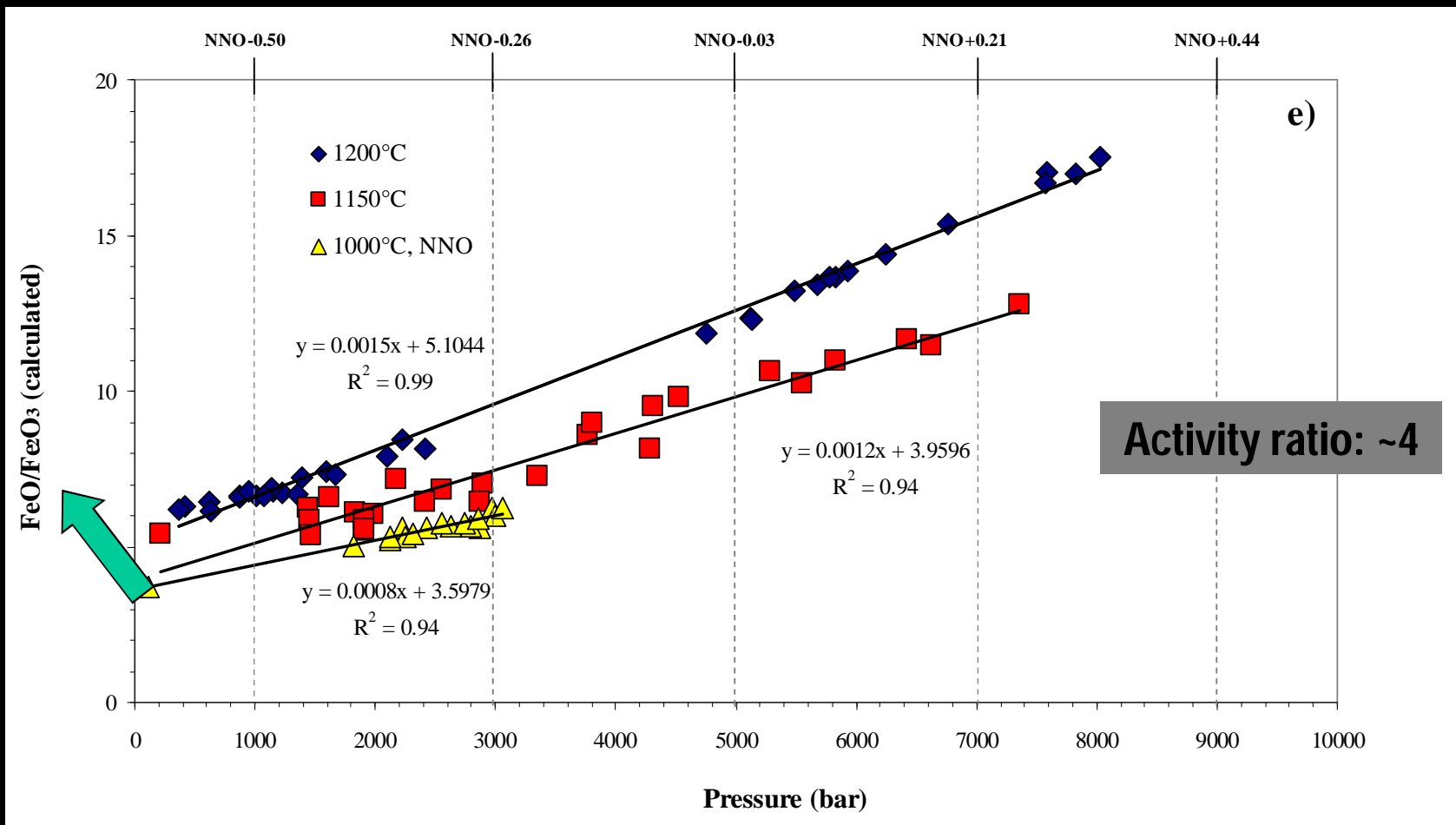
solubilities => acid-base properties, and so on...

That promotes our <u>full</u> understanding of the <u>role of bulk composition on the partioning of volatiles in magmatic systems</u>

Geo-Volcanological applications

-Mt. Erebus Volcano

-The deep source of Italian magmas

-Mt. Etna volcano

-Magmatic Degassing and Sulfur Isotopes

e)

- ◆ 1200°C
- ■ 1150°C
- △ 1000°C, NNO

NNO-0.50   NNO-0.26   NNO-0.03   NNO+0.21   NNO+0.44

$y = 0.0015x + 5.1044$
$R^2 = 0.99$

$y = 0.0012x + 3.9596$
$R^2 = 0.94$

$y = 0.0008x + 3.5979$
$R^2 = 0.94$

Activity ratio: ~4

FeO/Fe₂O₃ (calculated) — *FeO/Fe₂O₃ (calculated)*

Pressure (bar)

Why the lava lake is even further reduced ?

Late (1-10 bar) FeO/Fe_2O_3 increase (no more ol & cpx crystallization)

$$FeO_{(liq)} + Fe_2O_3{}_{(liq)} \rightarrow Fe_3O_4{}_{(magnetite)}$$
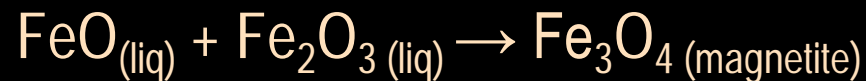
~1wt% crystallisation of magnetite => about a log unit drop in fO_2

XANES spectroscopy: pre-edge study of Fe-K edge spectra

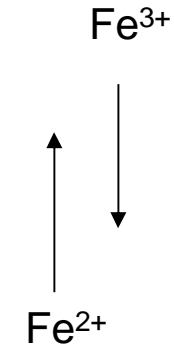Constant fO$_2$: 0.21
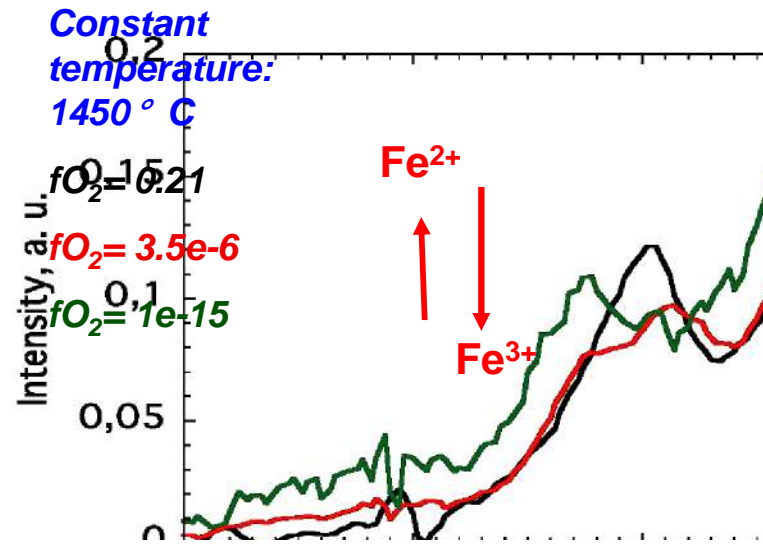
1100	
1150	° C
1550	
1550	
R.T. lava	

fO$_2$= 0.21

Constant temperature: 1450 ° C

fO$_2$= 0.21

fO$_2$= 3.5e-6

fO$_2$= 1e-15

Fe^{3+}

Fe^{2+}
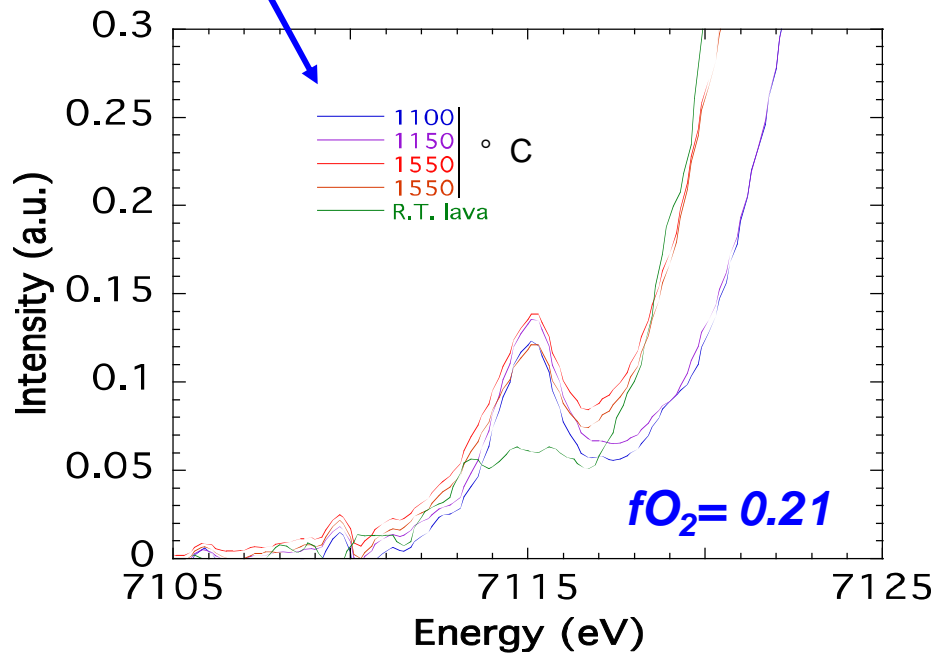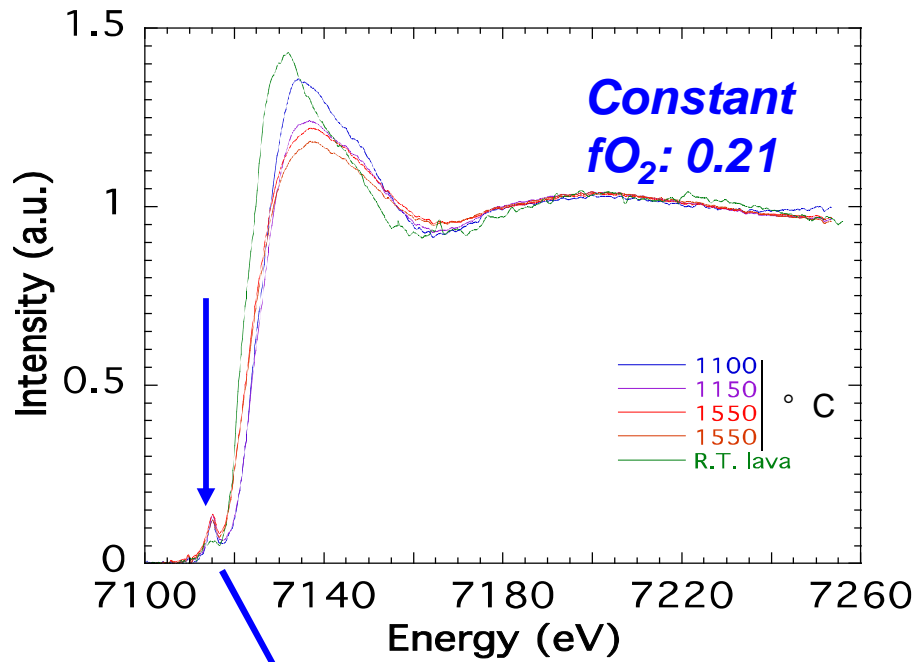
Evolution of the Fe^{2+}/Fe^{3+} equilibrium, depending on T or fO$_2$ = evolution of the pre-edge (Magnien, Neuville et al., 2004, 2008; Cochain, 2010)
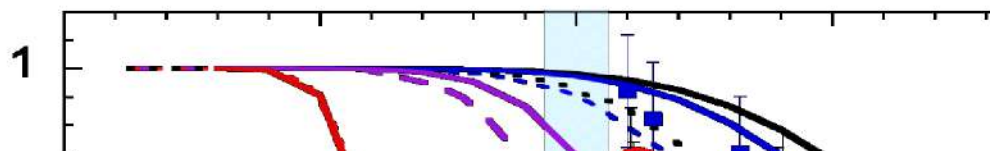
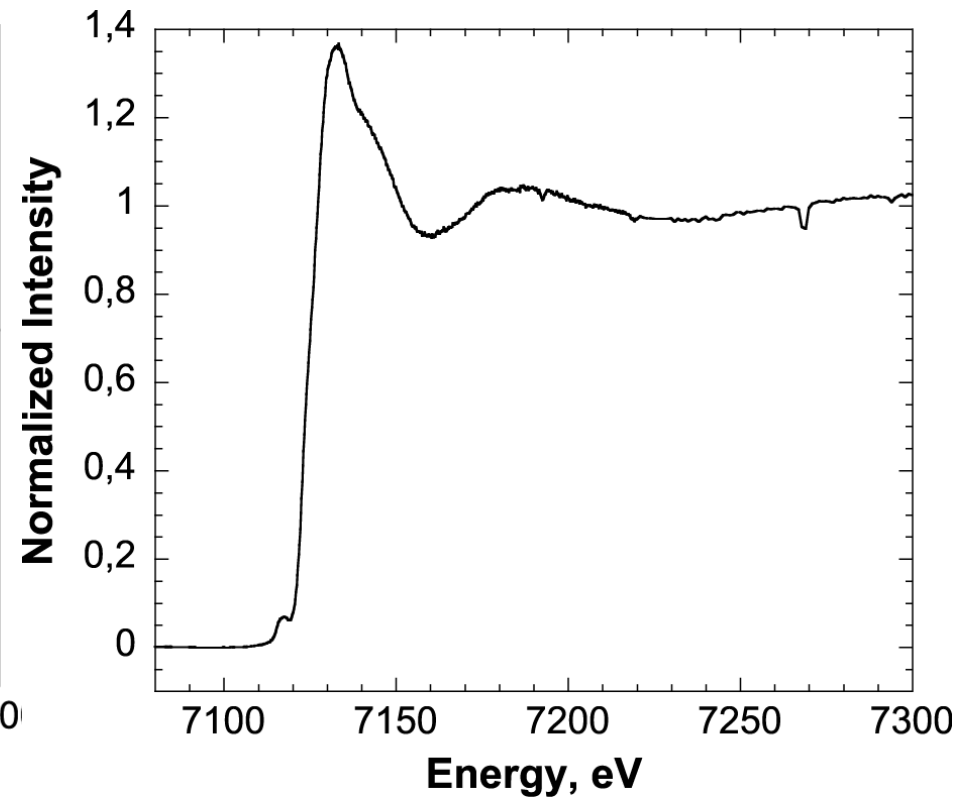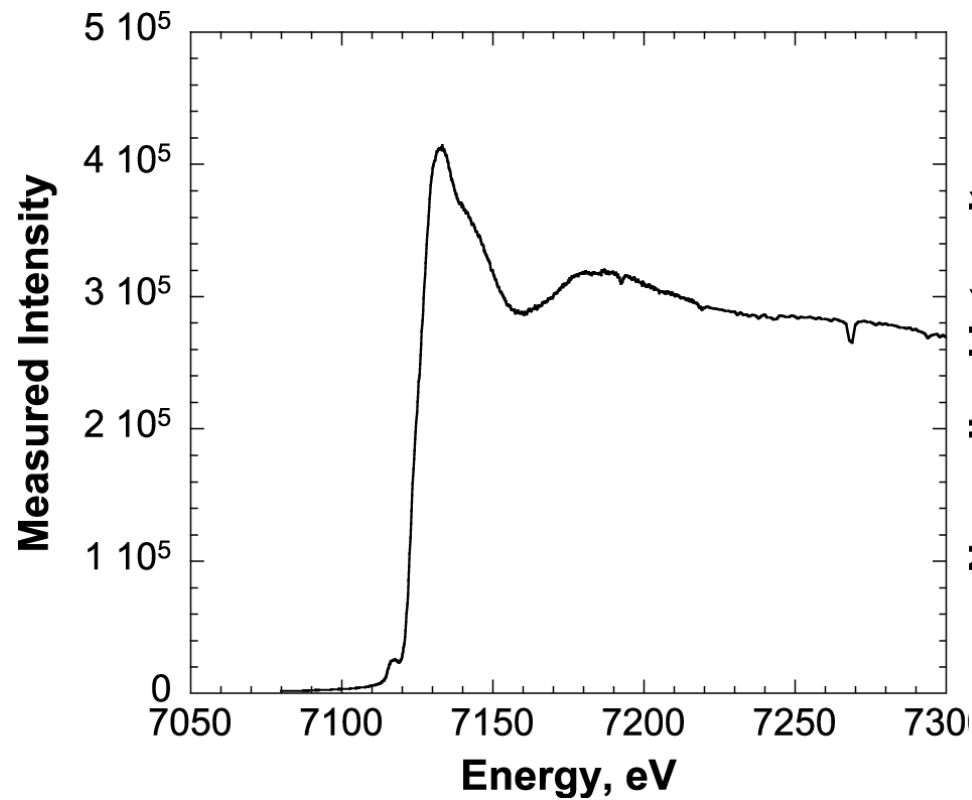## Redox determination by pre-edge deconvolution

pre-edge of Fe-K edge XANES spectra => 2 contributions from Fe in 2+/3+ state

Used to determine iron redox (Wilke et al., 2001, 2004, 2007; Galoisy et al., 2001; Berry et al., 2003; Magnien et al., 2004,2006,2008; Cochain et al., 2009)

Constant temperature: 1450° C

$fO_2 = 0.21$

$fO_2 = 3.5e\text{-}6$

$fO_2 = 1e\text{-}15$

Fe^{2+}

Fe^{3+}

Good agreement with the Moretti (2005) model

Red circles: Measurements difficult under O_2 atm=> crystallization
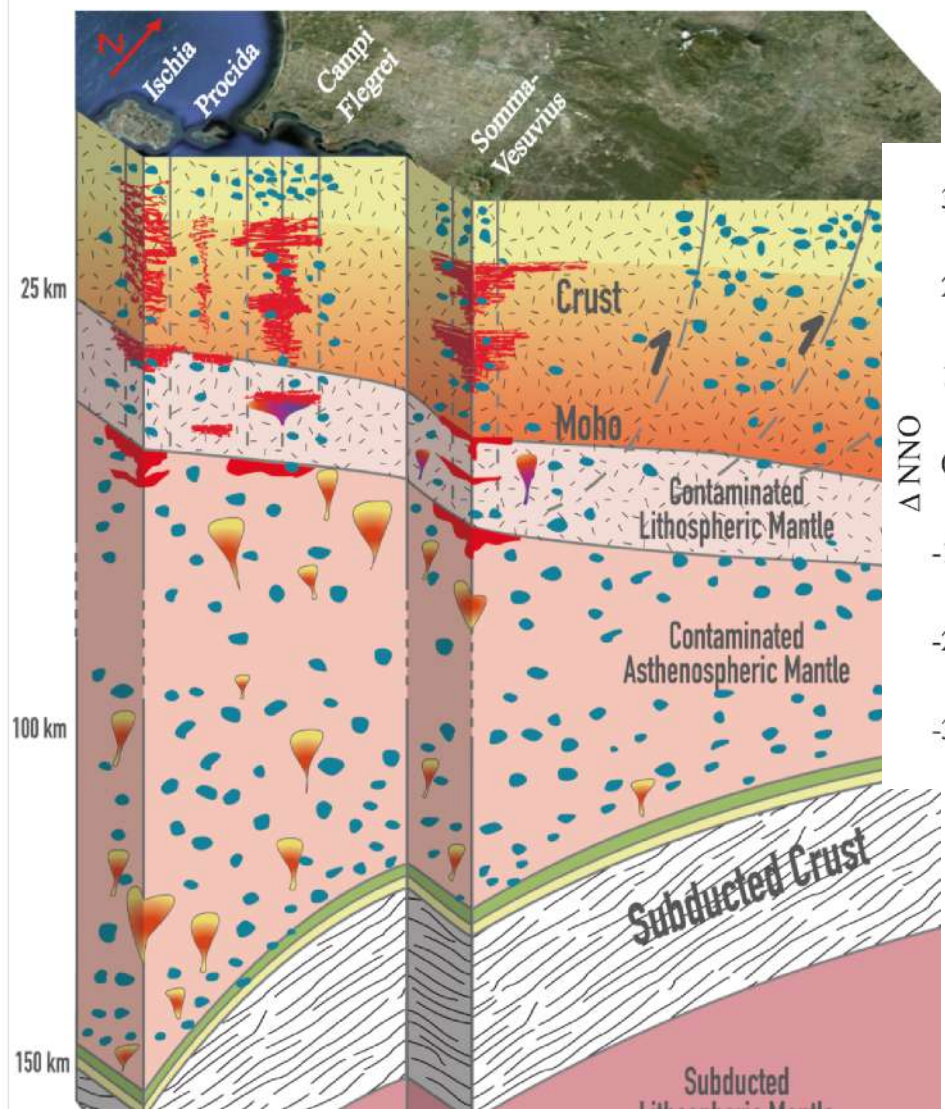
Ischia/Procida/Vesuvius MIs

Volcanic site	Sample	$Fe^{3+}/Fetot$					
Procida	Pro78ol1or2_01		0.47	20	Oui	Oui	
Procida	Procida78ol2or1_01		0.47	21	Oui	Oui	

Volcanic site	Sample	$Fe^{3+}/Fetot$	Volcanic site	Sample	$Fe^{3+}/Fetot$	Volcanic site	Sample	$Fe^{3+}/Fetot$
Vesuvio	VES3_a_DX_1	///	Ischia	C184_185_BIG_01	0.44	Procida	PRO78OL4_at_the_right_01	0.39
Vesuvio	VES01	0.49	Ischia	C186_01	0.41	Procida	PRO78OL6_01	0.51
			Ischia	C187_Big_01	0.42	Procida	PRO78OL7_new_01	0.49
			Ischia	C188_	0.38	Procida	Pro78ol1or2_01	0.47
			Ischia	C189asterix_01	0.47	Procida	Procida78ol2or1_01	0.47
			Ischia	C189obelix_01	0.46			
			Ischia	C190moyen_01	0.51			
			Ischia	C191_01	0.3			
			Ischia	C192bigDX_01	0.34			
			Ischia	C193big1_01	0.38			
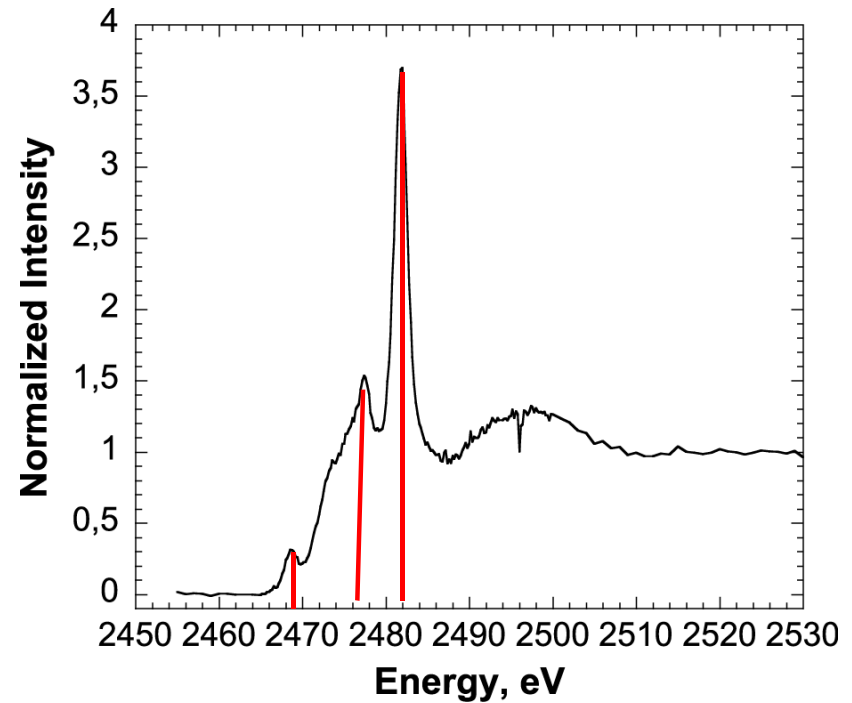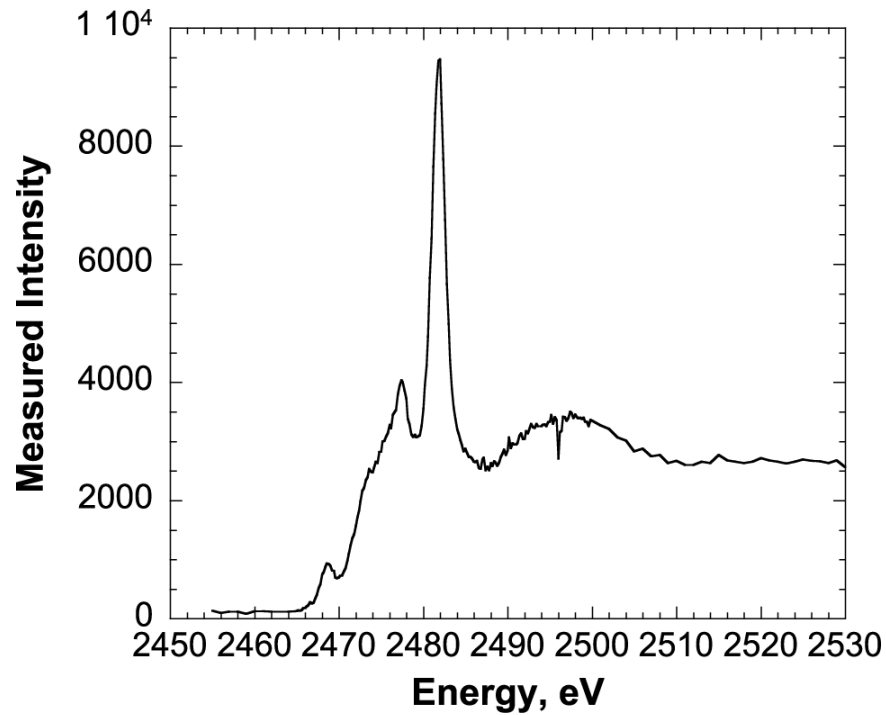
$S_{\#}^{6+}/Stot > 70\%$

$S_{\#}^{6+} = S^{6+} + S^{4+}$

S^{4+} : peak appears as soon as you start measuring, at the expense of the S^{6+}
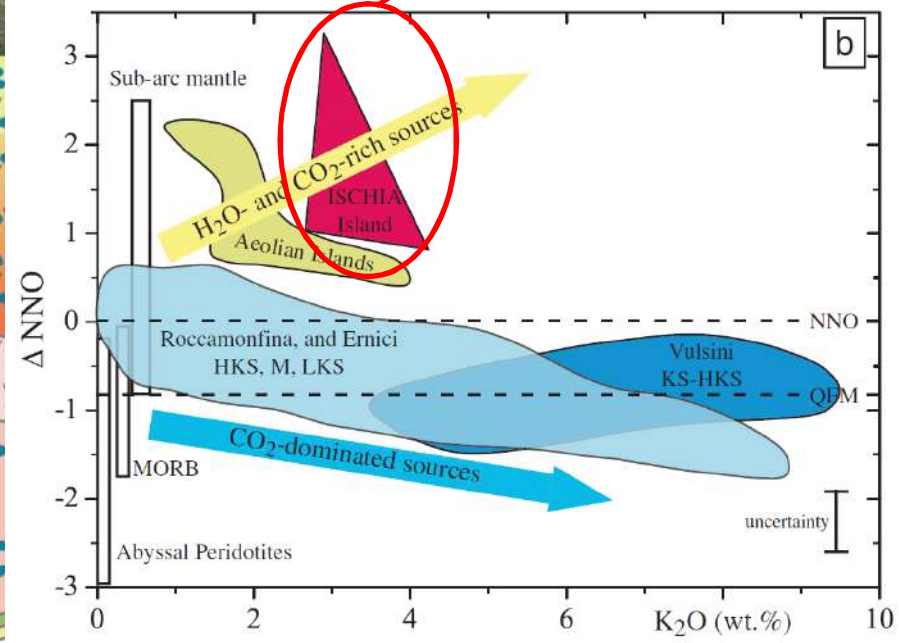
From early Cr-spinels

Legend: ◆ SEC 99 ▲ 122 BC ● BN 97-98 ◆ 2001 eruption (XANES)

$$S^{2-} + 2O_2 \Leftrightarrow SO_4^{2-}$$

$$y = -0.3858x + 16.575$$
$$R^2 = 0.9566$$

Y-axis: $\log(K_{SO_4}/K_{S_2})$

X-axis: H_2O (wt%)

Figure 10

Legend:
- 122 BC
- 2001 eruption (XANES)
- 122 BC (fO$_2$ estimated)
- SEC 99
- BN 97-98
- BN 97-98 (fO$_2$ estimated)

A (top panel): logfS$_2$ (y-axis, –2 to 2) vs ΔNNO (x-axis, –1.5 to 1)

y=x+0.71

B (bottom panel): log(fS$_2$/fO$_2$) (y-axis, 4 to 10) vs S (ppm) (x-axis, 0 to 5000)

Figure 8

$$SO_4^{2-} + 4CO_{2(g)} + 8Fe^{2+} + \Leftrightarrow 8Fe^{3+} + S^{2-} + 4CO_3^{2--}$$

nS^{2-} (mmol/kg of melt)

50
40
30
20
10
0

Reduction without S-loss

$SO_4^{2-} \leftrightarrow SO_{2(g)} + O^{2-} + \frac{1}{2}O_{2(g)}$
$SO_4^{2-} + Ca^{2+} \leftrightarrow CaSO_{4(anh)}$

Melt Initial Composition

$3SO_4^{2-} + S^{2-} \leftrightarrow 4SO_{2(g)} + 4O^{2-}$

$SO_4^{2-} + S^{2-} + H_2O_{(g)} \leftrightarrow H_2S_{(g)} + SO_{2(g)} + 2O^{2-} + \frac{1}{2}O_{2(g)}$

$H2O_{(g)} + S^{2-} \leftrightarrow H_2S_{(g)} + O^{2-}$

$S^{2-} + Fe^{2+} \leftrightarrow FeS_{(liq\ or\ po)}$

Oxidation without S-loss
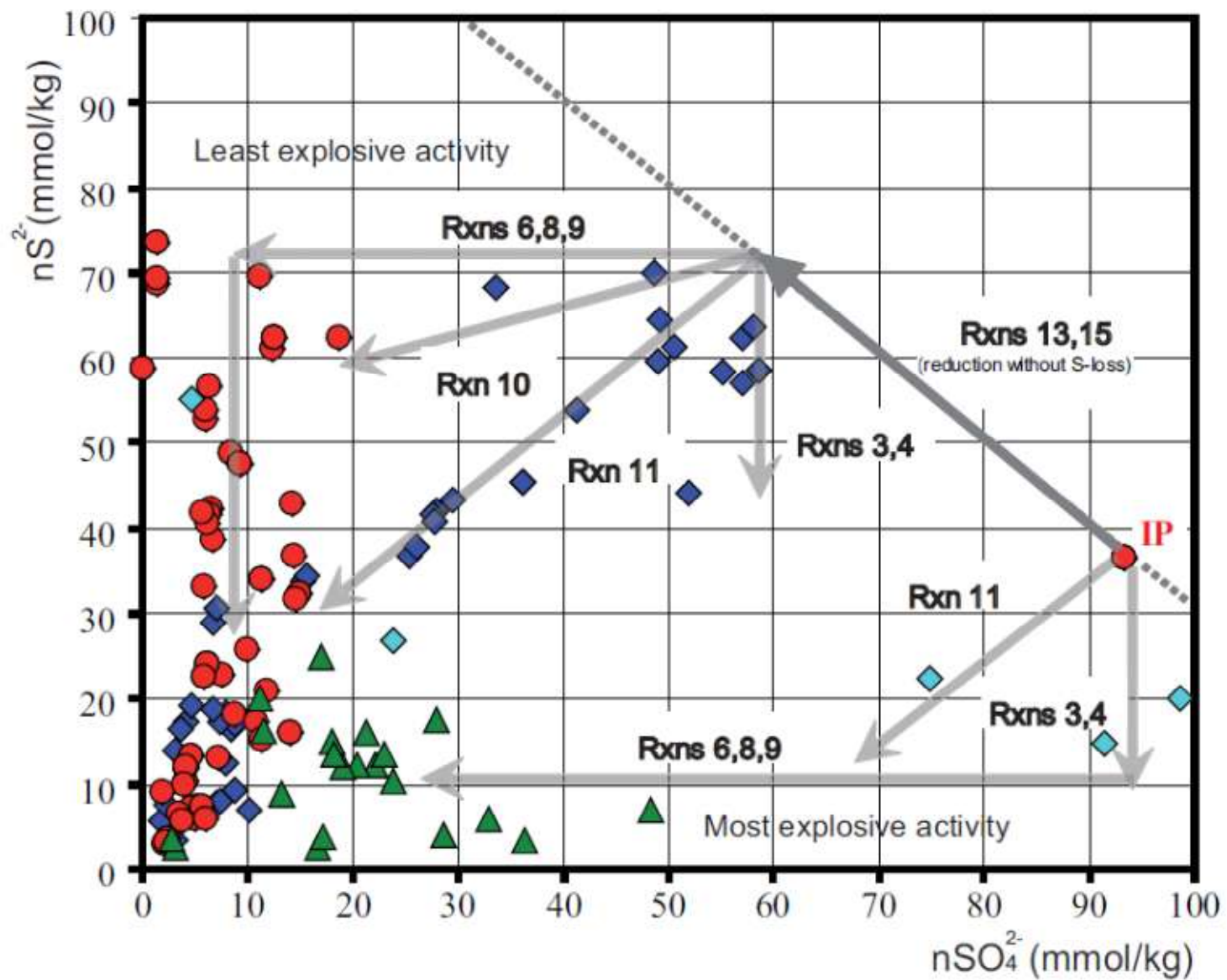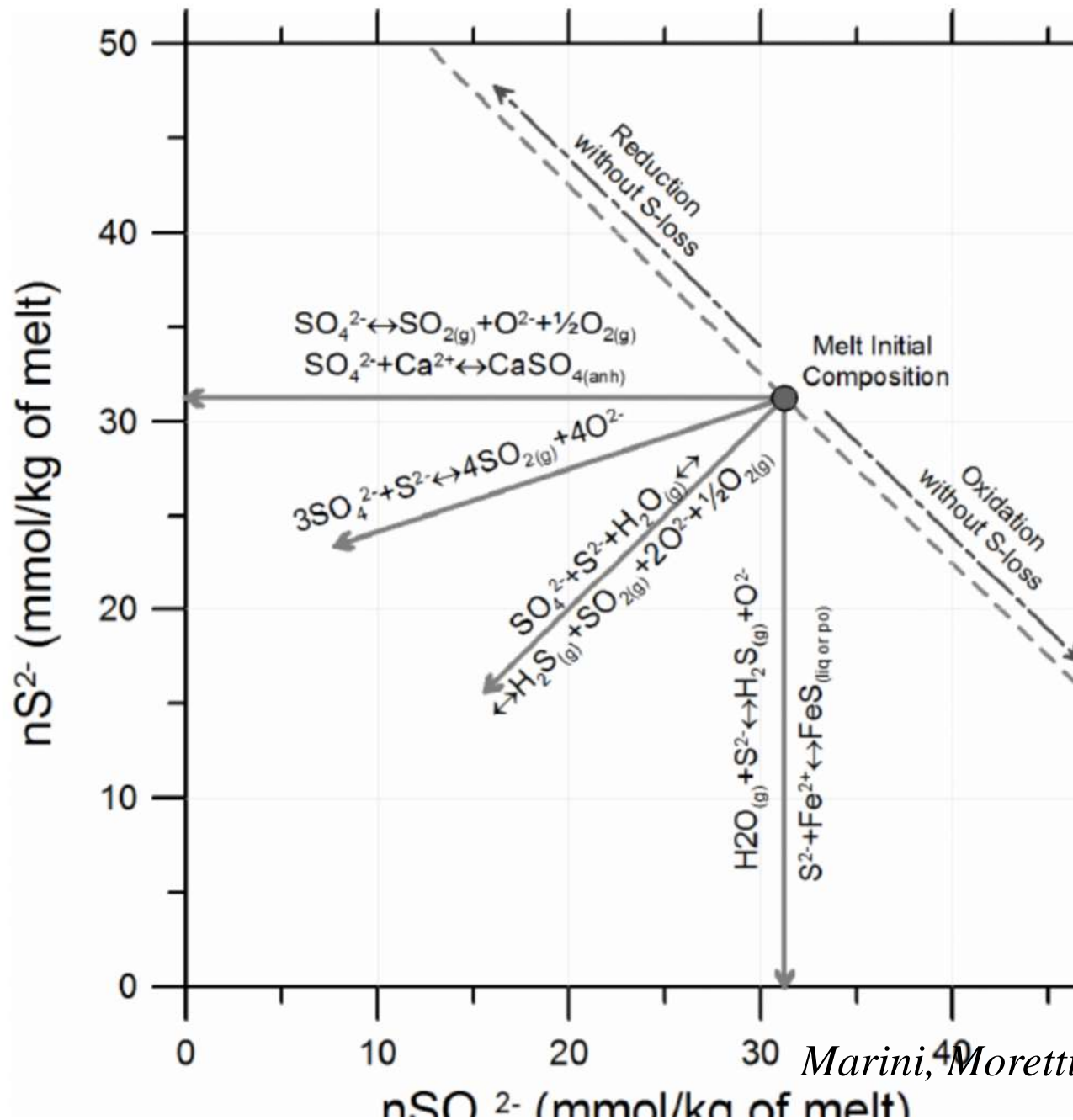
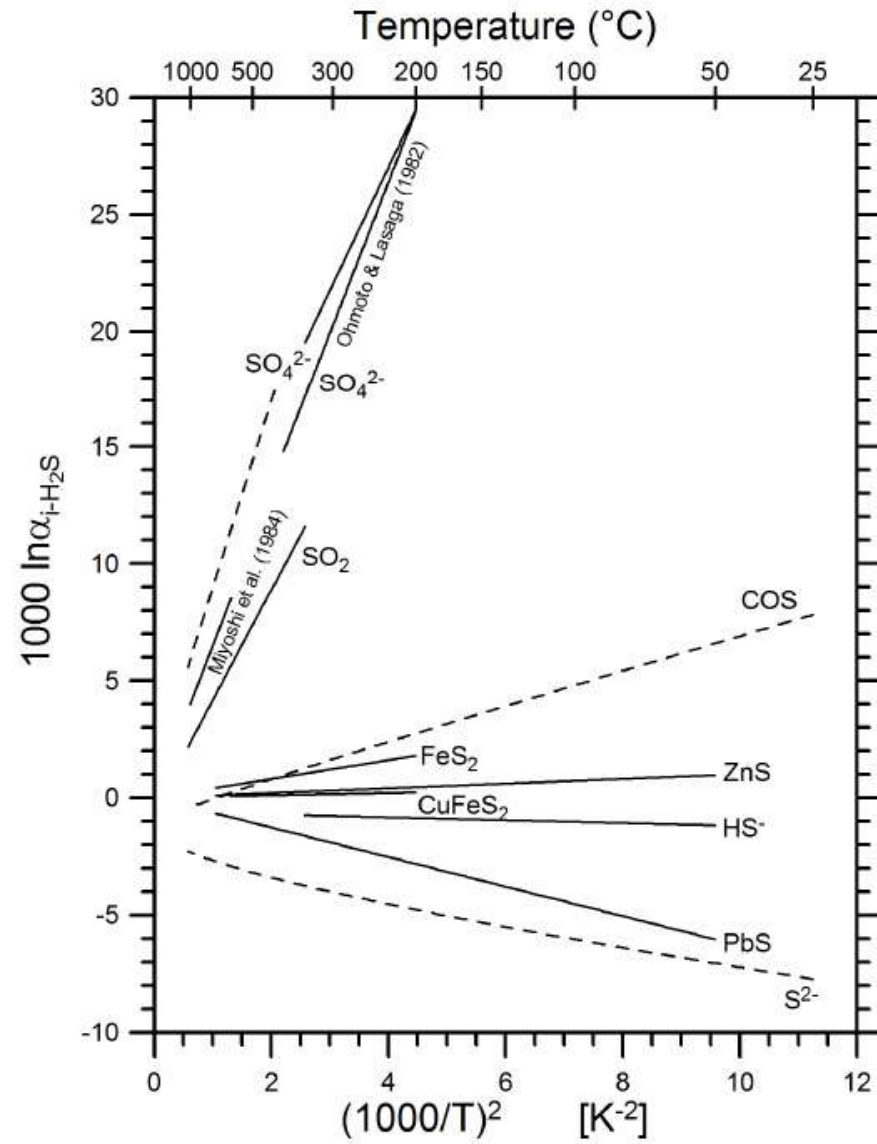nSO$_2^{2-}$ (mmol/kg of melt)

0   10   20   30   40

S-species and reactions involved in the **full tracking** *of volcanic degassing…*

High reactivity

many degassing paths

Marini, Moretti & Accornero (2011)

Ohmoto-Rye, 1979

Sulfur chemical behavior AND isotopic composition largely depends on (equilibrium or near-equilibrium) **redox conditions**

$\Rightarrow$parameterization of sulfur **speciation** becomes a major issue aldo for isotopes (large fractionation factors are involved) **!**.

$\Rightarrow$ Not simple, linear, behaviors should be expected for S isotopic composition in a phase (...because of the interplay with **temperature** and **bulk isotopic composition $\rightarrow$** source...)

$$\delta^{34}S_{\Sigma S} = \delta^{34}S_{SO_2} \cdot y_{SO_{2(g)}} + \delta^{34}S_{H_2S} \cdot \left(1 - y_{SO_{2(g)}}\right),$$

$$y_{SO_{2(g)}} = X_{SO_{2(g)}} \Big/ \left(X_{SO_{2(g)}} + X_{H_2S_{(g)}}\right).$$

$$1000 \ln \alpha_{SO_2-H_2S} = \delta^{34}S_{SO_2} - \delta^{34}S_{H_2S}$$

Degassing...

$$1000\ln\alpha_{gas-melt} \cong \delta^{34}S_{\Sigma S,gas} - \delta^{34}S_{\Sigma S,melt} =$$

$$= \left[Y_{SO_2} \cdot \delta^{34}S_{SO_2} + \left(1 - Y_{SO_2}\right) \cdot \delta^{34}S_{H_2S} \right] - \left[Y_{SO_4^{2-}} \cdot \delta^{34}S_{SO_4^{2-}} + \left(1 - Y_{SO_4^{2-}}\right) \cdot \delta^{34}S_{S^{2-}} \right] =$$

$$= Y_{SO_2} \cdot 1000\ln\alpha_{SO_2-H_2S} + Y_{SO_4^{2-}} \cdot 1000\ln\alpha_{S^{2-}-SO_4^{2-}} + 1000\ln\alpha_{H_2S-S^{2-}}$$

Sulfide separation...

$$1000\ln\alpha_{FeS-melt} \cong \delta^{34}S_{FeS} - \delta^{34}S_{\Sigma S,melt} =$$

$$= \delta^{34}S_{FeS} - \left[Y_{SO_4^{2-}} \cdot \delta^{34}S_{SO_4^{2-}} + \left(1 - Y_{SO_4^{2-}}\right) \cdot \delta^{34}S_{S^{2-}} \right] =$$

$$= Y_{SO_4^{2-}} \cdot 1000\ln\alpha_{S^{2-}-SO_4^{2-}} + 1000\ln\alpha_{FeS-H_2S} + 1000\ln\alpha_{H_2S-S^{2-}}$$

We MUST know <u>how $Y_{SO_4^{2-}}$ and $Y_{S^{2-}}$ are related to P, T and composition</u>

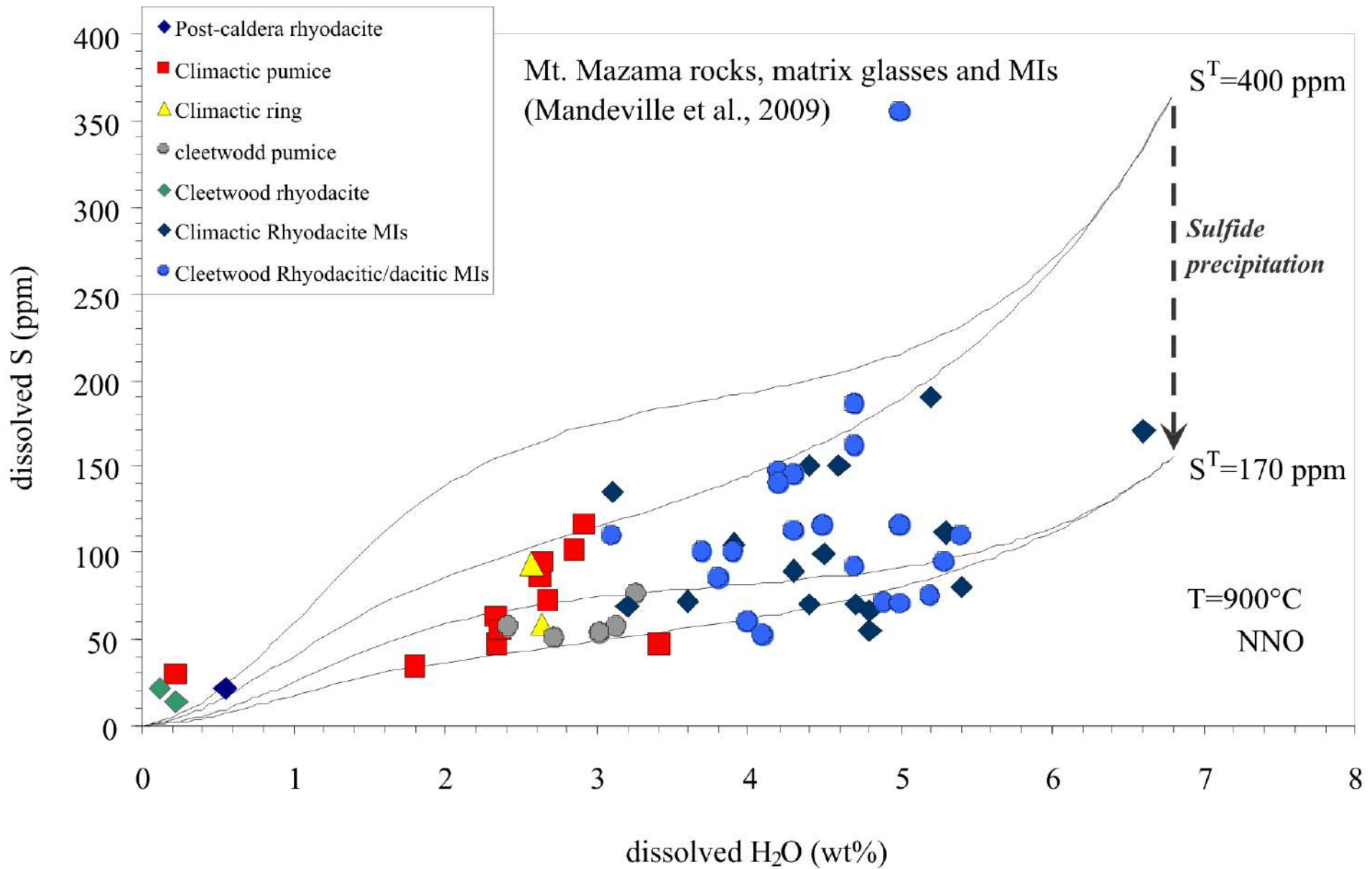$\Rightarrow$ AVOID EMPIRICAL LAWS, such as :

$$S_{wt\%} = a \log f_{SO2}{}^{b}$$

S is too reactive !

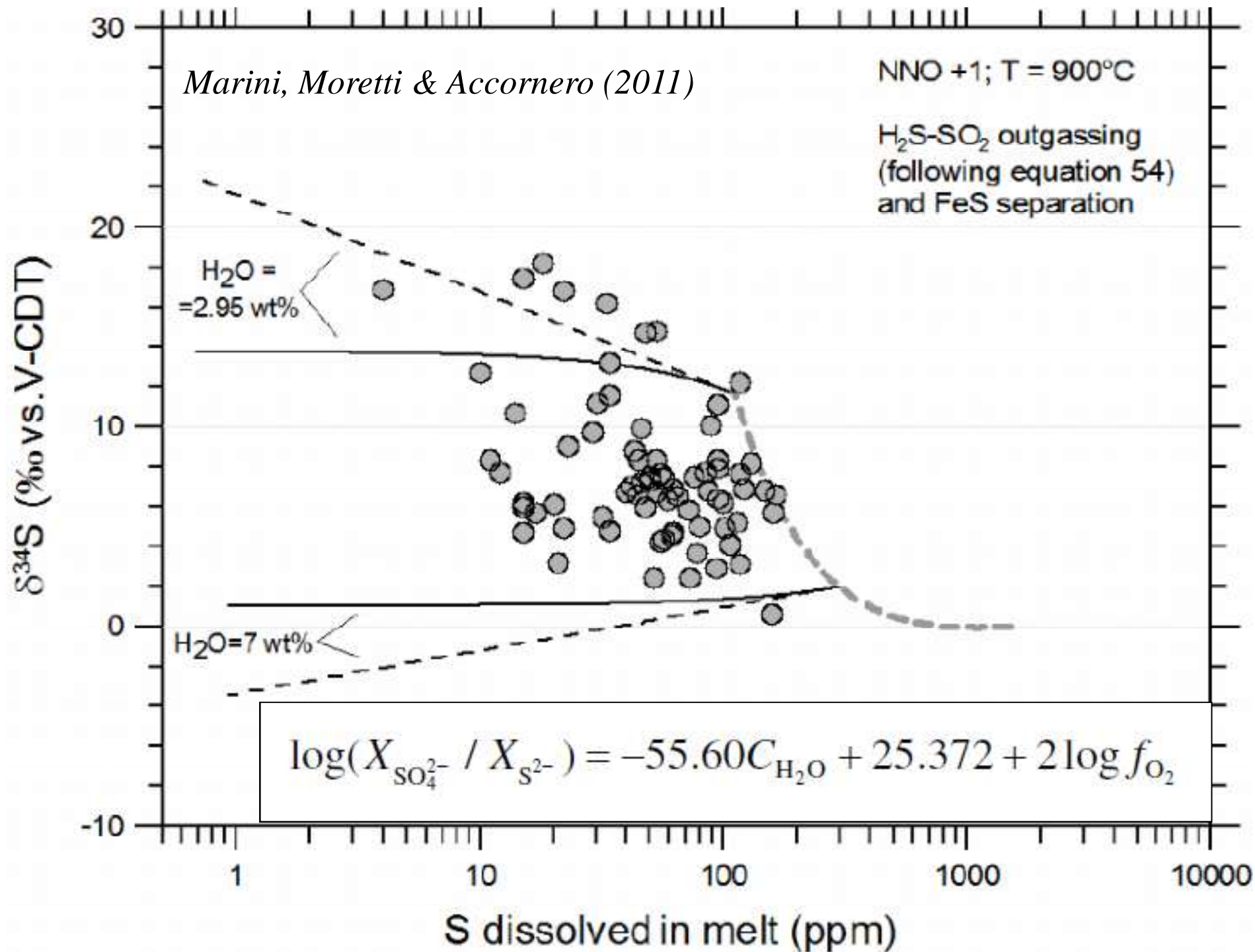…we need to measure and then parameterize SO_4^{2-} and S^{2-} in melts!

=> we need to well account for fO_2 and composition

$$\log(X_{SO_4^{2-}} / X_{S^{2-}}) = -55.60 C_{H_2O} + 25.372 + 2 \log f_{O_2}$$

Marini, Moretti & Accornero (2011)

Marini, Moretti & Accornero (2011)

NNO +1; T = 900°C

H_2S-SO_2 outgassing (following equation 54) and FeS separation

$H_2O = =2.95$ wt%

$H_2O = 7$ wt%

$$\log(X_{SO_4^{2-}} / X_{S^{2-}}) = -55.60 C_{H_2O} + 25.372 + 2\log f_{O_2}$$
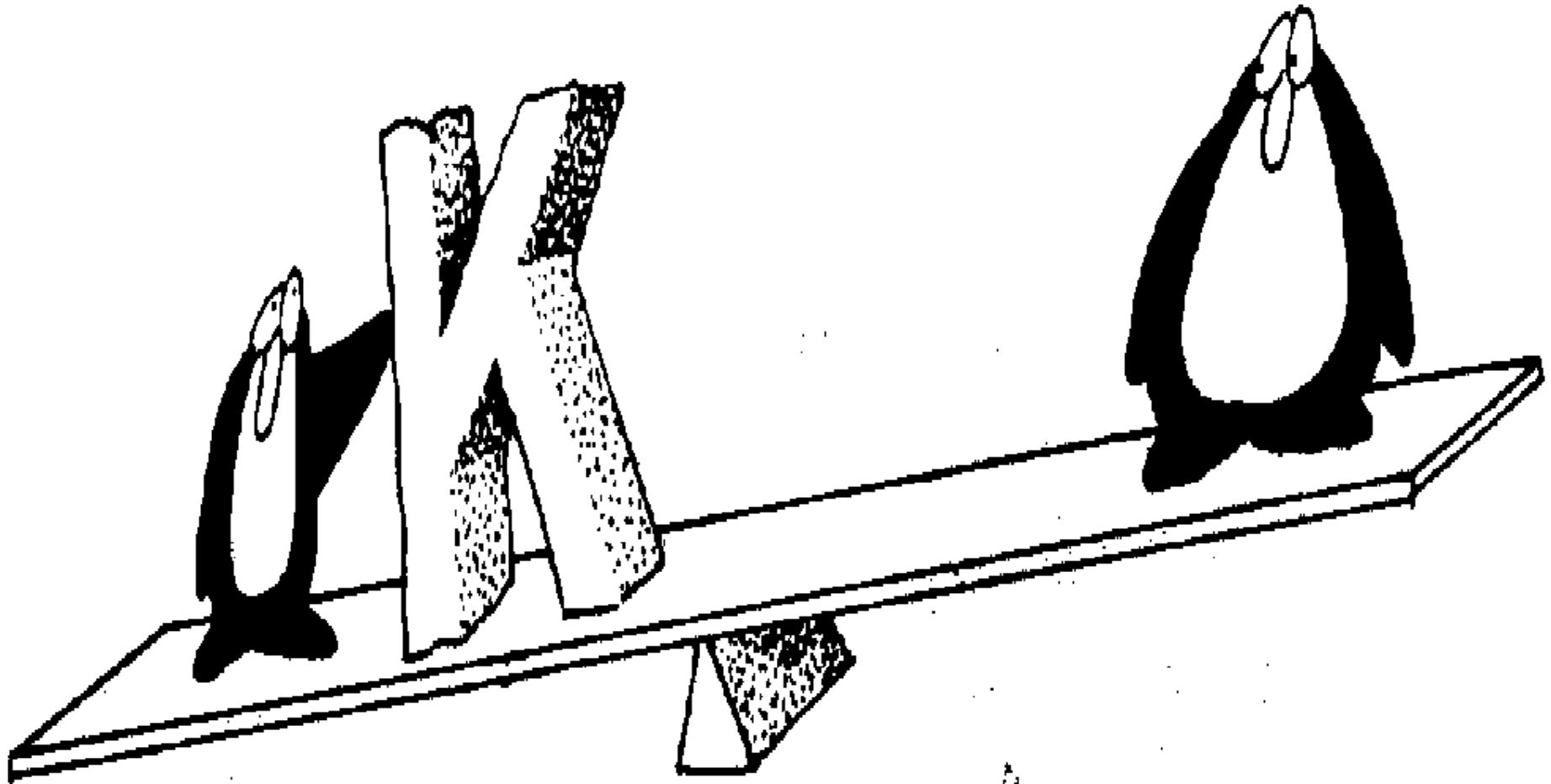
$\delta^{34}S$ (‰ vs. V-CDT)

S dissolved in melt (ppm)
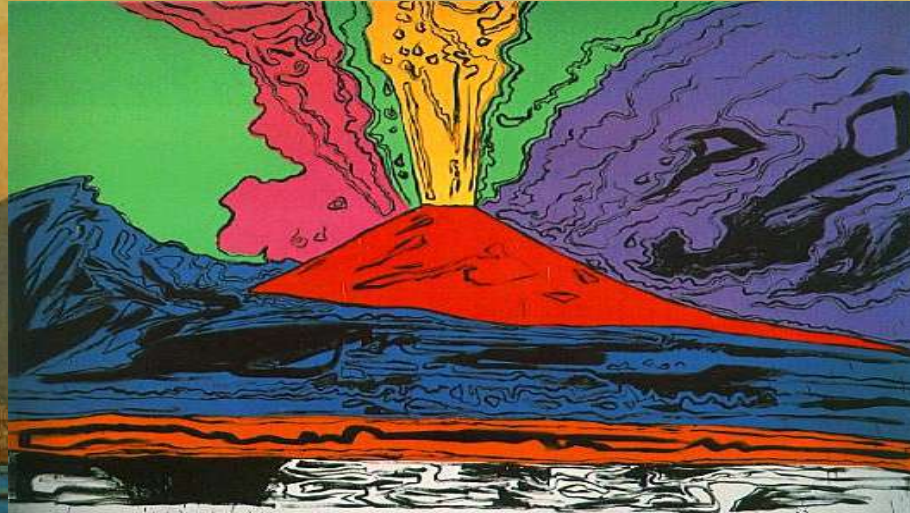
"Free energy" is needed...to work well

Nordstrom and Munoz (1986) *Geochemical Thermodynamics*
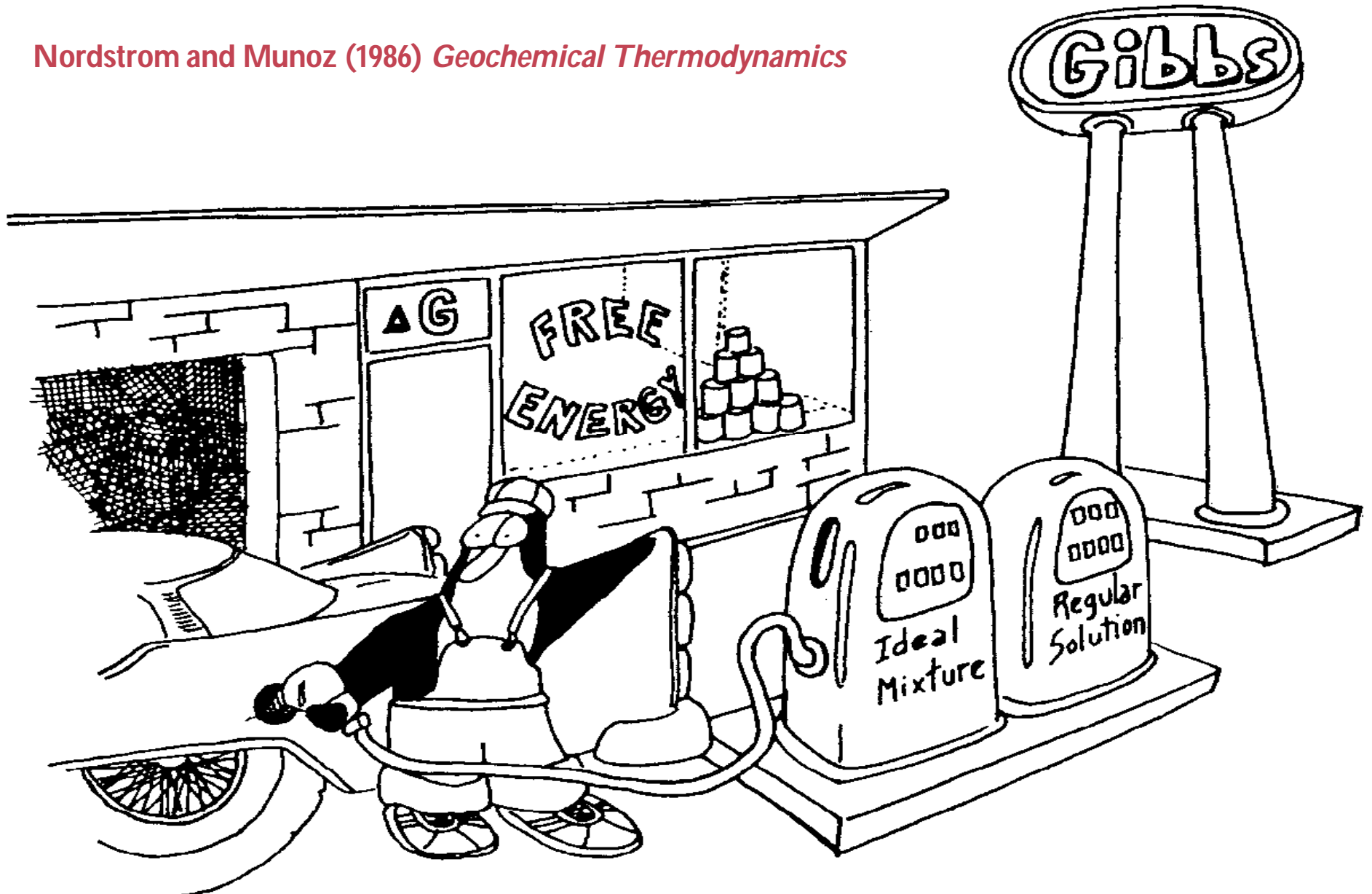
Nordstrom and Munoz (1986)
Geochemical Thermodynamics

Merci de votre attention !

Andy Warhol, 1985